View metadata, citation and similar papers at core.ac.uk
brought to you by CORE
provided by ScholarBank@NUS

Development and Evaluation of Sucrose Ester Stabilized Oleanolic Acid Nanosuspensions

LI WENJI

NATIONAL UNIVERSITY OF SINGAPORE

2011

DEVELOPMENT AND EVALUATION OF SUCROSE ESTER STABILIZED OLEANOLIC ACID NANOSUSPENSIONS

LI WENJI

M. Sc. (NUS)

A THESIS SUBMITTED FOR THE DEGREE OF DOCTOR OF PHILOSOPHY

DEPARTMENT OF PHARMACY

NATIONAL UNIVERSITY OF SINGAPORE

2011

ACKNOWLEDGEMENT

I wish to express my deepest appreciation to my respected supervisors, Dr Heng Wan Sia, Paul and Dr Ng Ka-Yun, Lawrence for their expert guidance and constant encouragement throughout my study. Their invaluable guidance, enlightening discussions and great patience had benefited me a considerably.

I wish to extend my heartiest gratitude to the Head, Department of Pharmacy, Dr Chan Sui Yung for her support. I am also very grateful to Dr Go Mei Lin for her guidance during my postgraduate studies.

I feel greatly appreciated to Dr Chan Lai Wah and Dr Celine Valeria Liew for their help and care. I also wish to thank Dr Loh Zhi Hui, Dr Tay Li Mei, Stephanie, Mrs Ang Swee Har, Teresa, Ms Wong Mei Yin and all the other GEA-NUS staff and students for their help and support.

I am greatly indebted to Dr Ho Chi Lui, Paul, Dr Chiu Ngar Chee, Gigi and Dr Eric Chan Chun Yong for allowing the use of the equipment under their charge. Thank you for your timely help.

I wish to thank my laboratory mates, Dr Leslie Gapter, Dr Zhang Yaochun, Dr Ling Hui, Dr Surajit Das, Ms Wu Jiao, Dr Wang Li kun, Mr Kou Xiang, Ms Chin Wun Chyi, Mr Shubhajit Paul, Mr Srimanta Sarkar, Dr Atul D Karande, Ms Christine Cahyadi, Mr Tan Bing Xun, Mr Wong Poh Mun, Ms Sweta Rathore, and Mr Asim Kumar Samanta for their constant help and encouragement.

I am particularly grateful to Dr Lin Haishu and Dr Sun Feng for their assistance in the

use of animals and in the pharmacokinetics study.

I am also greatly indebted to Ms Ng Sek Eng, Ms New Lee Sun, Mdm Oh Tang Booy, Ms Tan Bee Jen, Ms Yong Sock Leng, Ms Lye Pey Pey, Ms Ng Swee Eng, Mdm Napsiah Binte Suyod, Ms Chan Wei Ling, Mdm Nor Hazliza Binte Mohamad, Ms Chen Yee Ju, Mdm Lim Sing, Mdm Pakiavathi and all the other staff members of the Department of Pharmacy. They directly or indirectly helped me in the preparation of my research work and thesis.

I wish to thank Mdm Loy Gek Luan and Mr Chong Ping Lee, Department of Biological Sciences, for their support with the TEM experiments.

I am most greatly indebted to my beloved wife, Liu Hong Juan and daughter, Li zexuan, for their full support and encouragement. Finally, I wish to thank my parents for their constant care and love. It was their inspiration and constant encouragement which has helped me to come so far.

TABLE OF CONTENTS

Acknowledgement ..... **i**
TABLE OF CONTENTS ..... **iii**
Summary ..... **vi**
List of Tables ..... **ix**
List of Figures ..... **x**
Abbreviations ..... **xiv**
CHAPTER 1. ..... **1**
INTRODUCTION **1**
CHAPTER 1: Introduction **2**
1.1 Oleanolic acid (OA) - a hydrophobic natural product **2**
1.1.1 Natural products 2
1.1.2 Oleanolic acid pharmacological effect 4
1.1.2.1Hepatoprotection effect 4
1.1.2.2 Anti-cancer 4
1.1.2.3 Anti-HIV 5
1.1.2.4 Anti-inflammatory 5
1.1.2.5 Other pharmacological effect 6
1.1.3 Dose and administration 6
1.1.4 Bioavailability of oleanolic acid 6
1.2 Formulation strategies of increasing water solubility and dissolution rate **7**
1.3 Nanosuspensions **9**
1.3.1 Methods of preparation nanosuspensions 10
1.3.1.1 Milling 12
1.3.1.2 Homogenization 13
1.3.1.3 Bottom-up method 14
1.3.2 Nanosuspensions characterization 15
1.3.2.1 Mean particle size and particle size distribution 15
1.3.2.2 Particle morphology and crystalline state 16
1.3.2.3 Saturation solubility 16
1.3.2.4 *In vitro* dissolution rate and *in vivo* pharmacokinetics profile 17
1.3.2.5 Stability 18
1.3.3 Stabilizers in preparation of nanosuspensions 19
1.4 Sucrose ester as stabilizers in preparation of nanosuspensions **20**
1.5 Aims and objectives **22**
Chapter 2. ..... **24**
Development and evaluation of SEOA NS via emulsion-solvent evaporation method **24**
Chapter 2. Development and evaluation of SEOA NS via emulsion-solvent evaporation method **25**
2.1 Introduction **25**
2.2 Materials **27**
2.3 Methods **28**

2.3.1 Critical micellar concentration (CMC) determination by surface tension 28
2.3.2 OA equilibrium solubility.....28
2.3.3 Preparation of NS 29
2.3.4 Particle size and polydispersity index (PDI) analysis.....30
2.3.5 FT-IR measurement.....31
2.3.6 Transmission electron microscopy (TEM) 32
2.3.7 Percent encapsulation efficiency (EE %) and saturation solubility 32
2.3.8 Lyophilisation of SEOA NS and free OA solution.....34
2.3.9 Stability Study 34
2.3.9.1 Stability of storage in suspension form.....34
2.3.9.2 OA stability in plasma 34
2.3.9.3 Stability in simulated gastric and intestinal fluids 35
2.3.10 *In vitro* dissolution test 36
2.3.11 Cytotoxicity of OA and SEOA NS 37
2.3.12 Cellular uptake study.....37
2.3.13 Pharmacokinetics study 39
2.3.13.1 Intravenous and oral administration of OA to rats.....39
2.3.13.2 Sample preparation and calibration 40
2.3.13.3 Chromatography and tandem mass spectrometry analysis 41
2.3.13.4 Results analysis.....42
2.3.14. Statistical analysis 43
2.4. Results and discussion 43
2.4.1 Characteristics of SEOA NS.....43
2.4.1.1 Critical micellar concentration (CMC) of SEL and SEP 43
2.4.1.2 Particle size and PDI of different SEOA NS 45
2.4.1.3 Morphology determination by TEM.....48
2.4.1.4 Free OA equilibrium aqueous solubility at 25 ℃, SEOA NS encapsulation efficiency (EE) and saturation solubility 49
2.4.1.5 FT-IR.....53
2.4.1.6 Stability of SEOA NS.....56
2.4.2 *In vitro* dissolution.....57
2.4.3 Cytotoxicity of SEOA NS 60
2.4.4 Cellular uptake of SEOA NS.....63
2.4.5 SEOA NS pharmacokinetics profile.....66
2.4.5.1 Recovery, precision and accuracy in analysis of plasma samples 66
2.4.5.2 Pharmacokinetics results after intravenous administration.....67
2.4.5.3 Pharmacokinetics results after oral administration 67
2.5. Conclusion 73
Chapter 3. Development and evaluation of SEOA NS via wet ball milling optimized by design of experiments (DOE).....75
Chapter 3. Development and evaluation of SEOA NS via wet ball milling optimized by design of experiments (DOE).....76
3.1 Introduction 76
3.2 Materials.....77

3.3 Methods 78
3.3.1 Preparation of SEOA NS by wet ball milling 78
3.3.2 Particle size and polydispersity index analysis 80
3.3.3 FT-IR measurement 80
3.3.4 Transmission electron microscopy (TEM) 81
3.3.5 Percent encapsulation efficiency (EE %) and saturation solubility 83
3.3.6 Lyophilization of SEOA NS and free OA solution 84
3.3.7 *In vitro* dissolution test 84
3.3.8 Stability study 85
3.3.9 Cytotoxicity of OA and SEOA NS 85
3.3.10 Pharmacokinetics study 86
3.3.10.1 Intravenous and oral administration of OA to rats 86
3.3.10.2 Sample preparation and calibration 87
3.3.10.3 Chromatography and tandem mass spectrometry analysis 88
3.3.10.4 Results analysis 89
3.3.11 Statistical analysis 90
3.4 Results and discussion 90
3.4.1 Character of SEOA NS 90
3.4.1.1 Particle size and polydisperse index (PDI) of different SEOA NS formulations 90
3.4.1.2 Morphology of milled NS determined by TEM 94
3.4.1.3 SEOA NS encapsulation efficiency (EE %) and saturation solubility 95
3.4.1.4 FT-IR 96
3.4.1.5 Stability of SEOA NS 100
3.4.1.6 Analysis of the influence of process variables on NS properties 103
3.4.1.6.1.Analysis of particle size influencing factors 103
3.4.1.6.2. Analysis the factors influencing the PDI of NS products 108
3.4.1.6.3 Analysis of the saturation solubility influencing factors 113
3.4.1.6.4 Analysis of physical stability influencing factors 117
3.4.1.6.5 Analysis of chemical stability influencing factors 122
3.4.2 *In vitro* dissolution 129
3.4.3 Cytotoxicity of SEOA NS 131
3.4.4 SEOA NS Pharmacokinetics profile 134
3.4.4.1 Pharmacokinetics results after intravenous administration 134
3.4.4.2 Pharmacokinetics results after oral administration 134
3.5. Conclusion 138
Chapter 4. 140
General conclusions 140
Chapter 4. General conclusions 141
Reference 146

SUMMARY

Background: Oleanolic acid is a poorly water-soluble natural-derived triterpenoid with diverse and important activity, such as hepatoprotective, anti-cancer, anti-inflammatory, hypolipidemia and anti-diabetes etc. However, its application is limited for its low water solubility and poor oral bioavailability.

By reducing the particle size to nano range, nanosuspension has been proven to be one of the most expeditious and cost-effective methods to improve the solubility and bioavailability of poorly water-soluble drugs. Nanosuspension can be produced by top-down or bottom-up method and stabilized by polymer and/or surfactants.

Sucrose esters are a group of nonionic surfactants synthesized by esterification of sucrose with fatty acids. They are widely used in food, cosmetic and pharmaceutical area for their environmental compatibility: ready biodegradability, low toxicity, low irritation to eyes and skin, nontoxic and nonallergenic. Although sucrose esters were found with the ability of producing nanoproducts with little energy input, there were not frequently used in preparing nanoscaled products.

Purpose: The aim of this study was to develop sucrose ester stabilized oleanolic acid nanosuspension to enhance delivery of oleanolic acid by increasing its solubility, bioefficacy and bioavailability. Two manufacturing methods, bottom-up and top-down, would be used to develop sucrose ester stabilized oleanolic acid nanosuspensions. The product characteristics would be evaluated and compared.

Methods: O/W emulsion and organic solvent evaporation method, a bottom-up method, and wet ball milling method, a top-down method, were both used to prepare sucrose ester stabilized oleanolic acid nanosuspension. Designs of experiments were utilized to optimize the multiple parameters in wet ball milling method. The particles' size and polydispersity index were measured by nanosizer. Their percent encapsulation efficiency, saturation solubility and *in vitro* dissolution rate were obtained via HPLC. The *in vitro* bioefficacy was analyzed by MTT measurements in A549 human non-small cell lung cancer cell line. The cellular uptake of oleanolic acid and *in vivo* pharmacokinetics profile were determined using LC-ESI-MS/MS.

Results: Both methods yielded nano ranged particles (around 100 nm in diameter), which were found to be spherical in shape and covered by distinct sucrose ester coating on the periphery by TEM observation. Saturation solubility of nanosuspension prepared via solvent evaporation method and wet ball milling method were both much larger than free drug (3.43 μg/mL). It ranged from 0.66 mg/mL (SEOA91101 NS) to 1.89 mg/mL (SEOA4121 NS) in solvent evaporation method, and 2.08 mg/mL (SEOA-EAC NS) to 5.49 mg/mL (SEOA-HBD NS) in wet ball milling method respectively. However, nanosuspension produced by solvent evaporation method was physically and chemically more stable than that produced by wet ball milling method. The dissolution rate and cytotoxicity were both increased by either of the two methods. Preliminary studies indicated that cellular uptake of SEOA nanosuspension by A549 cells was temperature-, concentration- and time-dependent. The oral bioavailability also gained a big increase, from 6-7 folds (SEOA4121 NS) to 12

folds (SEOA-GBD NS) more than that of oleanolic acid coarse suspension.

Conclusion: Solvent evaporation method and wet ball milling were both successfully in preparing SEOA nanosuspension, providing a novel way to enhance saturation solubility, *in vitro* dissolution rate, bioefficacy and *in vivo* bioavailability of free oleanolic acid and/or other potentially useful hydrophobic drugs.

LIST OF TABLES

Table 1.1 Summary of nanosuspension-based formulations of drugs in market or in different clinical trials, modified from reference (47) **11**

Table 2.1 Detailed compositions of nanosuspension (NS) formulations **31**

Table 2.2 Comparison of SEOA NS properties **47**

Table 2.3 Chemical and physical stability of SEOA NS **55**

Table 2.4 SEOA 4121 NS incubation with rat plasma **56**

Table 2.5 SEOA 4121 incubated in SGF and SIF **57**

Table 2.6 IC_{50} comparison of SEOA NS and free OA **61**

Table 2.7 The recovery, precision and accuracy (n=5) of the assay method **67**

Table 2.8 Oral pharmacokinetics profiles of SEOA NS and coarse suspension **68**

Table 3.1 Detailed settings of SEOA NS made from wet ball milling **82**

Table 3.2 Comparison of size and PDI **93**

Table 3.3 Comparison of OA saturation solubility and EE % **98**

Table 3.4 Physical stability of SEOA NS **101**

Table 3.5 Chemical stability of SEOA NS **102**

Table 3.6 IC_{50} comparison of SEOA-GBD NS and free OA **133**

Table 3.7 Oral pharmacokinetics profiles of SEOA NS and coarse suspension **137**

Table 4.1 character comparison between bottom-up and top-down methods **143**

LIST OF FIGURES

Figure 1.1 Molecular structure of oleanolic acid **3**

Figure 2.1 Chemical structure of sucrose monolaurate (SEL) (a) and sucrose monopalmitate (SEP) (b). **26**

Figure 2.2 Determination of CMC of SEP (a) and SEL (b) by surface tension method. X axis represents the concentrations of the surfactant (%, w/v) and Y axis shows the surface tension readings of surfactant solutions (mN/meter). **44**

Figure 2.3 Representative particle size distribution data obtained from Zetasizer Instrument by the intensity of signal. **46**

Figure 2.4 Representative TEM of SEOA-NS produced by emulsion-organic solvent evaporation method. (c=encapsulated OA; d= thickness of SE coating) **49**

Figure 2.5a HPLC chromatogram of OA showing OA retention time is approximately 6.8 min. 2.5b Calibration curve of OA standards: 0.02, 0.04, 0.06, 0.08, 0.1, 0.2, mg/mL; R2 =0.9983. X axis indicates OA concentration (mg/mL), Y-axis indicates UV absorption. **51**

Figure 2.6 FTIR spectra of pure oleanolic acid (A), lyophilized SEOA4121 NS (B), and blank SEL and SEP mixture (4 : 1, w/w) (C). **54**

Figure 2.7 Dissolution profiles of OA coarse suspension (▲) (suspended in N,N-DMAC : PEG400 : Water at 2 : 4 : 1, v/v/v), SEOA 4121 NS (■) and SEOA 4121 lyophilized powder(◆) (2.7a) and SEOA4121 NS in dialysis bag (▲) (2.7b) in pH 7.4 phosphate buffer solution saline containing 1 % sodium dodecyl sulfate (SDS) (n = 3). **59**

Figure 2.8 Dose- and time-dependent growth inhibition of A549 cells by (a) Free OA dissolved in media containing 0.05 %DMSO, (b) SEOA91101 NS (*, $p<0.05$ between 24 h and 72 h) (c) SEOA4121 NS(*, $p<0.05$ between 24 h and 72 h) (d) blank SE 41 NS (SEL : SEP at 4 : 1 w/w) and blank SE 91 NS (SEL : SEP at 9 : 1 w/w) without OA. *, $p<0.05$ between SE41 24 h and SE41 72 h; #, $p<0.05$ between SE91 24 h and SE91 72 h. Data is presented as mean (μg/mL) ± std from three independent experiments repeated in quadruplicate. **62**

Figure 2.9 Cellular uptake of SEOA NS. (a) Mass peak of OA by LCMS. The left peak is the internal standard and the right one is OA peak. Cellular uptake of SEOA NS is (b) temperature-dependent, (c) concentration-dependent, and (d) time-dependent. Data is presented as mean (μg/mg protein.mL) ± Std from three independent experiments repeated triplicate. *, *p<0.05*; **, *p<0.01*. 66

Figure 2.10 Mass spectra of $[M-H]^-$ of oleanolic acid (a, OA) and glycyrrhetinic acid (b, GA, internal standard) 69

Figure 2.11 Calibration curve of OA standards ranged from 20-2000 ng/mL; R^2 =0.9942 70

Figure 2.12 Mean plasma concentration-time profiles comparison of OA in rats after (a) IV injection at 2 mg/kg (■,n=5), (b) oral administration of OA NS at 10 mg/kg (○, n=5), 20 (■, n=5) mg/kg doses and oral administration of OA coarse suspension (△, n=5, control) at 20 mg/kg dose. Vertical bars represent standard deviation 72

Figure 3.1 Ball mill used for wet milling (Technical specifications: 220 V, 50 Hz, 75 W. Container dimensions (ø) x (H): 7.5 x 6.5 cm). 79

Figure 3.2a Representative particle size distribution data obtained from Zetasizer (Nano-ZS90) Instrument by the intensity of volume. Figure 3.2b Particle size of different SEOA NS. Data is presented as mean (nm) ± Std from three independent experiments repeated triplicate. 92

Figure 3.3 Representative TEM of SEOA NS produced by wet ball milling method. In Figure 3.3a, bar = 200 nm, magnification 15,000 times. In Figure 3.3b, bar = 100 nm, magnification 40,000 times. 95

Figure 3.4 OA saturation solubility in SEOA NS. Data is presented as mean (mg/mL) ± Std from three independent experiments repeated triplicate. 97

Figure 3.5 FTIR spectra of lyophilized SEOA-GBD NS (A), free OA (B) and physical mixture of SEL and SEP at 9 : 1 (w/w) (C). 99

Figure 3.6 Minitab analysis of Particle Size influence factors. Normal Probability Plot of the Standardized Effects (3.6a), Pareto Chart of the Standardized Effects (3.6b), Main Effects Plot (data means) for Particle Sizes (3.6c), Interaction Plot (data means) for Particle sizes between milling speed and SE : OA (3.6d1),. Interaction Plot (data means) for Particle sizes between SE : OA and SEL : SEP (3.6d2), and Interaction Plot (data means)

for Particle sizes between milling speed and SEL : SEP (3.6d3). 107

Figure 3.7 Minitab analysis of PDI influence factors. Normal Probability Plot of the Standardized Effects (3.7a), Pareto Chart of the Standardized Effects (3.7b), Main Effects Plot (data means) for PDI (3.7c), Interaction Plot (data means) for PDI between milling time and SE : OA (3.7d1),. Interaction Plot (data means) for PDI between SE : OA and milling speed (3.7d2), and Interaction Plot (data means) for PDI between SE : OA and SEL : SEP (3.7d3). 112

Figure 3.8 Minitab analysis of Saturation Solubility influence factors. Normal Probability Plot of the Standardized Effects (3.8a), Pareto Chart of the Standardized Effects (3.8b), Main Effects Plot (data means) for Saturation Solubility(four parameters) (3.8c), Main Effects Plot (data means) for Saturation Solubility (two major parameters) (3.8d), and Interaction Plot (data means) for Saturation Solubility (3.8e). 116

Figure 3.9 Minitab analysis of Physical Stability influence factors. Normal Probability Plot of the Standardized Effects (3.9a), Pareto Chart of the Standardized Effects (3.9b), Main Effects Plot (data means) for 30-day size change (3.9c), Interaction Plot (data means) for 30-day size change between milling time and SE : OA (3.9d1),. Interaction Plot (data means) between SE : OA and milling speed (3.9d2), and Interaction Plot (data means) between milling speed and milling time (3.9d3). 121

Figure 3.10 Minitab analysis of 30-day chemical stability influence factors. Normal Probability Plot of the Standardized Effects (3.10a), Pareto Chart of the Standardized Effects (3.10b), Main Effects Plot (data means) for 30-day relative concentration (3.10c), Interaction Plot (data means) for 30-day relative concentration between milling time and SE : OA (3.10d1), and Interaction Plot (data means) between SE : OA and SEL : SEP ratio (3.10d2). 127

Figure 3.11 Response optimization of 30-day physical stability, PDI, particle size, saturation solubility and 30-day chemical stability with optimized conditions in brackets. 128

Figure 3.12 Dissolution profiles of OA coarse suspension (▲) (suspended in N,N-DMAC : PEG400 : Water at 2 : 4 : 1, v/v/v), SEOA-GBD NS (◇) and SEOA-GBD NS lyophilized powder(◆) (3.12a) and SEOA GBD NS in dialysis bag (▲) (3.12b) in pH 7.4 phosphate buffer solution containing 1 % sodium dodecyl sulfate (SDS) (n = 3). 130

Figure 3.13 Dose- and time-dependent growth inhibition of A549 cells by Free

OA dissolved in media containing 0.05 %DMSO, and SEOA-GBD NS.X axis shows OA concentration (μg/mL) and Y shows the percentages of viable A549 cells normalized to that of control (%). 132

Figure 3.14 Mean plasma concentration-time profiles comparison of OA in rats after (a) IV injection at 2 mg/kg (■,n=5), (b) oral administration of OA NS at 10(▲, n=5),20 (■, n=5) mg/kg doses and oral administration of OA coarse suspension (▼, n=5, control) at 20 mg/kg dose. Vertical bars represent standard deviation. 136

ABBREVIATIONS

APIs	**Active pharmaceutical ingredients**
AUC	**Area under the plasma concentration**
$AUC_{0\rightarrow t}$	**Area under the plasma concentration versus time curve**
BCS	**Biopharmaceutics Classification System**
CCl_4	**Carbon tetrachloride**
Cl	**Clearance**
C_{max}	**Maximum plasma concentration**
CMC	**Critical micellar concentration**
COST	**Changing one separate factor at a time**
Cs	**Saturation solubility**
DLS	**Dynamic light scattering**
DMSO	**Dimethyl sulfoxide**
DOE	**Design of experiments**
DSC	**Differential scanning calorimetry**
EE	**Encapsulation efficiency**
EE %	**Percent encapsulation efficiency**
ESE	**Emulsion-solvent evaporation method**
ESI	**Electrospray ionization**
F %	**Absolute bioavailability**
F12K	**F12 Ham Kaighn's modification**

FBS	**Fetal bovine serum**
FDA	**Food and Drug Administration**
GA	**Glycyrrhetinic acid**
GI	**Gastrointestinal**
HEPES	**4-(2-hydroxyethyl)-1-piperazineethanesulfonic acid**
HLB	**Hydrophilic-lipophilic balance**
HPF	**Human pleural fluid**
HPLC	**High performance liquid chromatography**
HRTEM	**High resolution TEM**
HSF	**Human synovial fluid**
IS	**Internal standard**
LC-ESI-MS/MS	**Liquid chromatography-electrospray ionization tandem mass spectrometry assay**
LSW	**Lifshitz–Slesov–Wagner theory**
MRM	**Multiple selected reaction monitoring**
MTT	**Methyl thiazolyl tetrazolium**
NS	**Nanosuspensions**
NSCLC	**Non small cell lung cancer cell line**
OA	**Oleanolic acid**
OVAT	**One variable at a time**
PBMC	**Peripheral mononuclear cells**
PBS	**Phosphate buffered saline**

PCS	**Photon correlation spectroscopy**
PDI	**Polydispersity index**
PTA	**Phosphotungstic acid**
rF %	**Relative bioavailability**
SDS	**Sodium dodecyl sulphate**
SE	**Sucrose ester**
SEL	**Sucrose monolaurate**
SEM	**Scanning electron microscopy**
SEP	**Sucrose monopalmitate**
SGF	**Simulated gastric fluid**
SIF	**Simulated intestinal fluid**
Std	**Standard deviation**
$T_{1/2}$	**Elimination half-life**
TEM	**Transmission electronic microscopy**
TPGS	**D-α-tocopheryl polyethylene glycol 1000 succinate**
WBM	**Wet ball milling**
XRD	**X-ray diffraction analysis**
ΔG	**Gibbs free energy**

CHAPTER 1.

INTRODUCTION

CHAPTER 1: INTRODUCTION

1.1 OLEANOLIC ACID (OA) - A HYDROPHOBIC NATURAL PRODUCT

OA is a poorly water-soluble natural-derived triterpenoid (Figure 1.1). It has a long history of therapeutic use in many Asian countries. In China, it has been marketed as an over-the-counter drug to treat liver diseases. However, the low water solubility of OA limits its bioavailability, and hence, possibly its efficacy.

1.1.1 NATURAL PRODUCTS

Discovery and development of new active pharmaceutical ingredients is always a multidisciplinary effort and is both time and resource consuming process. Recent studies revealed that the average time to discover, develop, and approve a new drug in the United States (US) take approximately 14.2 years, with the estimated cost of US $1.3–$1.6 billion (1). Adams and Branter also claimed that the cost of drug development is $1 billion and it was not an absolute number, however, as there was a substantial variation in drug development expenditure depending on the therapeutic category (2).

Natural products or natural compounds have been the main source of many of the medicines in use. More than 80 % of drug substances discovered were from natural sources or inspired by a natural compound before the era of high-throughput screening (3). Natural products still remain to be the major resource to look for new drugs as almost half of the

drugs approved since 1994 are based on natural compounds (4). From Alan L. Harvey's review, natural products are also found to be averagely more readily absorbed than synthetic drugs (3).

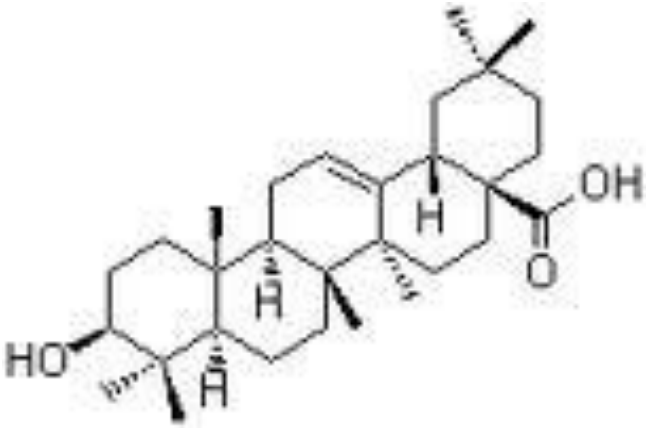

Figure 1.1 Molecular structure of oleanolic acid

However, many nature-derived drug candidates have problem with aqueous solubility. Poor dissolution rates and consequently, low bioavailabilities of these compounds are the consequence of poor aqueous solubility, may result in delays in development or cause the compounds to be dropped from clinical use (5-7). To address this problem, chemically modified derivatives of nature-derived compounds with improved aqueous solubility have been produced (8, 9). Although effective, chemical modification and selection take time as well as the need for expensive toxicological studies and not all nature derived compounds are amenable to chemical modifications (10).

1.1.2 OLEANOLIC ACID PHARMACOLOGICAL EFFECT

1.1.2.1HEPATOPROTECTION EFFECT

The hepatoprotective effects of OA include protection of acute chemically induced liver injury and chronic liver fibrosis as well as cirrhosis (11). OA is still being used either alone or in combination with other hepatoprotective ingredients as oral medications. In China, it is an over-the-counter drug sold for treating liver disease. OA has shown to be effective at alleviating the adverse effects of carbon tetrachloride (CCl_4) consumption by enhancing the hepatic antioxidant defence system (12). It is believed that at the gene level, OA exerted hepatoprotection effect through the dramatic induction of metallothionein (MT) and the nuclear factor E2-related factor 2 (Nrf2) by increasing the expression of genes related to cell proliferation and suppressing the expression of several cytochrome P450 genes, possibly to switch cellular metabolic energy to an acute-phase response mode (13).

1.1.2.2 ANTI-CANCER

OA has been shown to act at various stages of tumour development, including inhibition of tumour genesis, inhibition of tumour promotion, and induction of tumour cell differentiation. It can effectively inhibit angiogenesis, invasion of tumour cells and metastasis (14). In an experiment examining its ability to inhibit the tumour growth and modify haematopoiesis after irradiation, OA showed that it might be effective as an anti-cancer agent and possess the ability to decrease undesirable radiation damages on the hematopoietic tissue

after radiotherapy (15). OA also has been shown to inhibit mouse skin tumour induced by 12-O-tetradecanoylphorbol-13-acetate (16).

1.1.2.3 ANTI-HIV

Based on the research of Kashiwada et al., OA inhibited HIV-1 replication in acutely infected H9 cells with an EC_{50} value of 1.7 μg/mL, and inhibited H9 cell growth with an IC_{50} value of 21.8 μg/mL [therapeutic index (T. I.) 12.8] (17). Mengoni et al. also found that OA inhibited the HIV-1 replication in all the cellular systems used (EC_{50} values: 22.7 μM, 24.6 μM and 57.4 μM for *in vitro* infected human peripheral mononuclear cells (PBMC), naturally infected PBMC and monocyte/macrophages, respectively) by inhibiting the HIV-1 protease activity (18).

1.1.2.4 ANTI-INFLAMMATORY

From experiments carried out by Singh et al., OA displayed anti-inflammatory activity in carrageenan and dextran-induced oedema in rats via reducing exudate volume and inhibiting leukocyte infiltration in carrageenan-induced pleurisy (19). In an *in vitro* study, PC12 cells were used to examine the *in vitro* antioxidative and anti-inflammatory effects of OA. The pre-treatment from OA significantly reduced release of IL-6 and TNF-alpha induced by $H_2O_2^-$ or MPP^+- (20). $sPLA_2$ is a key enzyme in inflammatory reactions. Recent studies showed OA inhibited indirect haemolytic activity and mouse paw oedema by inhibiting of *in vitro* and *in vivo* $sPLA_2$. OA inhibited $sPLA_2$ activities of human synovial fluid (HSF),

human pleural fluid (HPF) and VIPERA RUSSELLI (VRV-PL-V) and NAJA NAJA (NN-PL-I) snake venoms in a concentration-dependent manner (21).

1.1.2.5 OTHER PHARMACOLOGICAL EFFECT

OA showed anti-pruritic effect on pruritic model in mice induced by a compound 48/80 (22). OA demonstrated its spasmolytic activity mediated through blockade of calcium influx (23). It is also reported to possess other pharmacological effects such as hypolipidemia and anti-diabetes (24).

1.1.3 DOSE AND ADMINISTRATION

OA is marketed as oral over-the-counter tablets (Shen Zhen Haiwang Pharmaceutical Ltd. Co., Shen Zhen, Guangdong, China; reference link: http://www.0514zx.com/jiuyizhinan/yaopin/gdyy/200910/623732.html). Each tablet contains 10 mg of OA together with other excipients. The usual oral dose for adult patients with acute hepatitis is 2-4 tablets thrice daily, whereas that of adult patients with chronic hepatitis is 4-8 tablets thrice daily.

1.1.4 BIOAVAILABILITY OF OLEANOLIC ACID

Like other natural compounds, although with diverse effect, and its derivatives CDDO-Me and CDDO-Imm showed promising antitumor activities and are presently under evaluation in phase I clinical studies (25, 26), the application of OA is limited due to its low

bioavailability arising from its low aqueous solubility.

According to the USA FDA Biopharmaceutics Classification System (BCS) Guidance (http://www.fda.gov/AboutFDA/CentersOffices/CDER/ucm128219.htm), OA should fall in the Class IV category because of its low aqueous solubility (4.37 μg/mL) (27) and low permeability (Papp = 1.1–1.3×10^{-6} cm/s in the apical-to-basolateral direction at 10 and 20 μM) (28). As a result, the oral bioavailability values of OA in rats at doses of 25 and 50 mg/kg were as low as 0.7 % (28).

Besides chemical modifications, which is not applicable to all naturally derived compounds, a variety of formulation strategies have been developed to improve the solubility and, thus, the bioavailability of OA and other natural products.

1.2 FORMULATION STRATEGIES OF INCREASING WATER SOLUBILITY AND DISSOLUTION RATE

Solubility, in particular equilibrium solubility, is a quantitative term that describes the concentration of a solute in a saturated solution at a certain temperature. It is defined as the concentration of a compound in solution which is in contact with an excess amount of the solid compound when the concentration in solution do not change over time (29). Solubility can be influenced by a number of physicochemical means such as intrinsic equilibrium solubility or pH alteration, particle size reduction, solid dispersions, emulsions/microemulsions, complexation (e.g. cyclodextrins), liposomes, co-solvent systems, micelles among others.

Low equilibrium solubility of hydrophobic compounds can also be the result of poor dissolution rate. Hydrophobic compounds are usually poorly water-wettable as well. Upon adding to water, the hydrophobic particles often float with minimal wetting, which result in their very slow rates of dissolution. According to Nernst-Brunner equation (30):

$dM/dt = S*D/h*(C_S - C)$

where M is the mass of drug dissolved in time t, C_S is the saturation solubility of the solute, C is the bulk concentration of the solute in the medium at time t, D is the diffusion coefficient of the solute in the dissolution medium, S is the specific surface area of the solids, and h is the stagnant layer thickness.

Dissolution process is defined by a time-dependent differential equation (dM/dt). Two major steps are normally involved in the dissolution of molecules from the solid surface (31). The first step involves the detachment of molecules from the solid surface, which is followed by diffusion of the detached molecule across the diffusion layer adjacent to the solid surface. In most cases, the first step is easily achievable whereas the second step is usually the rate-limiting step that determines the overall dissolution rate. Step two often limits the solubility of hydrophobic compounds.

By changing the solute's intrinsic equilibrium solubility, modification of drug crystal form improves solubility and dissolution rate (32). Using pH-solubility and pH-dissolution rate interrelationships, diffusion layer pH was found to influence solubility and dissolution rates for haloperidol and its two different salt forms, hydrochloride and mesylate (33).The solubility and dissolution rate of a poorly water-soluble drug can also be significantly enhanced by the preparation of solid dispersions (34). Likewise, other formulation methods

achieved success in enhancing the solubility and dissolution rate of water-insoluble drugs. For example, using liposomes (35), emulsions (36), microemulsions (37), micelles (38) and inclusion complexes employing cyclodextrins (39-41) had all been reported to be capable of improving drug dissolution. However, these formulation methods all have their restricted application scope and are not universal in approach, applicable to most poorly water-soluble drugs. Therefore, a formulation strategy which can suit most of hydrophobic drugs is much preferred.

The aqueous solubility, dissolution rate and bioavailability of poorly soluble drugs are often intrinsically related to drugs' particle sizes (42, 43). As indicated in Nernst-Brunner equation, the dissolution rate of a compound can be increased by reduction of particle size which increases the total surface area for dissolution. Therefore, by reducing particle size, nanosuspension (NS) can increase surface area that leads to improved the dissolution rate and of hydrophobic compounds and this is often accepted as one of the most expeditious and effective methods to improve the solubility and bioavailability of poorly water-soluble drugs. For the point of simplicity and efficaciousness, NS preparation confers over other formulation strategies, NS has revealed its potential to be the universal technique to tackle the most of the problems associated with the delivery of poorly water-soluble drugs (44).

1.3 NANOSUSPENSIONS

In more recent years, more and more NS products have come into market or are under clinical trials (Table 1.1). NS refers to a colloidal dispersion of drug nanoparticles that are

produced using by a suitable method (precipitation, pearl milling, or high-pressure homogenization) and stabilized by adjuvants such as polymers and/or surfactants (27, 45, 46). In either method, a high Gibbs free energy (ΔG) is produced with the nanoscaled products. In the formula forwarded by B.E. Rabinow (47), $\Delta G = \gamma s/l \bullet \Delta A$, where γs/l is the interfacial tension and ΔA is the increased surface area. The Gibbs free energy (ΔG) arises because water molecules incur less attractive forces with other water molecules when located at the free solids' surfaces (47). Since the Gibbs free energy is higher, the nanosuspensions formed are thermodynamically unstable and will tend to minimize their total energy by precipitation or agglomeration (48). As indicated by the Rabinow's formula, Gibbs free energy can be lowered down by decreasing the interfacial tension (γs/l), which can be achieved by adding stabilizers (polymers and / or surfactants) to the system. Stabilizers are needed to wet the surface of the hydrophobic surfaces of the drug particles first and then form barriers against agglomeration or precipitation. These barriers include electrostatic coats produced by charged surfactants or steric coats with the non-ionic surfactants or polymers (49).

1.3.1 METHODS OF PREPARATION NANOSUSPENSIONS

In general, NS preparation methods consist two categories. One category can be described as a top-down method, i.e. by breaking of large drug particles into nanosized fragments through milling or homogenization. The other category is bottom-up method, by the build-up of nanoparticles from dissolved drug molecules via precipitation from solution (50).

Table 1.1 Summary of nanosuspension-based formulations of drugs in market or in different clinical trials, modified from reference (47)

Drug	Indication	Pharma Company	Route	Status
Paclitaxel	Anti-cancer	American Pharmaceutical Partners	Intravenous	Phase III
Rapamune (Sirolimus)	Immuno-suppressant	Wyeth	Oral	Marketed
Emend (aprepitant)	Anti-emetic	Merck	Oral	Marketed
Cytokine inhibitor	Crohn's disease	Cytokine PharmaSciences	Oral	Phase II
Diagnostic agent	Imaging agent	Photogen	Intravenous	Phase I/ II
Thymectacin	Anticancer agent	NewBiotics./Ilex Oncology	Intravenous	Phase I/ II
Budesonide	Asthma	Sheffield Pharmaceuticals	Pulmonary	Phase I
Tricor (fenofibrate)	Lipid Lowering	Undisclosed	Oral	Marketed
Fenofibrate	Lipid Lowering	Undisclosed	Oral	Phase I
Busulfan	Anticancer	Supergen	Intrathecal	Phase I
Silver	Eczema, atopic dermatitis	Self-developed	Topical	Phase I
Insulin	Diabetes	Self-developed	Oral	Phase I
Calcium phosphate	Mucosal Vaccine adjuvant for herpes	Self-developed	Oral	Phase I

1.3.1.1 MILLING

NS can be produced by high shear media milling or pearl milling. The milling medium is usually made of glass, zirconium oxide or highly cross-linked polystyrene resin. Nanosized particles were broken down from micron-sized drug particles by the energy generated from the impaction of the milling media with drug at high energy and shear forces supplied during milling process (44) .

Liversidge et al. first introduced and patented the pearl milling technology (51) and it was later acquired by Elan Drug Delivery Company. The pearl mill generally consists of a stainless steel vessel filled with steel, glass or hard polystyrene balls. The mill operates by moving the balls with an impeller while keeping the vessel either static or with movements while the balls inside also move. Advantages of pearl milling include suitability for most drugs with poor solubility, usable for both aqueous and organic media, easy to scale up, little batch-to-batch variation and narrow size distribution of the final nanosized products (44).

However, the milling methods associated with high energy input and are regarded as being highly inefficient (52). Considerable amount of heat is generated which may cause degradation of heat sensitive active pharmaceutical ingredients (APIs). Milling has also been shown to cause mechanical activation at drug particle surfaces (53). One of the other major concerns is the potential erosion of the milling media and the contribution to product contamination hazard (54).

1.3.1.2 HOMOGENIZATION

The two most frequently reported homogenization methods are the microfluidizer technology and piston gap high pressure homogenization.

The microfluidizer technology can generate small particles by a frontal collision of two fluid suspensions under high pressures (55). The high speed collisions of sprayed suspension lead to particle collisions with high shear forces as well as cavitation forces (56). Surfactants are required to stabilize particles produced at the desired particle size. The disadvantages of this method are the relatively large size distribution of particles produced and a high number of cycles needed for a sufficient particle size reduction to occur (57).

Another technology used is the piston gap high pressure homogenization method. This patented technology is also referred as the Dissocubes technology developed and patented by Muller et al. (58) and technology owned by SkyePharma PLC. In this homogenization method, the NS particles are produced in water at room temperature. A drug powder is first dispersed in an aqueous surfactant solution and subsequently forced by a piston through the tiny homogenization gap with pressures ranging up to 4000 bars (57).

Homogenization methods have the similar advantages like milling and they include flexibility in handling drug in quantities ranging from 1 to 400 mg/mL (59) , ease of scale-up, little batch-to-batch variation (60), suitable for drugs with poor solubility in both aqueous and organic media, and narrow size distribution of the nanoparticulate drug among others (44).

The main concerns of homogenization for preparing NS are the use of water which may contribute to the hydrolysis effect on water-sensitive drugs (57) and the prerequisite of

suspension formation using high-speed mixers before processing by homogenization (44).

1.3.1.3 BOTTOM-UP METHOD

As reported by B. Van Eerdenbrugh et al. (49), among all the products that were approved by the United States Food and Drug Administration (FDA) from the year 2000 onwards, of all five registered products are based on top-down approaches, four relied on media milling and one by high pressure homogenization (49). Although the bottom-up approaches hold tremendous potential with respect to improving bioavailability by making products of smaller particle sizes and amorphous drug particles, no commercial application of these systems has yet been realized (61).

By the bottom-up approach, the drug is first dissolved in an organic solvent and is then precipitated on addition of an anti-solvent in the presence of a stabilizer. Various adaptations of this approach include: (i) solvent–anti-solvent method; (ii) supercritical fluid processes; (iii) spray drying; and (iv) emulsion–solvent evaporation (47). The method of manufacture can significantly impact the formation and stability of NS and hence their overall performance (62).

The main advantages include preparation methods that are relatively simple to carry out and do not require expensive equipment, and relatively easy to scale up. The main disadvantages of these approaches are related to the use of organic solvents in preparation giving rise to concerns association to toxicity of organic solvents as well as difficulties of their completely removal (44). Any residual solvent can cause physical and chemical

instability of the formulation. This may partially explain why bottom-up method is not as frequently used as the top-down method. However, compared with either milling or homogenization, bottom-up method does not require as much energy or generate as much heat, which can be problematic for unstable or heat sensitive drug. With lower toxicity and / or improved technique, it may be promising to prepare NS using the bottom-up method.

1.3.2 NANOSUSPENSIONS CHARACTERIZATION

A prerequisite for the development of optimized NS is the availability of precise characterization procedures. The frequently analysed characteristic parameters for NS are described in the following discussions.

1.3.2.1 MEAN PARTICLE SIZE AND PARTICLE SIZE DISTRIBUTION

The mean particle size and the width of particle size distribution are important attributes and are also related to factors such as saturation solubility, dissolution velocity, physical stability and even biological performance of NS. It has been reported by Muller and Peters (63) that saturation solubility and dissolution velocity showed considerable variations with the changing particle size of the drug.

Dynamic light scattering (DLS) together with photon correlation spectroscopy (PCS) are most popular techniques for determining the particle size and size distribution of sub-micron particles. DLS is fast and suitable for screening a large quantity of samples with the

measuring range from 0.02-2,000 μm (64). PCS is also fast but with a narrower sizing range, for particles affected by Brownian motion, from 0.02-3 μm (65).

1.3.2.2 PARTICLE MORPHOLOGY AND CRYSTALLINE STATE

It is helpful to understand the morphological or polymorphic changes during nanosizing by the particle morphology and crystalline state assessments.

In order to obtain the actual particle morphology, scanning electron microscopy (SEM) (66, 67) or transmission electron microscopy (TEM) (68, 69) can be applied. Magnification in a SEM can be ranged from about 10 to 500,000 times. TEM's observation magnification capability can range from 80 to 1 million times. High resolution TEM (HRTEM) can magnify even further, to above 50 million times (70).

It is also vital to investigate the extent of amorphous state during the preparation of NS. The changes in the physical state of the drug particles as well as the extent of the amorphous fraction can be determined by x-ray diffraction analysis (XRD) (71, 72) and findings can be supplemented by measurements using the differential scanning calorimetry (DSC) (67, 73).

1.3.2.3 SATURATION SOLUBILITY

As discussed, NS has the ability to improve the saturation solubility of hydrophobic drugs, the determination of the saturation solubility as well as the increase in saturation solubility remains an important investigational parameter. The amount of dissolved drug after equilibrium can be quantified usually by either ultraviolet spectroscopy or high pressure

liquid chromatography.

1.3.2.4 *IN VITRO* DISSOLUTION RATE AND *IN VIVO* PHARMACOKINETICS PROFILE

The determination of dissolution rate is very important for anticipating any possible change in the *in vivo* performance (pharmacokinetics and bioavailability) of the drug product (74, 75).

Since low drug solubility, slow dissolution rate and poor oral bioavailability are generally associated with poorly formulated drug products, there is the impetus to improve drug formulation to produce drug products that are readily bioavailable. According to Ostwald-Freundlich's equation, $\log (Cs/C\alpha)= 2\sigma V/(2.303RT\rho r)$, where Cs is the saturation solubility, Cα is the solubility of the solid consisting of large particles, σ is the interfacial tension of substance, V is the molar volume of the particle material, R is the gas constant, T is the absolute temperature, ρ is the density of the solid and r is the radius. By decreasing the particle size (r), NS can increase the saturation solubility of OA (Cs).When the nanoscaled drug particles are presented with dramatic increase in surface area, the drug's solubility and dissolution rate will be enhanced, and hence, high oral bioavailability can be possible.

Sigfridsson et al. (74) found that with the reduction of particle size from 12 μm (in microsuspensions) to 190 nm (in nanosuspensions), the poorly soluble drug UG558 showed a big increase in dissolution rate, absorption rate and bioavailability. The dissolution rate and bioavailability of fenofibrate were also shown to be obviously enhanced when formulated as

a nanosuspension (76).

1.3.2.5 STABILITY

As mentioned earlier, a high Gibbs free energy (ΔG) with the nanosuspensions formed caused the nanoparticles present to be thermodynamically unstable and tended to minimize their total energy by precipitation or agglomeration (48). In their suspended state, the stability issues of nanosuspensions can be both physical (e.g. Ostwald ripening) and chemical (e.g. hydrolysis) (49).

In the classical theory of Ostwald ripening, the ripening rate can be calculated using Lifshitz–Slesov–Wagner (LSW) theory (77, 78): $\omega = \frac{dr_N^3}{dt} = \frac{8}{9}[C(\infty)\gamma V_m D/\rho RT]$

where ω is the Ostwald ripening rate, r_N is the droplet radius, C(∞) is bulk solubility (i.e., the molecular concentration that is in thermal equilibrium with a macroscopic bulk phase), γ is the interfacial tension, V_m is the molar volume of the dispersed compound, ρ is the density of the dispersed phase, D is the diffusion coefficient in the solvent, R is the gas constant and T is the temperature (K).

As the suspension form is not stable, NS is usually stored as a more stable solid form by either spray drying or freeze drying. However, some short term stability is also important as otherwise it may be very problematical when the NS needed further *in vivo* or *in vitro* analysis. The most extreme example is hydrosols developed by Gassmann et al. (79). Hydrosols developed were colloidal aqueous suspensions containing drug nanoparticles of

poorly water-soluble drugs for intravenous administration. They were stabilized by “short term stabilizers” agents such as poloxamer and modified gelatines and were stable for only about 60 min. To prevent crystallization from occurring, the hydrosols were immediately spray dried after production with excipients such as lactose or mannitol and spray dried products reconstituted with water just before use.

The frequently measured short-term stability of products reported ranged from within 7 days (80), within 14 days (81) to within 30 days (82, 83).

1.3.3 STABILIZERS IN PREPARATION OF NANOSUSPENSIONS

Stabilizers used in preparation of NS can be classified into two main categories.

(a) Electrostatic stabilizer: charged surfactants or polymers, such as isotactic poly(4-methyl-1-pentene) (84) and sodium dodecyl sulfonate (85, 86) among others. (b) Steric stabilizer: non-ionic surfactants or polymers, such as poloxamers (87), Tween 80 (88, 89), hydroxylpropylmethyl cellulose and hydroxylpropyl cellulose (90) among others.

Combinations of more than one stabilizers have at times been preferred for enhanced long-term stability (91). Unlike nonionic materials (steric stabilizers), which stabilize NS by the steric effect, ionic surfactants and polymers (electrostatic stabilizers) stabilize the NS system by electrostatic action or, depending on the molecular weight (chain length), by electrosteric action (92).

Electrostatic stabilizers are effective in aqueous environment, but may become less effective in dry state for the ionized state is not maintained (93). They are also sensitive to changes in pH and ionic strength. By comparison, steric stabilizers are superior in being less

sensitive to electrolyte additions, and are equally efficient in both aqueous and nonaqueous environments (92).

1.4 SUCROSE ESTER AS STABILIZERS IN PREPARATION OF NANOSUSPENSIONS

Sucrose ester (SE) is a group of nonionic surfactants synthesized by esterification of sucrose, the hydrophilic head, with fatty acids.

SEs are widely used in food and cosmetic industries. Tual et al. found that with the recipe and manufacturing process used to produce dairy foams, sucrose ester was important in manufacture and storage dairy foams (94). SEs were also found useful in stimulating peptide YY release in the distal intestine and inhibiting protein-induced pancreatic secretion in pancreatico-biliary diverted rat model (95). The research investigations carried out by Calderilla-Fajardo et al. showed that nanoemulsions formulated with sucrose laureate exhibited the highest penetration in the stratum corneum (96).

Besides the application in food and cosmetic areas, SEs are also important excipients in preparing pharmaceutical formulations. SEs have been used to prepare micelles in increasing solubility of timobesone acetate (97). The bioavailability of superoxide dismutase was improved when encapsulated in reverse micelles prepared by poly (epsilon-caprolactone) and SE (98). SEs was also reported to aid in the preparation of microemulsions (99, 100). In transdermal drug delivery, Ayala-Bravo et al. found that as penetration enhancers, combination of sucrose esters (oleate or laureate) and transcutol was able to temporally alter

the stratum corneum barrier properties and promoted penetration of 4-hydroxybenzonitrile (101). Cazares-Delgadillo et al. discovered that sucrose laureate enhanced the transdermal flux of the ionized form of lidocaine and sucrose oleate promoted permeation of the unionized lidocaine (102).

The broadness of the SE application may be aroused by the fact that SE can be synthesized with an extremely wide range of hydrophilic-lipophilic balance (HLB) values, i.e., HLB 1–18 (103).

Biodegradability is a critical factor for ensuring that the concentrations of surfactants or polymers remain below deleterious levels. In contrast with petrochemically derived surfactants, those derived from food sources such as SEs are attractive because of their environmental compatibility: ready biodegradability, low toxicity, low irritation to eyes and skin, nontoxic and nonallergenic (104-106). This factor becomes even more apparent in the preparation of nanoscaled products where it is usual to require much larger amounts of surfactants to stabilize the markedly increased specific surface area. Thus, the availability of an environmentally compatible, nontoxic surfactant may be of greater interest to stabilize nanonized particles (107).

Producing nanoscaled products are often associated with the input of high energy and shear forces, which is of concern to the chemical and physical stability of final product, and amount of drug incorporation (108). SEs were found to have the capability to produce nanosized, physiologically acceptable dispersions only by the application of gentle heat with moderate shear stress (109).

As a consequence, SE stabilized nano products may be prepared easily and with less

worry of the final product toxicity. However, despite these favourable amenities, SEs had been overlooked as stabilizers in preparation of nanoparticles or nanosuspensions till recent years (107, 109-113). Some possible reasons for this are the relative lack of SE manufacturers and difficulties to secure high purity SE samples.

1.5 AIMS AND OBJECTIVES

Although NS is a good method to enhance the saturation solubility and oral bioavailability of natural compounds, there is very little research on developing OA NS. Chen et al. (27) have reported preparing OA NS stabilized by using polysorbate 80 with 6-fold increase in saturation solubility but oral bioavailability was not determined. There are only a few literature reports on the pharmacokinetics profile of OA *in vivo* (28, 114, 115). Jeong et al. (28) first published the oral bioavailability of OA suspension in rats and it was as low as 0.7 %.

Specific objectives of this present study were designed to address the knowledge gaps and they are listed below.

(a) Investigation of the characteristics (including *in vitro* dissolution rate) of OA NS stabilized by blended SEs using top-down and bottom-up methods

(b) Since OA was reported to possess anticancer property (14, 116) and Gao et al. (117) had reported that OA showed weak cytotoxicity effect against A549 cell line, the bioefficacy would also be examined by comparing the cytotoxcity of both free and nanosized OA using the A549 cell line.

(c) With the liquid chromatography-electrospray ionization tandem mass

spectrometry assay (LC-ESI-MS/MS) modified from the method used by Song and Jeong (28, 115), comparison would be on the *in vivo* pharmacokinetics profile with OA NS and OA coarse suspension. By this method, the intracellular OA concentration change can also be monitored to determine its cellular uptake manner.

(d) Comparisons of the top-down and bottom-up approaches will be made for evaluating the effects of the preparation methods on nanosuspension properties

This present research is the first reported study for employing SEs as main stabilizer when preparing NS of OA. Our hypothesis is by formulating OA into nanosuspension form, it can have better saturation solubility, bioefficacy and bioavailability. The results of this study would provide a clearer understanding of the significance and impact of the formulation method for enhancing saturation solubility, dissolution rate and bioavailability of hydrophobic natural compound. This study would also provide the opportunity to enable the study of the pharmaceutical application of a water-insoluble natural compound which would have otherwise be deemed as unsuitable during the screening stage based on the compound's water insolubility.

CHAPTER 2.

DEVELOPMENT AND EVALUATION OF SEOA NS VIA EMULSION-SOLVENT EVAPORATION METHOD

CHAPTER 2. DEVELOPMENT AND EVALUATION OF SEOA NS VIA EMULSION-SOLVENT EVAPORATION METHOD

2.1 INTRODUCTION

SE group contains a series of nonionic surfactants prepared by esterification of sucrose with fatty acids of different chain lengths. From the chemical structures as shown in Figure 2.1, the fatty acid chain of sucrose monolaurate (SEL) possesses 11 alkyl groups while that of sucrose monopalmitate (SEP) has 15 alkyl groups. Although both SEs are hydrophilic nonionic surfactants, with shorter fatty acid chain, SEL (HLB: 15, xLogP3: 1.5) (118) is more hydrophilic than SEP (HLB: 13, xLogP3: 3.2) (119). The term, xLogP3 refers to the logarithm of the ratio of concentrations of the unionized solute in octanol and water, calculated by XlogP version 3 software (120). NS stabilized with blended SEL and SEP may exert synergistic advantage over single SE as the stabilizer surfactant.

Both SEL and SEP are potentially important surfactants especially in pharmaceutical product development research. They have shown to possess good abilities in enhancing the solubility and absorption of hydrophobic compounds. Experiments by Lerk (121) showed that numerous poorly water-soluble drugs could be solubilised by aqueous sucrose laureate solutions at high concentrations, and solubilisation procedures were uncomplicated. In determining the ability of surfactants to enhance the absorption of digoxin and celiprolol *in vitro,* the efficacy of surfactants tested were found to be: SEL > polysorbate 20 > d-α-tocopheryl polyethylene glycol 1000 succinate (TPGS) > polysorbate 80 (122). Henry et al. (123) found the optimal formulation for the sub-micron emulsion with SEL, SEP and

other surfactants, would minimize droplet size during processing and minimize or prevent Ostwald ripening.

a. b.

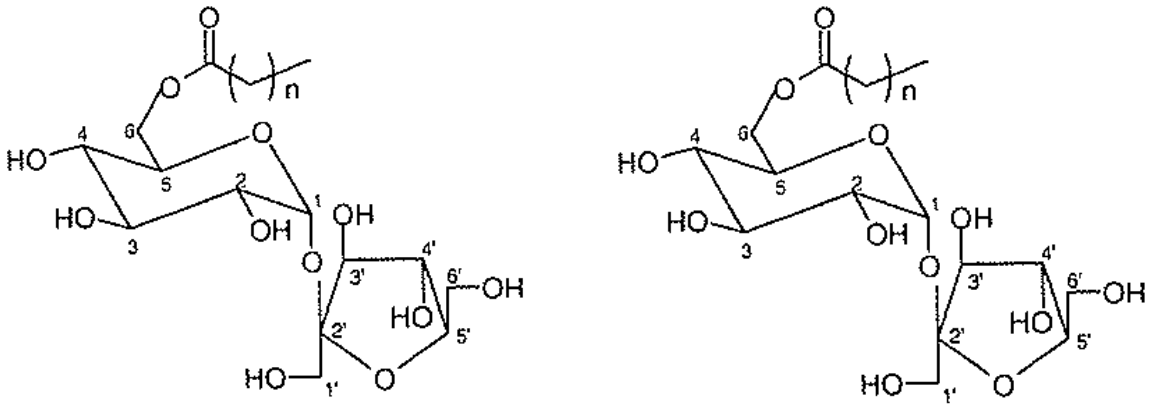

Sucrose monolaurate (n=10) Sucrose monopalmitate (n=14)

Figure 2.1 Chemical structure of sucrose monolaurate (SEL) (a) and sucrose monopalmitate (SEP) (b).

SEL was also found to be helpful in fabricating micelles used to solubilise the water-insoluble drug, sodium diclofenac (124).

However, there are very few reported literature studies on nanoscaled products produced using either SEL or SEP (96, 123). In comparison with top-down preparation methods, the bottom-up method does not require as much energy or heat and hence is more suitable for unstable or heat sensitive drugs. However, bottom-up methods are not as frequently used as top-down techniques. With lower toxicity and / or improved technique, the bottom-up method may become the promising alternative as a technique to prepare NS of poorly water-soluble drugs. To meet the increasing needs of biocompatible and low toxicity surfactants for the

production of nanosized drugs, this study was proposed with one of the aims to study the preparation of SE stabilized OA NS by the emulsion-solvent evaporation method, a bottom-up technique.

Many organic solvents can be used in emulsion-solvent evaporation method including acetone (125, 126), chloroform (127, 128) and dichloromethane (129, 130). As the residual content of the more toxic organic solvent was a main concern of this method, the lower toxicity of acetone was deemed as a more favourable choice of organic solvent for adoption as the organic solvent to use.

2.2 MATERIALS

OA was purchased from Nanjing Qinze Pharmaceutics (Nanjing, China). SEL (batch M07A001, 90 % purity) and SEP (batch M07C003, 90 % purity) were donated by Compass Foods (Singapore). Methyl thiazolyl tetrazolium (MTT) and F12 Ham Kaighn's modification (F12K) medium were purchased from Sigma Aldrich (St. Louis, MO, USA). A549 human non-small cell lung cancer cell line (NSCLC) was purchased from American Type Culture Collection (Rockville, MD, USA). Foetal bovine serum (FBS) was purchased from Hyclone Laboratories (Logan, UT, USA). 4-(2-hydroxyethyl)-1-piperazineethanesulfonic acid (HEPES) was purchased from Applichem (Darmstadt, Germany). MilliQ water (18.2 MΩ cm at 25 ℃) was obtained from a Millipore Direct-Q ultra-pure water system (Billerica, MA, USA) and used throughout the study as the water used, unless otherwise mentioned.

2.3 METHODS

2.3.1 CRITICAL MICELLAR CONCENTRATION (CMC) DETERMINATION BY SURFACE TENSION

The air/water surface tension measurements of SEL and SEP solutions were determined at 20 ℃ with a tensiometer (Torsion Balance Supplies, Alcester, Warwickshire, UK) equipped with a 4 cm circumference platinum ring. Surfactant solutions (from 0.0005 to 0.2 g, %) were prepared in double distilled deionized water and equilibrated at room temperature for 24 h before use. The surface tension of purified water was measured and found to be 72 mN/m at 20 ℃. The critical micellar concentration (CMC) of SE was determined graphically by the plot of surface tension (mN/m) versus the concentration of the detergent. The CMC was read off from the intersection of two straight lines, one from the descending part of the curve, and the other, through the levelled part of the curve.

2.3.2 OA EQUILIBRIUM SOLUBILITY

Equilibrium solubility of OA was determined by saturation shake-flask method according to the US Pharmacopoeia (USP) XXI (United States Pharmacopeia Convention, Inc., Rockville, MD, USA, 1985). The drug was added to distilled water until excess undissolved drug appeared which indicated that the solution had reached its saturated solubility. Briefly, excess drug was added to conical tubes, each filled with 50 mL distilled water, shaken at 100 rpm at 25 ℃ for 24 h, and observed for the presence of any undissolved

drug. If no drug crystals were detected, more drug was introduced and the process repeated until undissolved drug crystals appeared and remained undissolved after prolonged agitation. The saturated amount of dissolved drug was determined by filtering an aliquot through a 0.22 μm filter and assaying the supernatant solution using high performance liquid chromatography (HPLC) assay as according to the USP prescribed procedure.

2.3.3 PREPARATION OF NS

NS trials were prepared by emulsion-organic solvent evaporation method, adapted from the report by Chen et al. (27). In brief, SEP or / and SEL was / were dissolved in 30 mL water in a 50 mL beaker with a magnetic bead at room temperature. The aqueous solution was stirred at 800 rpm on a stir plate (Sybron, East Lyme, CT, USA) for about 30 min until all the surfactant(s) added was(were) completely dissolved. OA in 15 mL acetone was next added to the solution. The resulting o/w emulsion was stirred at 800 rpm overnight in a fume hood under a small jet of nitrogen to facilitate diffusion and evaporation of the organic solvent. This action resulted in nanoprecipitation and the formation of NS. In the last step of the preparation, precipitated materials including OA NS, free OA and SE were suspended in same volume of water (30 mL) and stirred for 24 h. Next, the suspension, with excess undissolved material, was centrifuged at13, 000 g for 10 min. The centrifuged supernatant was filtered through a 0.22 μm membrane to give a visually clear NS. The resulting NS was used immediately for determination of OA saturation solubility and percent encapsulation efficiency (EE %). Detailed compositions of various SEOA NS are shown in Table 2.1.

2.3.4 PARTICLE SIZE AND POLYDISPERSITY INDEX (PDI) ANALYSIS

Dynamic light scattering (DLS) measurements were performed on Zetasizer-3000 (Malvern Instruments, Malvern, UK) at a wavelength of 532 nm. The scattering angle was fixed at 90° and the temperature of the sample was maintained at 25 ℃. Particle size and PDI determination were carried out using a diluted suspension by adding 4 times of its volume with MilliQ water.

Table 2.1 Detailed compositions of nanosuspension (NS) formulations

Group	SEL (mg)	SEP (mg)	OA (mg)
SELOA	250.00	0.00	25.00
SEPOA	0.00	250.00	25.00
SEOA 91101	225.00	25.00	25.00
SEOA 9121	225.00	25.00	125.00
SEOA 9151	225.00	25.00	50.00
SEOA 4121	200.00	50.00	125.00
SEOA 4151	200.00	50.00	50.00
SEOA 2151	167.00	83.00	50.00

SELOA (SEL : OA at 10 : 1, w/w), SEPOA NS (SEP : OA at 10 : 1, w/w), SEOA91101 NS (SEL : SEP at 9 : 1, w/w; SE : OA at 10 : 1, w/w), SEOA9121 NS (SEL : SEP at 9:1, w/w; SE : OA at 2 : 1, w/w), SEOA9151 NS (SEL : SEP at 9 : 1, w/w; SE : OA at 5 : 1, w/w), SEOA4121 NS (SEL : SEP at 4 : 1, w/w; SE : OA at 2 : 1, w/w), SEOA4151 NS (SEL : SEP at 4 : 1, w/w; SE : OA at 5 : 1, w/w), SEOA2151 NS (SEL : SEP at 2 : 1, w/w; SE : OA at 5 : 1, w/w).

2.3.5 FT-IR MEASUREMENT

Pure oleanolic acid, blank SEL and SEP mixture (4 : 1, w/w) and lyophilized SEOA4121 NS were analysed using a FT-IR Spectrometer (PerkinElmer Spectrum 100 Series, Norwalk, CT, USA). Samples were mixed with anhydrous potassium bromide (1 : 100) and ground in a mortar and then pressed in a hydraulic press (14 tons) to small discs. The discs were placed under the infrared beam and the FT-IR spectra were collected in a spectral region between 4000 and 450 cm^{-1}.

2.3.6 TRANSMISSION ELECTRON MICROSCOPY (TEM)

Copper grids were coated with 0.25 % Formvar film and carbon in sequence.

The film faces of the grids were applied with the NS sample and stained with 5 % phosphotungstic acid (PTA) subsequently. Excess suspension was carefully blotted off during each step. After drying for over 10 min under a bench top lamp, the sample was ready for use. TEM photomicrographs were obtained using a transmission electron microscope (JEM 2010, JEOL, Tokyo, Japan) operated at 200 kV.

2.3.7 PERCENT ENCAPSULATION EFFICIENCY (EE %) AND SATURATION SOLUBILITY

HPLC analysis was carried out on an Aglient model 1100 (Agilent, Palo Alto, CA, USA) using a C18 column (ODS 5 μm, 3.9 mm x 150 mm; Waters, Milford, MA, USA) with 65 % acetonitrile and 35 % MilliQ water as the mobile phase. Column temperature was set at 24 ℃. Flow rate was 1 mL/min and UV detection wavelength was 210 nm. Standard samples were dissolved in methanol. Each freshly prepared NS sample was dissolved in at least 5 times its volume of methanol to ensure that OA was fully dissolved and fell within the standard calibration curve. All samples were filtered through 0.22 μm membranes before measurements. The calibration curve over the concentration range of 0.02–0.20 mg/mL was constructed by plotting the peak area of the analyte against the concentration spiked for each

media. Six independently weighed concentrations (0.02, 0.04, 0.06, 0.08, 0.10, 0.20 mg/mL) were used to obtain the calibration plot. The linearity of the assay procedure was determined by calculation of a regression line. Each standard, i.e. 20, 40, 60, 80, 100 or 200 μg/mL, was tested respectively with five repetitions for each concentration.

The precision of the HPLC method was assessed by carrying out repeatability and intermediate precision tests. The repeatability was evaluated by analysing ten solutions containing a known quantity of analyte. The inter-day precision was assessed by testing three concentrations (40, 60 and 100 μg/ml) over 3 consecutive days.

The accuracy of the method was checked for three known concentration levels (40, 60 and 100 μg/ml) and peak area was recorded. All analyses were repeated six times, and the recoveries and respective standard deviations were calculated.

Concentrations of OA in diluted SEOA NS samples were obtained from the resulting peak areas and the regression equation of the calibration curve. Saturation solubility of OA was calculated from the amount of OA dissolved in diluted sample multiplied by the dilution factor. For calculation of the EE % of OA, the following equation was used,

$$EE\ \% = OA_{NS} / OA_{T} \times 100\ \%$$

where, OA_{NS} indicates amount (mg) of OA in NS and OA_{T} indicates total amount (mg) of OA added during formulation.

2.3.8 LYOPHILISATION OF SEOA NS AND FREE OA SOLUTION

SEOA NS and free OA solution were frozen at -80 ℃ overnight and then freeze dried (Labconco Corp., Kansas City, MO, USA) for 24 h at -70 ℃ and 0.02 mbar.

2.3.9 STABILITY STUDY

2.3.9.1 STABILITY OF STORAGE IN SUSPENSION FORM

From our preliminary study, the nanosuspensions stored at 37 ℃ and room temperature were found not to be stable, so the effects of storage time on the chemical and physical stability of SEOA NS were investigated at 4 ℃. Chemical stability was measured as the dissolved OA concentration changes in NS after storage at 1 month and 3 months intervals (after filtration) by HPLC. Physical stability was determined by the extent of particle size changes of SEOA NS after storage at 15 days and 30 days intervals. All experiments were in triplicates, and results averaged.

2.3.9.2 OA STABILITY IN PLASMA

SEOA4121 NS (SEL : SEP at 4 : 1, w/w; SE : OA at 2 : 1, w/w) was diluted with 60 x volumes of normal rat plasma, vortexed (1 min) and incubated in a shaking water bath (100 rpm) at 37 ℃. Samples were removed at 0, 1, 2, 4 and 24 h after incubation and centrifuged

(13,000 g x 10 min). Supernatant (50 μL) of each sample was removed and placed into a new tube. Ethyl acetate (1 mL) containing 1000 ng glycyrrhetinic acid (GA) as the internal standard (IS) was then added, vortexed (1 min) and centrifuged (13,000 g x 10 min). The supernatant was carefully removed, dried under nitrogen flow for 1 h at 40 ℃ and reconstituted in 1 mL methanol for LC-ESI-MS/MS measurement. The LC-ESI-MS/MS analysis method will be discussed in Section 2.3.13.3 Chromatography and tandem mass spectrometry analysis. All experiments were in triplicates, and results averaged.

2.3.9.3 STABILITY IN SIMULATED GASTRIC AND INTESTINAL FLUIDS

Non-enzyme simulated gastric fluid (SGF, pH 1.2) and simulated intestinal fluid (SIF, pH 6.8 and 7.4) were prepared following USP 29 (United States Pharmacopeia Convention, Inc., Rockville, MD, USA, 2006) with modification. SGF was prepared by dissolving 2 g of sodium chloride in 0.2 N hydrochloric acid and diluting with sufficient distilled water to make a 1000 mL solution and adjusting pH to 1.2 ± 0.1. SIF was prepared by dissolving 6.8 g of monobasic potassium phosphate in 250 mL distilled water, mixing and adding 77 mL of 0.20 N sodium hydroxide. The resulting solution was adjusted with either 0.2 N sodium hydroxide or 0.2 N hydrochloric acid to pH 6.8 ± 0.1 and 7.4 ± 0.1 and made up with distilled water to 1000 mL.

One millilitre SEOA4121 NS was separately diluted with 10 x volumes of SGF (pH 1.2) and SIF (pH 6.8 and 7.4), vortexed (1 min), and incubated in a shaking water bath (100 rpm)

at 37 ℃. Samples were removed after 0, 0.5, 1, 2, 4 and 24 h incubation, and centrifuged (13,000 g x 10 min) and supernatant (50 μL) of each sample was transferred to a new tube for lyophilisation and subsequent dilution for HPLC analysis. All experiments were in triplicates, and results averaged.

2.3.10 *IN VITRO* DISSOLUTION TEST

Dissolution experiments were carried out using a dissolution apparatus (Model 2100c; Distek, North Brunswick, NJ, USA) according to the USP 29 Apparatus 2 (United States Pharmacopeia Convention, Inc., Rockville, MD, USA, 2006). The dissolution medium was 500 mL pH 7.4 phosphate buffered saline containing 1 % sodium dodecyl sulphate (SDS), thermostated at 37 ± 0.5 ℃ with 100 rpm paddle rotating speed. SEOA 4121 NS, SEOA 4121 NS lyophilized powder, OA coarse suspension (suspended in N,N-DMAC : PEG400 : water in the ratio of 2 : 4 :1, v/v/v) and SEOA4121 NS in dialysis bags (MWCO 2,000; Spectrum Medical Industries Inc, Singapore) were all added into the dissolution media, each bag contained an estimated amount equivalent to 8 mg OA. Samples (3 mL) were withdrawn at predetermined time intervals and filtered through 0.22 μm filters. After each withdrawal, an equal volume of the dissolution medium was added to maintain the volume constant. The content of dissolved OA was determined using HPLC. All dissolution experiments were performed in triplicates, and all sample analyses were carried out in triplicates, and results averaged.

2.3.11 CYTOTOXICITY OF OA AND SEOA NS

A549 human NSCLC cells were cultured in F12 Ham Kaighn's modification (F12K) medium, supplemented with 10 % FBS, 10 mM HEPES, 100 U/mL penicillin G and 100 µg/mL streptomycin. The cells were maintained at 37 ℃ in a 5 % CO_2 humidified incubator. To determine cytotoxicity of OA and SEOA NS, A549 cells were seeded in 96-well plates at a density of 6 x 10^3 cells per well and incubated for 24 h at 37 ℃ in a 5 % CO_2 humidified incubator. Culture media were then removed and replaced with 100 µL fresh media (blank) or fresh media containing 0.5 % Dimethyl sulfoxide (DMSO) (control) or different concentrations of OA (in media with 0.5 % DMSO) or SEOA NS or the same ratio blank SE NS without OA. After 24 and 72 h incubation, 10 µL MTT solution (5 mg/mL in Phosphate buffered saline (PBS)) was added to each well. After incubation at 37 ℃ for 4 h, the mixtures in the wells were removed, and 110 µL DMSO was added to each well and shaken at 100 rpm for 30 min. Absorbance was measured using a multiplate reader (Molecular Devices, Sunnyvale, CA, USA) at 590 nm. Proliferation rate (%) was calculated as ((sample reading-blank reading) / (control reading-blank reading)) × 100.

2.3.12 CELLULAR UPTAKE STUDY

A549 cells (100,000 cells/mL) were seeded into each well of the 6-well plates (Falcon; Becton Dickinson, Sparks, MD, USA) and allowed to attach for 24 h. After cell attachment, the cell culture media were replaced with fresh media containing different concentrations of

SEOA NS. After incubation for 1 and 3 h respectively, the cells were washed thrice with cold PBS (4 ℃, pH 7.4, 10 mM). The cells were then lysed by incubating with 0.2 mL cell lysis buffer (Cell Signaling Technology, Beverly, MA, USA). After brief sonication on ice, the cell lysates were processed to determine the OA levels by LC-ESI-MS/MS using a modified published method (28, 115), which will be elaborated in Section 2.3.13.3 Chromatography and tandem mass spectrometry analysis.

To determine the levels of cellular uptake of NS, 5 μL of glycyrrhetinic acid (GA) solution (1 μg/mL) as the internal standard (IS) was added to 50 μL of cell lysate sample, and vortexed for 1 min. The samples were extracted with ethyl acetate (900 μL) by vortex-mixing (1 min) and centrifuged (13,000 g x 10 min) at room temperature. The organic layer was carefully transferred and dried under nitrogen flow at 40 ℃. The residues were dissolved in methanol and transferred to clean vials for sample injection. Calibration standards were prepared with 50 μL blank cell lysate sample by the same method. Cell protein was assayed by BCA Protein Assay Kit (Thermo Fisher Scientific, Waltham, MA, USA) according to the kit protocol. Results were expressed as amount (μg) of OA per mg total cell protein.

To study the effect of temperature on SEOA NS uptake, as control groups, A549 cells were pre-incubated in regular growth medium at 4 ℃ for 30 min and co-incubated with SEOA NS (15 μg/mL) at 4 ℃ for 3 h. Normal groups were pre-incubated in regular growth medium at 4 ℃ for 30 min then co-incubated with SEOA NS (15 μg/mL) at 37 ℃ for 3 h. The dose and time effects on cellular uptake of NS were also examined. To study the dose-dependent NS uptake effect, cells were incubated with different concentrations of NS (15 and 30 μg /mL) for 1 h. To study the time-dependent NS uptake effect, cells were

incubated with NS (15 μg/mL) for 1 and 3 h.

2.3.13 PHARMACOKINETICS STUDY

2.3.13.1 INTRAVENOUS AND ORAL ADMINISTRATION OF OA TO RATS

The study design and animal handling protocol of this pharmacokinetic study were modified from our previous study (131) and approved by the Institutional Animal Care and Use Committee of the National University of Singapore. Adult male Sprague–Dawley rats (250 – 300 g) were purchased from the Laboratory Animal Centre of the National University of Singapore. The rats were housed under temperature (22 ± 1 ℃) and relative humidity (60 – 70 %) controlled environment in Animal Holding Unit of the university operated at a 12-h light / dark cycle. The rats were given free access to food and water before surgery. On the day before the pharmacokinetic study, a polyethylene tube (i.d. 0.58 mm, o.d. 0.965 mm, Becton Dickinson, Sparks, MD, USA) was placed into the right jugular vein through surgical implant under anaesthesia. The intravenous (iv) drug administration and blood sample collection were performed through this cannula. The rats were randomly divided into four groups (n = 5 per group). Group I received iv administration of OA while three other groups received oral dosing through gavages. It is known that oral absorption may be influenced by different dietary regimens and the inherent bile salt solubilisation capacity in the intestine. Hence, the rats for oral administration (Groups II – IV) were kept in fasting condition overnight prior to the oral gavages and during blood collection but free access to water were

allowed. However, such restriction was not applied to the rats that received iv administration. Rats in Groups II and III were administered single dose of SEOA 4121 NS by oral gavages at the dose of 10 and 20 mg/kg, respectively. As controls and comparisons, rats in Groups I and IV would receive either SEOA4121 NS by iv administration (2 mg/kg) or oral administration of coarse OA suspensions in N, N-DMAC : PEG400 : water (2 : 4 : 1, v/v/v) at the dose of 20 mg/kg. Serial blood samples (200 μL) were collected from each animal at 1, 5, 15, 30, and 45 min, and 1, 1.5, 2, 3, 4, 6, 8, 10 and 12 h after iv administration and at 5, 15, and 30 min, and 1, 1.5, 2, 3, 4, 6, 8, 10 and 12 h after oral administration. The cannula was flushed and blood was replaced by an equivalent volume of heparin–saline (20 IU/mL heparin in normal saline) after each draw of blood sample. Plasma samples were collected after centrifugation (3,000 g x 5 min) of the blood samples and stored at −80 ℃ until LC-ESI-MS/MS analysis.

2.3.13.2 SAMPLE PREPARATION AND CALIBRATION

The sample preparation method (liquid-liquid extraction) was adopted from our previous study with minor modification (131). The plasma sample (100 μL) was spiked with methanol solution (5 μL) of GA (20 μg/mL) as IS and mixed briefly in a clean 2 mL centrifuge tube. Then ethyl acetate (300 μL) was added to the tube and mixed for 1 min to facilitate the extraction procedure. After this liquid-liquid extraction, the tube was centrifuged (13,000 g x 10 min) and the ethyl acetate layer was carefully transferred to another clean tube. The extraction procedure was repeated for two additional cycles and the ethyl acetate layer was collected in the same tube. The sample was then dried under nitrogen flow at 40 ℃. The

residue was reconstituted with methanol (75 μL) and centrifuged (13,000 g x 5 min). The supernatant was injected (10 μL) into the HPLC column. Calibration standards were prepared with 100 μL blank plasma samples using the same procedures. The calibration curve was obtained from the samples prepared by spiking OA and internal standard into pooled rat plasma. It was linear (r^2 = 0.9907) within the range of 20–2,000 ng/mL of OA.

The within-day and between-day accuracy and precision were evaluated at three concentration levels (40, 100, and 800 ng/mL) based on five measurements carried out in a single day and over five days of validation period, respectively, according to previous report with modifications (115). The accuracy was expressed as bias (the percentage of difference between the measured and spiked concentrations over that of the spiked value), whereas the precision was presented as the relative standard deviation (R.S.D. %). The absolute recovery of the extraction was determined by comparing the peak area obtained from the plasma sample with peak areas obtained by the direct injection of pure OA standard solutions in the HPLC column at three different concentration levels. The quantification of the chromatogram was performed by using peak area ratios of OA to internal standard.

2.3.13.3 CHROMATOGRAPHY AND TANDEM MASS SPECTROMETRY ANALYSIS

The concentrations of OA in plasma were determined by a previously reported LC-ESI-MS/MS method with modifications (28, 115). Briefly, the HPLC system was an Agilent 1100 series machine equipped with a G1312A binary pump and a G1379A degasser

(Agilent, Palo Alto, CA, USA). The HPLC column was a C18 column (300 mm × 2. mm i.d.) packed with 3 μm ODS stationary phase (Hypersil Aquasil, Thermo Scientific, Waltham, MA, USA) which was protected with a guard column (Inertsil ODS-3; GL Sciences, Tokyo, Japan). The HPLC mobile phase consisted of acetonitrile/10 mM ammonium acetate buffer pH 6.5 (15 : 85, v/v). The flow rate was set at 0.30 mL/min and analysis was performed in isocratic mode. The mass spectrometer was the Qtrap 3000 model with an electrospray ionization (ESI) interface (Applied Biosystems, Toronto, Canada). Negative ion ESI with the collision energy -30 V, curtain gas 10 psi and ion source temperature 200 ℃ were used. Quantification was performed with multiple selected reaction monitoring (MRM) mode. The transition of OA is 455.5/455.5 (m/z) (Figure 2.10a) and GA (IS) is 469.5/425.5 (m/z) (Figure 2.10b) with a scan time of 100 ms per transition.

2.3.13.4 RESULTS ANALYSIS

WinNonlin standard Version 5.01 (Scientific Consulting Inc., Apex, NC, USA) was used to analyze the pharmacokinetic parameters and non-compartmental model was adopted for the analysis. The area under the plasma concentration (AUC) versus time curve ($AUC_{0\rightarrow t}$) in rats that received oral administration (Groups II – IV) was calculated by the linear trapezoidal rule with the time point from 0 to the last detectable time point, whereas the $AUC_{0\rightarrow t}$ in rats that received iv dosing (Group I) was calculated through the same rule except the logarithmic scale was taken. Clearance (Cl) values were calculated using the equation: $Cl = \frac{Dose}{AUC_{0 \rightarrow t}}$. Absolute bioavailability (F %) of OA after oral administration (Groups II –

IV) was calculated using the following equation:

$$F\% = \frac{\frac{AUC_{0 \to t}(\text{Group II, III or IV})}{\text{Dose(Group II, III or IV)}}}{\frac{AUC_{0 \to t}(\text{Group I})}{2\text{mg/kg}}} \times 100 .$$

2.3.14. STATISTICAL ANALYSIS

Results were presented as mean ± standard deviation (std). Statistical significance of the results was analysed using two-tail independent sample t-test or one-way ANOVA. Values of $p<0.05$ were considered statistically significant.

2.4. RESULTS AND DISCUSSION

2.4.1 CHARACTERISTICS OF SEOA NS

2.4.1.1 CRITICAL MICELLAR CONCENTRATION (CMC) OF SEL AND SEP

To determine the concentration of SE in preparing SEOA NS by emulsion-organic solvent evaporation method, the CMC values of SEL and SEP needed to be confirmed. Figure 2.2 shows the surface tension readings of SEL and SEP solutions (mN/m) as a function of the concentrations of the surfactant (%, w/v). From the tendency equations, CMC of SEL and SEP were calculated to be 0.021 (%, w/v) and 0.00105 (%, w/v), respectively. The concentration of SE in preparing NS should be above the CMC level.

a.

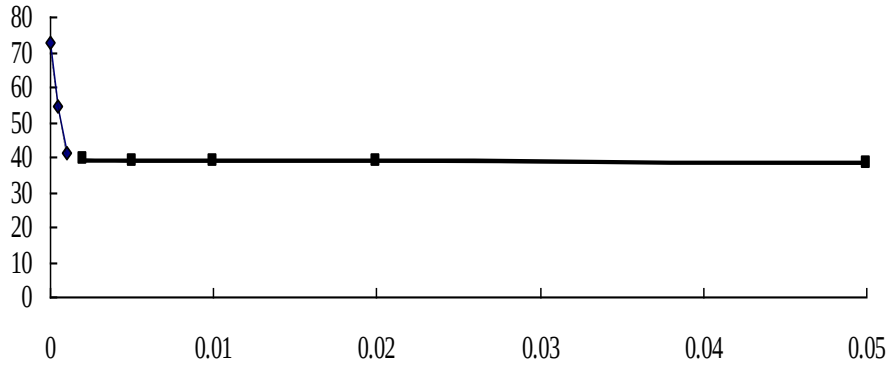

b.

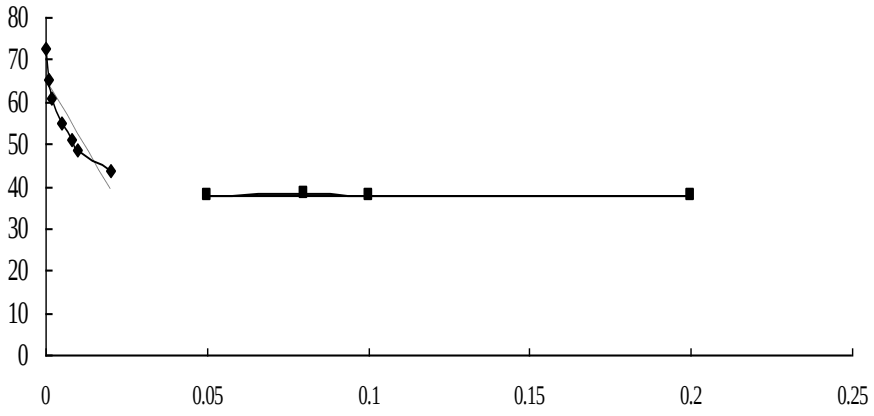

Figure 2.2 Determination of CMC of SEP (a) and SEL (b) by surface tension method. X axis represents the concentrations of the surfactant (%, w/v) and Y axis shows the surface tension readings of surfactant solutions (mN/meter).

2.4.1.2 PARTICLE SIZE AND PDI OF DIFFERENT SEOA NS

The size and PDI of SE-OA NS were characterized by DLS measurement. Figure 2.3 shows a typical size distribution curve of OA NS prepared with SEL and SEP. The graph shows the distribution of particle sizes, with the mode of particles around 100 nm. With the exception of SEOA9121 NS (SEL : SEP at 9 : 1, w/w; SE : OA at 2 : 1, w/w) ($p<0.01$), which had a mean size of 171.40 nm, the mean size of all other particles were all at around 100 nm in mean size. The PDI values were generally relatively high. SEOA 4121 NS and SEOA 9121 NS had the smallest PDI readings of around 0.41 (see also Table 2.2).

As indicated in Table 2.2, it was noted that the weight ratio of SEL to SEP may had influenced the particle size of drug particles in the NS.

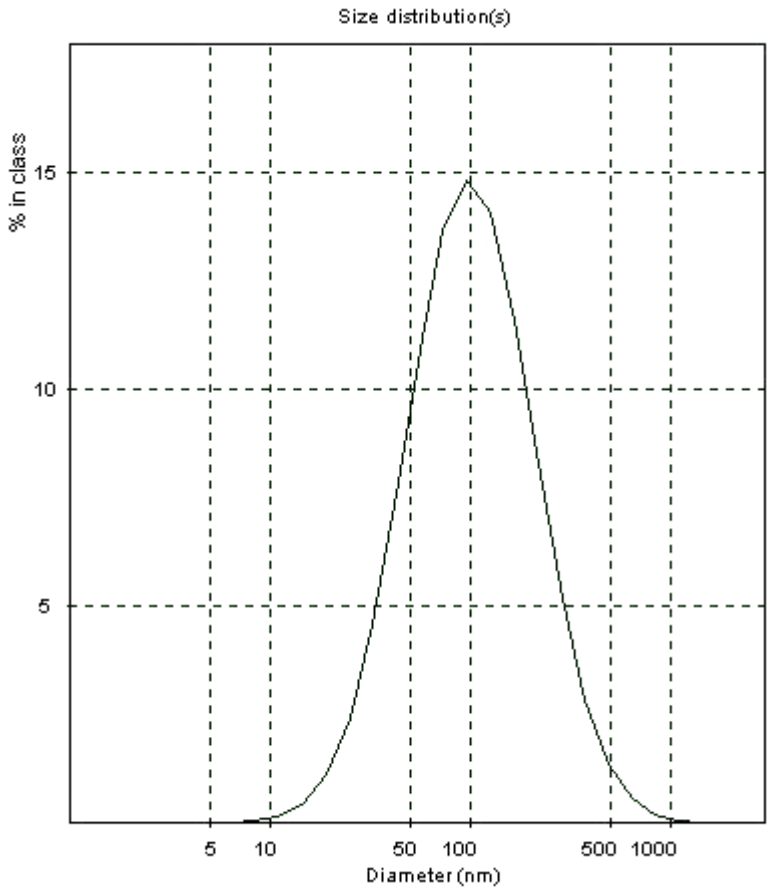

Figure 2.3 Representative particle size distribution data obtained from Zetasizer Instrument by the intensity of signal.

Table 2.2 Comparison of SEOA NS properties

Group	Size (nm)	PDI	EE %	Saturation solubility (mg/mL)
SELOA	101.60 ± 4.00 [e, f]	0.60 ± 0.09[d,e]	79.40 ± 0.06 [d, e, f, g, h]	0.66 ± 0.01 [d, g, h]
SEPOA	92.20 ± 2.10 [e, f, h]	0.61 ± 0.02[d,e]	79.82 ± 3.20 [d, e, f, g, h]	0.67 ± 0.03 [d, g, h]
SEOA91101	103.60 ± 5.30 [e, f]	0.57 ± 0.08[d,e].	79.29 ± 2.69 [d, e, f, g, h]	0.66 ± 0.02 [d, g, h]
SEOA9121	171.40 ± 3.40 [a, b, c, d, f, g, h]	0.41 ± 0.04[a,b,c,g,h]	18.07 ± 0.58 [a, b, c, d, f, g, h]	0.75 ± 0.02 [d, g, h]
SEOA9151	133.70 ± 1.20 [a, b, c, d, e, g, h]	0.49 ± 0.02[h]	40.73 ± 3.02 [a, b, c, e, g, h]	0.68 ± 0.05 [d, g, h]
SEOA4121	96.60 ± 2.30 [e, f, h]	0.41 ± 0.03[a,b,c,g,h]	45.38 ± 1.81 [a, b, c, e]	1.89 ± 0.08 [a, b, c,e,f, g, h]
SEOA4151	93.10 ± 1.50 [e, f, h]	0.59 ± 0.08[d,e]	54.31 ± 0.74 [a, b, c, e, f]	0.91 ± 0.01 [a, b, c, d, e, f]
SEOA2151	110.60 ± 6.80 [b, d, e, f, g]	0.66±0.07[d,e,f]	49.15±2.37 [a, b, c, e, f]	0.82 ± 0.04[a, b, c, d, e, f]

Data represent 3 independent experiments repeated in triplicate. Values are presented as means ± std. Statistics are carried out via one-way ANOVA. [a], significantly different compared with SELOA ($p<0.05$). [b], significantly different compared with SEPOA ($p<0.05$). [c], significantly different compared with SEOA91101 ($p<0.05$). [d], significantly different compared with SEOA4121 ($p<0.05$). [e], significantly different compared with SEOA9121 ($p<0.05$). [f], significantly different compared with SEOA9151 ($p<0.05$). [g], significantly different compared with SEOA4151 ($p<0.05$). [h], significantly different compared with SEOA2151($p<0.05$).

Among all the formulations, when the ratio of SEL to SEP equalled to 9 : 1, the particle size was found to be the largest. For instance, between SEOA 4121 and SEOA 9121, which only differed from the SEL to SEP weight ratios, the latter was found to contain much larger nanoparticulates. The conditions were about same with SEOA 2151(SEL : SEP at 2 : 1, w/w; SE : OA at 5 : 1, w/w), SEOA 4151(SEL : SEP at 4 : 1, w/w; SE : OA at 5 :1, w/w) and

SEOA 9151(SEL : SEP at 9 : 1, w/w; SE : OA at 5 : 1, w/w). These findings suggested at the above surfactant ratio (SEL : SEP at 9 : 1, w/w), the particles of SEOA NS were probably coated by much thicker surfactant layers, hence demonstrating larger particle sizes.

2.4.1.3 MORPHOLOGY DETERMINATION BY TEM

Confirmation of the NS size and morphology of SEOA NS were carried out using transmission electronic microscopy (TEM). Figure 2.4 shows examples of the TEM photomicrographs of SEOA NS. The constituent OA particles were generally spherical in shape with a mean diameter of around 30-40 nm. The smaller particle size estimated as compared with the results obtained using the DLS may be due to nano-aggregation effects and aggregates were seen during DLS measurements. Particles of NS tended to aggregate together due the their high surface energies and observations by the DLS methods only give the actually presented average size distribution which comprised considerably of the nanoaggregates, and the lesser isolated individual nanoparticles. TEM results showed the particles presented mainly as clustered agglomerates, encapsulated by distinct SE membrane-like layer, which appeared like an “outer shell”. This outer shell may function as a steric barrier that had ensured the stability of OA NS.

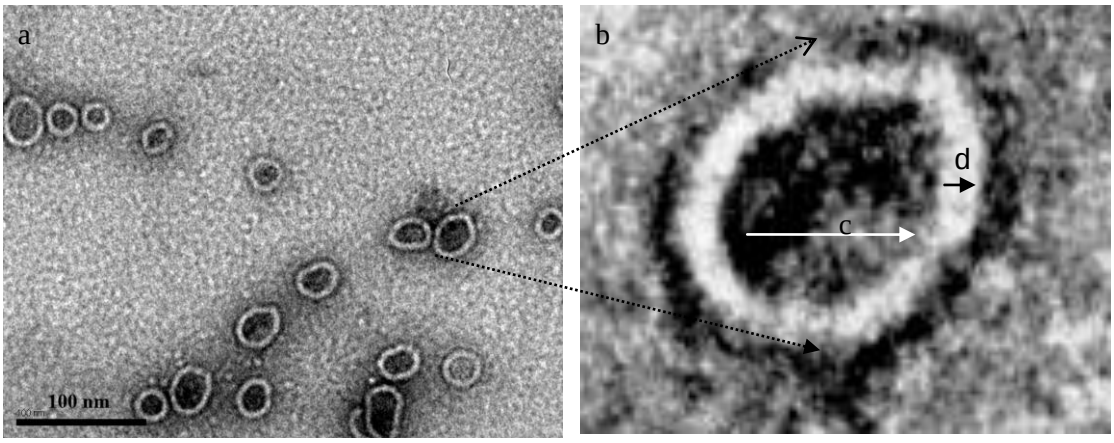

Figure 2.4 Representative TEM of SEOA-NS produced by emulsion-organic solvent evaporation method. (c=encapsulated OA; d= thickness of SE coating)

2.4.1.4 FREE OA EQUILIBRIUM AQUEOUS SOLUBILITY AT 25 ℃, SEOA NS ENCAPSULATION EFFICIENCY (EE) AND SATURATION SOLUBILITY

After the determination of the size and morphology of the SEOA NS, studies were next carried out to (a) compared the EE % of NS prepared with either pure SE or mixture of different ratios of SE types, combined at predetermined weight ratios and (b) study which of the formulations of NS gave rise to the highest OA saturation solubility.

The HPLC peak for OA was detected at a retention time of about 6.8 min, using the above mentioned settings, and SE did not have any significant effect on the separation of OA since the elution peak of SE merged with that of organic solvent, and occurred at the early elution phase. The concentrations of unknown OA samples can be determined by reference to the standard curve (Figures 2.5a and b). The intra-day coefficients of variation were 1.24, 1.86 and 3.55 % respectively, the inter-day coefficients of variation on three consecutive days were 1.21, 1.99 and 4.05 % respectively. The accuracy (%) of the method, expressed as the

mean deviation of all concentrations from theoretical value, were 1.43 %, 0.83 % and 1.06 % for OA respectively.

Since free OA equilibrium aqueous solubility was too low to be detected directly, the OA aliquot obtained from the equilibrium aqueous solution was freeze dried and concentrated in methanol solution before use for HPLC detection. From the results obtained by HPLC, equilibrium solubility of OA in water at 25 ℃ was found to be approximately 3.43 ± 0.11 (μg/mL), which is close to the value reported by Chen et al. (4.37 μg/mL) (27).

From Tables 2.2 and 2.3, of all the SEOA NS, SEOA4121 NS preparations had much higher OA saturation solubility, at about 1.89 mg/mL, which is almost 550 folds higher than free OA solubility in water. Meanwhile, SEOA91101 NS showed the highest percent encapsulation efficiency (79.29 %) as well as possessing the highest level of product stability. Upon consideration of these observations, it was decided that these two SEOA formulations would be chosen for further studies, and to be used for the subsequent *in vitro* efficacy study.

a

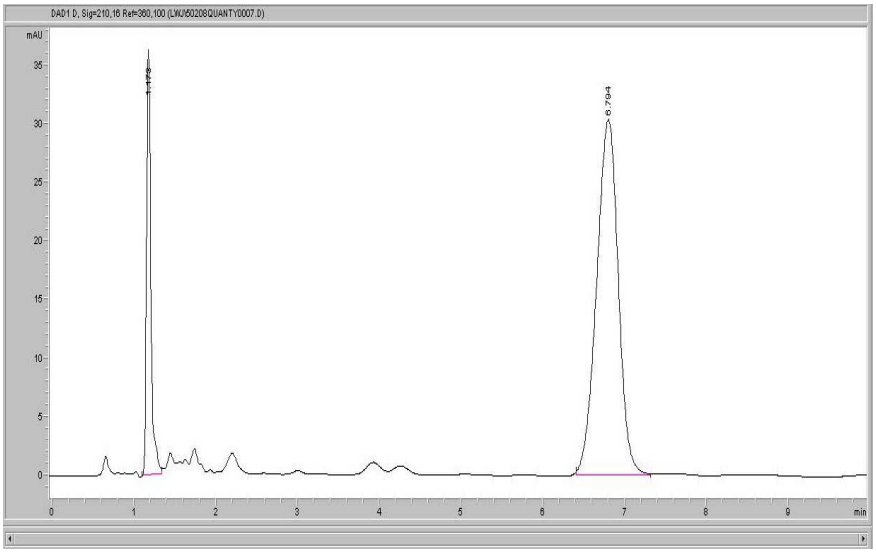

b.

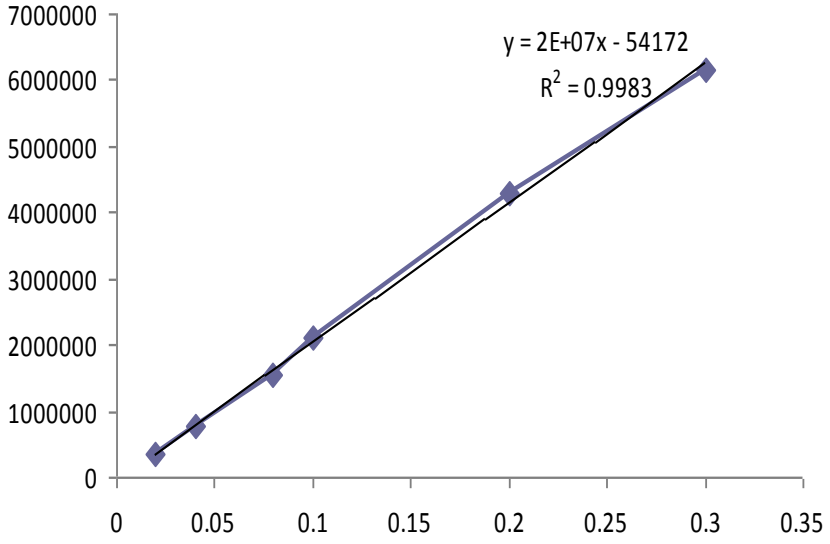

Figure 2.5a HPLC chromatogram of OA showing OA retention time is approximately 6.8 min. 2.5b Calibration curve of OA standards: 0.02, 0.04, 0.06, 0.08, 0.1, 0.2, mg/mL; R2 =0.9983. X axis indicates OA concentration (mg/mL), Y-axis indicates UV absorption.

According to Ostwald-Freundlich's equation (44), $\log (C_s/C_\alpha) = 2\sigma V/ (2.303RT\rho r)$, where Cs is the saturation solubility, C_α is the solubility of the solid consisting of large particles, σ is the interfacial tension of substance, V is the molar volume of the particle

material, R is the gas constant, T is the absolute temperature, ρ is the density of the solid and r is the radius. By decreasing the particle size (r), NS should show an increase the saturation solubility (Cs) of OA. Comparing with a previous report by Chen et al. (27), the saturation solubility increased by 191 to 550 folds when SE stabilized, and SE was much more effective than the 6 folds increase by polysorbate 80. This is the first report on the use of SEL and SEP to stabilized NS.

From the chemical structure, SEL has a shorter fatty acid chain than SEP. According to the literature and in the product manufacturer's manual, SEL is listed as being more hydrophilic than SEP, with smaller logP value (1.5 vs. 3.2) (118, 119) and a higher HLB value(13 vs. 15). Stabilization of NS with the combination of SEL and SEP could produce synergistic advantages as the combined properties of both surfactants could bring about improved affinity of the SE to the hydrophobic drug and resultant NS stabilized by SE are more readily dissolving in aqueous solution. It would also be expected that the complementary nature of these two SEs should lead to the formation of a more stable NS. Indeed, when the surfactant to drug ratio (10 : 1) was kept constant for SELOA NS (SEL : OA at 10 : 1, w/w), SEPOA NS (SEP : OA at 10 : 1, w/w) and SEOA91101 NS (SEL : SEP at 9 : 1, w/w; SE : OA at 10 : 1, w/w), the three OA NS formulations all exhibited similar values in their mean particle sizes, encapsulation efficiency and OA solubility. However, SEOA91101 NS was more stable upon prolonged storage than SELOA and SEPOA. (Table 2.2).

The weight ratios of surfactant (SEL and SEP) to OA may have influenced the NS characteristics. As shown in Table 2.2, when the SEL : SEP weight ratios were kept constant

and the amount of OA to SE was increased (from 10 : 1 to 2 : 1) for the three OA NS (SEOA 91101, SEOA9151, and SEOA9121), it resulted in an increase in the particle size (from 103.60 nm to 171.40 nm) and OA saturation solubility, but a decrease in the EE % (from 79.29 % to 18.07 %) and stability (Tables 2.2 and 2.3). The findings indicated that additions of OA at low OA concentrations brought about an increase in the saturation solubility of SE stabilized OA NS, but it did not keep on increasing and beyond a level, further OA increase was at the expense of sacrificing encapsulation efficacy and stability. Since the overall amount of SE was constant for all the formulations, the increase of OA beyond the stabilizing ability of SE may probably caused the decrease in the EE % and stability.

2.4.1.5 FT-IR

From TEM findings, nanoprecipitated particles of OA were observed to be encapsulated by SE membranes. Thus, it may be pertinent to examine the possibility of any interaction of SE with the hydrophobic drug. The SE OA samples were examined by determining the FT-IR spectra. According to Figure 2.6, all of the major peaks of OA remained clearly seen in the lyophilized SEOA NS, thus, indicating that OA was not chemically modified when formulated into SEOA NS.

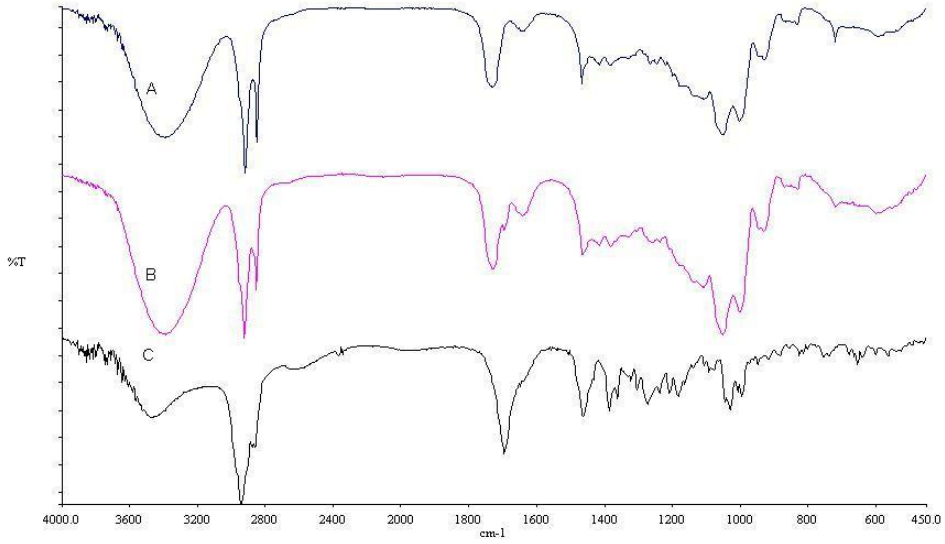

Figure 2.6 FTIR spectra of pure oleanolic acid (A), lyophilized SEOA4121 NS (B), and blank SEL and SEP mixture (4 : 1, w/w) (C).

Table 2.3 Chemical and physical stability of SEOA NS

Group	Original (%)	1 month relative concentration (%)	3 month relative concentration (%)	15 days size change (%)	30 days size change (%)
SEOA4151	100.00	82.52 ± 1.63[e]	67.75 ± 0.56[c, e, g]	16.58 ± 3.20[b, c, d, g, h]	124.97 ± 17.76[e, g, h]
SEPOA	100.00	86.32 ± 1.12[e]	65.35 ± 0.70[c, e, g]	64.49 ± 13.30[a, e, f]	121.79 ± 59.99[e, g, h]
SEOA2151	100.00	88.50 ± 1.81[e]	82.24 ± 0.79[a, b, g, h]	53.11 ± 21.38[a, e, f]	93.10 ± 32.37[d, g, h]
SELOA	100.00	88.27 ± 4.79 [e]	76.79 ± 0.33 [g]	47.79 ± 6.57[a, e, f]	172.06 ± 28.89[c, e, g, h]
SEOA91101	100.00	98.61 ± 4.44 [a, b, c, d, f, g, ,h]	88.21 ± 1.30 [a, b, f, g, h]	4.89 ± 1.47[b, c, d, g, h]	39.03 ± 24.41[a, b, d, f, g, h]
SEOA9151	100.00	84.69 ± 4.63 [e]	71.12 ± 1.52[e,g]	13.54 ± 17.98[b, c, d, g, h]	153.27 ± 26.16[e, g, h]
SEOA9121	100.00	80.54 ± 2.97 [e]	44.88 ± 0.06[a, b , c, d, e, f, h]	57.28 ± 16.93[a, e, f]	376.37 ± 23.31[a, b, c, d, e, f]
SEOA4121	100.00	87.06 ± 4.86 [e]	68.17 ± 0.70[c, e, g]	43.74 ± 11.44[a, e, f]	403.93 ± 47.80[a, b, c, d, e, f]

Data represent 3 independent experiments repeated in triplicate. Values are presented as means ± std. Statistics are carried out via One-Way ANOVA. [a], significantly different compared with SEOA4151 ($p<0.05$). [b], significantly different compared with SEPOA ($p<0.05$). [c], significantly different compared with SEOA2151 ($p<0.05$). [d], significantly different compared with SELOA ($p<0.05$). [e], significantly different compared with SEOA91101 ($p<0.05$). [f], significantly different compared with SEOA9151 ($p<0.05$). [g], significantly different compared with SEOA9121($p<0.05$). [h], significantly different compared with SEOA4121($p<0.05$).

2.4.1.6 STABILITY OF SEOA NS

Table 2.3 demonstrates the comparison of stability values among the SEOA NS. It is noted that most of the NS samples were found to be relatively chemical stable (>80 %) for 1 month when stored at 4 ℃ but much degraded after 3 months' storage. SEOA 91101 NS and SEOA 2151 NS were found to be more chemically stable than other NS formulations. Among all the NS, SEOA91101 NS was the most stable, in both physical and chemical stability aspects. Since SEOA 4121 NS was stable up to 15 days of storage and with the highest OA content, it was hence selected for further *in vitro* study and *in vivo* pharmacokinetics application. From Tables 2.4 and 2.5, either in rat plasma or in SGF and SIF circumstances, SEOA4121 NS was shown to be relatively stable over the first 24 h *in vitro*.

Table 2.4 SEOA 4121 NS incubation with rat plasma

Time(h)	Relative Concentration (%)	Standard (%)
0	100.00	0.00
1	96.94	9.63
2	88.99	1.95
4	89.91	10.38
24	83.94	5.05

Data represent 3 independent experiments repeated in triplicate.

Table 2.5 SEOA 4121 incubated in SGF and SIF

	Sample Time (h)				
	0.5	1	2	4	24
Media	Relative Concentration (%)				
pH 7.4	97.97 ± 1.13	97.60 ± 1.31	93.05 ± 0.38	93.05 ± 0.28	92.21 ± 1.13
pH 6.8	100.00 ± 0.36	99.62 ± 0.51	97.46 ± 1.13	94.97 ± 0.51	94.97 ± 1.13
pH 1.2	100.00 ± 6.68	98.42 ± 1.31	98.16 ± 0.47	95.71 ± 0.24	95.60 ± 0.85

Data represent 3 independent experiments repeated in triplicate. Values are presented as means ± std

2.4.2 *IN VITRO* DISSOLUTION

In the preparation of a dosage form, it is important that the bioactive compound remains bioavailable upon ingestion into the gastrointestinal tract. The common assessment of bioavailability in *vitro* of a drug delivery system is by the use of the dissolution test method as prescribed by the USP. The dissolution rate of OA was determined by the *in vitro* dissolution profiles of different OA formulations (Figure 2.7a). The dissolution rate of OA coarse suspension (suspended in N, N-DMAC : PEG400 : water at 2 : 4 :1, v/v/v) was very

low, only about 15 % of the drug dissolved in 120 min. On the contrary, the SEOA 4121 NS either in suspension form or in lyophilized powder form both showed a great increase in the dissolution of OA over the coarse suspension, and 100 % of OA dissolved within 120 min. According to Noyes–Whitney equation, $\frac{dW}{dt} = \frac{DA(C_s - C)}{L}$ (132), where, $\frac{dW}{dt}$ is the rate of dissolution, A is the surface area of the solid, C is the concentration of the solid in the bulk dissolution medium, C_s is the concentration of the solid in the diffusion layer surrounding the solid, D is the diffusion coefficient, and L is the diffusion layer thickness.

An increase in saturation solubility (Cs) and decrease in particle size would led to increased dissolution rate ($\frac{dW}{dt}$). Thus, formulating the poorly water-soluble drug as nanosize particles had a dramatic effect on both its saturation solubility and dissolution rate, and the bioavailability could be consequently increased.

The fast dissolution of OA from SEOA 4121 NS may be derived from the release of OA as free dissolved molecular form or in NS form. Therefore, the dialysis bag, through which only free OA can pass, was needed to identify the different forms released. From Figure 2.7b, using the dialysis method, no free OA could be detected even after 6 h in the dissolution medium and the dissolution rate increased very slowly. The percent of dissolved OA did not reach 12 % even after 48 h. The present findings indicated that most of the dissolved OA released existed in the NS particles and not in the free molecularly dissolved form.

a.

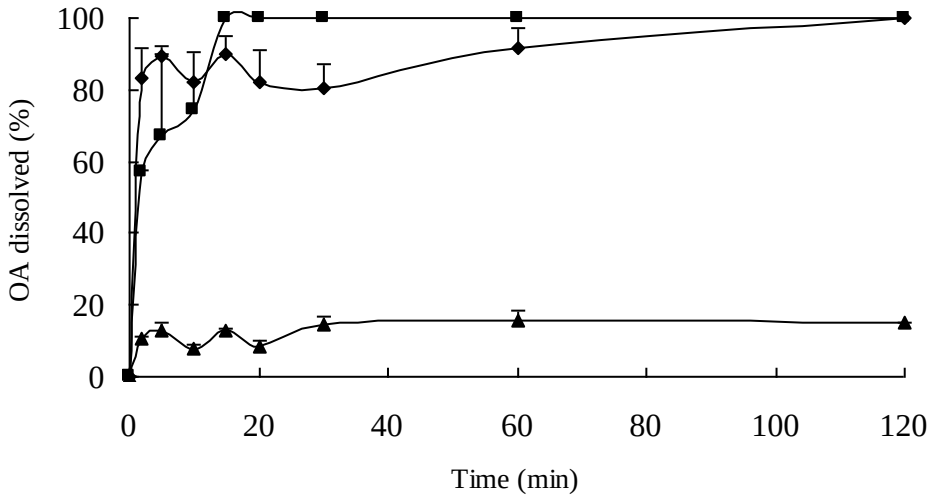

b.

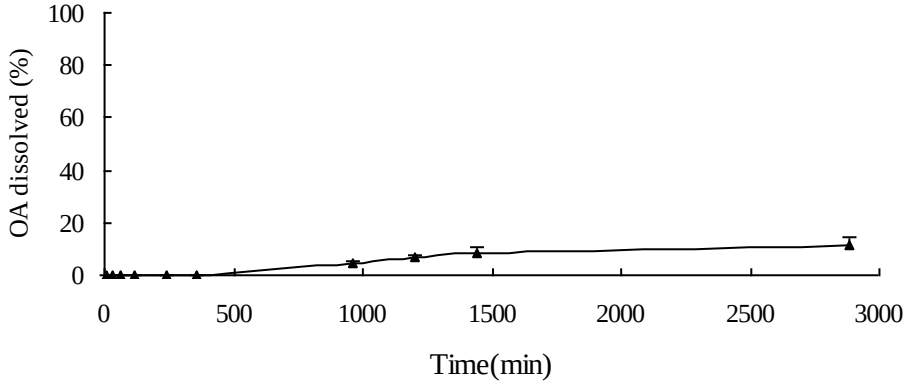

Figure 2.7 Dissolution profiles of OA coarse suspension (▲) (suspended in N,N-DMAC : PEG400 : Water at 2 : 4 : 1, v/v/v), SEOA 4121 NS (■) and SEOA 4121 lyophilized powder(◆) (2.7a) and SEOA4121 NS in dialysis bag (▲) (2.7b) in pH 7.4 phosphate buffer saline solution containing 1 % sodium dodecyl sulfate (SDS) (n = 3).

2.4.3 CYTOTOXICITY OF SEOA NS

In NS form, the saturation solubility of OA was increased markedly from 3.43 μg/mL (free OA) to 660 μg/mL (SEOA91101 NS) and 1890 μg/mL (SEOA4121 NS). Owing to the increase in OA saturation solubility, the *in vitro* cytotoxicity in A549 cell lines as determined by the MTT assay also saw an increased. As shown in Figure 2.8, formulation of SE-stabilized OA NS significantly increased the cytotoxicity of OA in both time- and dose-dependent manner (see data in Table 2.6). The 72 h IC_{50} dropped from 120 μM of free OA to 26 μM of SEOA4121 NS and 18 μM of SEOA91101 NS. Although free OA is not considered as potent in anti-lung cancer cells, formulated OA as NS form showed much enhanced bioefficacy even without any chemical modification.

The enhanced cytotoxic effect was most likely to be due to the increased saturation solubility of OA rather than the surface-active effects of the sucrose ester molecules.

Table 2.6 IC_{50} comparison of SEOA NS and free OA

Group	24h (μg/mL)	72h (μg/mL)
Free OA	59. 67 ± 1.01(130.00 μM)	56.75 ± 1.02 (120.00 μM)
SEOA91101 NS	13.10 ± 1.08 (28.00 μM)	8.30 ± 1.05 (18.00 μM)
SEOA4121 NS		12.10 ± 1.09 (26.00 μM)
SE(4 : 1) NS	211.40 ± 1.03	217.10 ± 1.03
SE (9 : 1) NS	249.10 ± 1.06	212.60 ± 1.00

IC_{50} values were calculated by nonlinear regression (curve fit) of cytotoxicity data in figures 2.8a-d using sigmoidal dose response (variable slope) equation, Graphpad Prism software (Graphpad 4.0, Graphpad software, Inc., La Jolla, CA, USA).

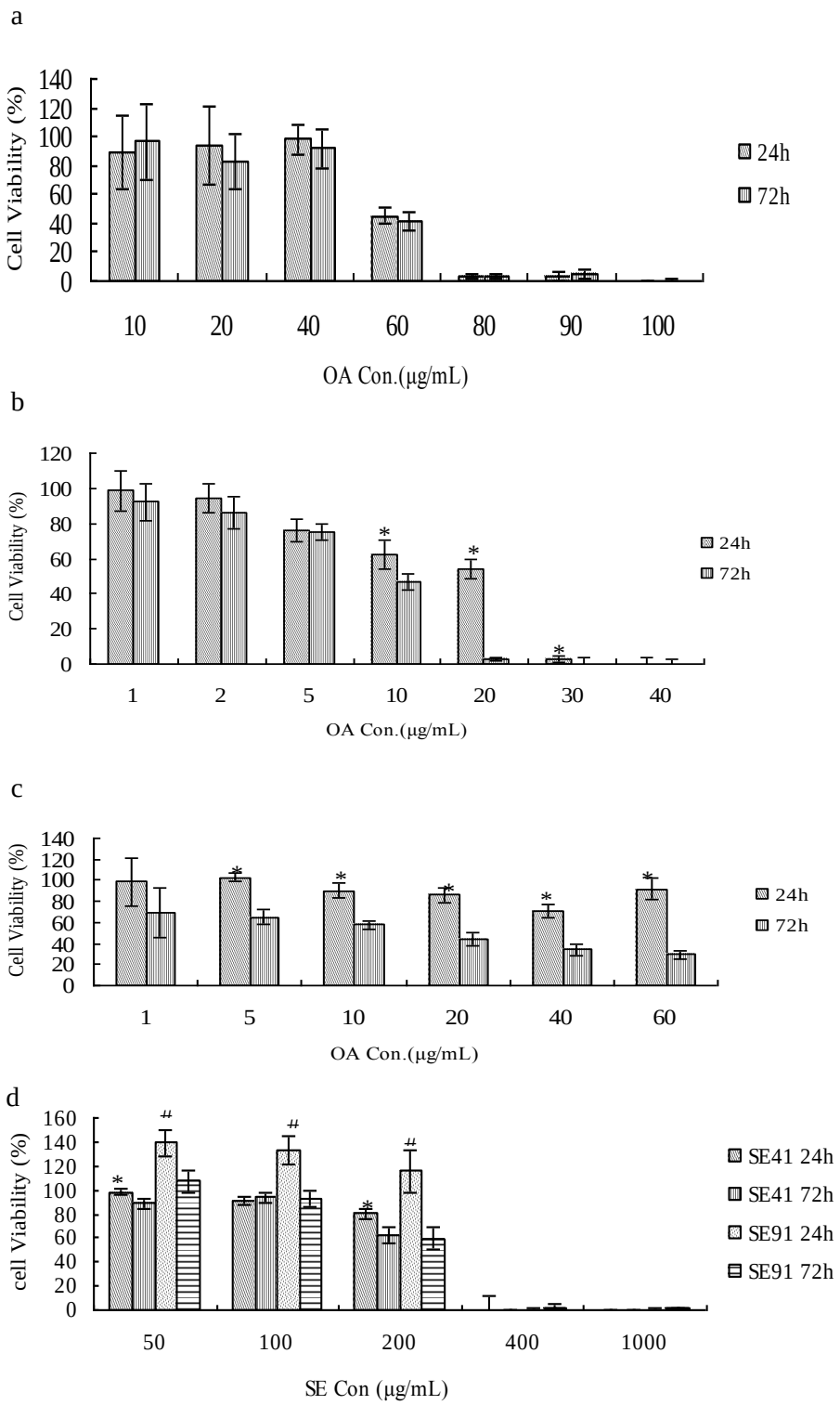

Figure 2.8 Dose- and time-dependent growth inhibition of A549 cells by (a) Free OA dissolved in media containing 0.05 %DMSO, (b) SEOA91101 NS (*, *p<0.05* between 24 h and 72 h) (c) SEOA4121 NS(*, *p<0.05* between 24 h and 72 h) (d) blank SE 41 NS (SEL : SEP at 4 : 1 w/w) and blank SE 91 NS (SEL : SEP at 9 : 1 w/w) without OA. *, *p<0.05* between SE41 24 h and SE41 72 h; #, *p<0.05* between SE91 24 h and SE91 72 h. Data is presented as mean (μg/mL) ± std from three independent experiments repeated in quadruplicate.

This contention was supported by the findings that treatment of A549 cells with drug-free NS resulted in a considerably much less cytotoxic effect than when the cells were treated with drug-loaded SEOA NS.

Since the encapsulation efficiency of SEOA 4121 NS and SEOA 91101 NS was 45.38 % and 79.29 % respectively (Table 2.6), without considering the loss of SE during preparation, the maximum yield SE : OA ratio in SEOA 4121 NS and SEOA 91101 NS was 4.41 : 1 $(\frac{2\times 100\,\%}{1\times 45.38\%})$ and 12.61 : 1 $(\frac{10\times 100\,\%}{1\times 79.29\%})$ respectively.

At 72 h after the treatment, the IC_{50} of NS prepared with SEL : SEP weight ratio at 4 : 1 was 17.57 times that of SEOA4121 NS (more than 4.41 times). Similarly, the IC_{50} of NS prepared with SEL : SEP weight ratio at 9 : 1 was 19.02 times that of SEOA91101 NS at 24 h and 25.61 times at 72 h after treatment (more than 12.61 times).These observations indicated that the cellular toxic effect of SEOA NS was mainly derived from the nanoparticulate drug rather than from the surfactants that formed and stabilized the NS (see Table 2.6).

2.4.4 CELLULAR UPTAKE OF SEOA NS

LC-ESI-MS/MS was used to quantify the cellular OA concentration. The mass peak of OA was demonstrated in Figure 2.9a. Using the pre-determined settings, the GA (internal stand) peak and OA peak emerged at around 2.20 min and 4.29 min respectively.

Suitable temperature, around 37 ℃, is crucial for intracellular metabolism (133). When A549 cells were incubated at 4 ℃, cellular uptake of SEOA NS was significantly lower than

that at 37 ℃ (Figure 2.9b). Our results suggested that uptake of SEOA NS into the A549 cells required suitable temperature. To determine the effect of varying the NS concentration and incubation time on uptake of NS by the A549 cells, the cells were treated with different OA concentrations (15 μg/mL or 30 μg/mL) for same incubation time (1 h) or same OA concentration (15 μg/mL) for different times (1 h or 3 h). As shown in Figures 2.9c and d, significantly higher uptake of SEOA NS compared to control was observed when the cells were treated with a higher concentration of OA or longer incubation time. This may explain that SEOA 4121 NS and SEOA 91101 NS had better cytotoxicity effect than free OA and they yielded better effect after 72 h incubation.

From the *in vitro* dissolution study, it was demonstrated that most of the dissolved OA existed as NS droplets and not as the free molecular form. This may imply that the uptake of OA was mainly in NS form, and by endocytosis.

However, further experiments will be needed to verify this hypothesis and to explore the underlying mechanism for OA intake as well as to study the full extent of *in vivo* bioeffect of SEOA NS as a potential therapeutic agent.

a.

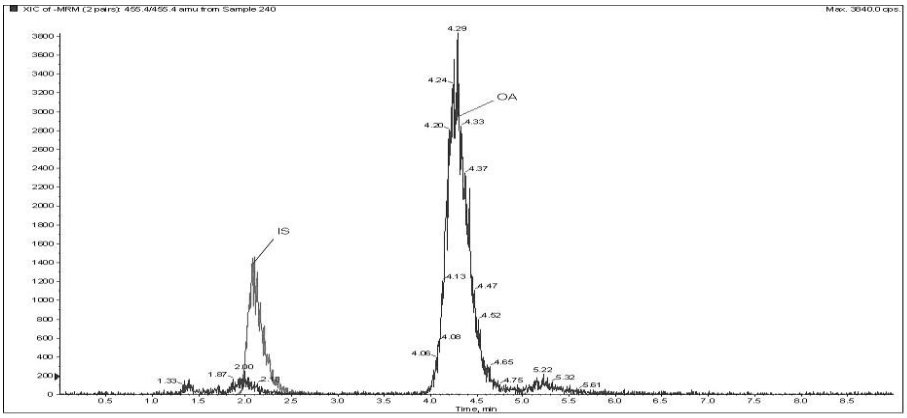
IS
OA
Time, min

b

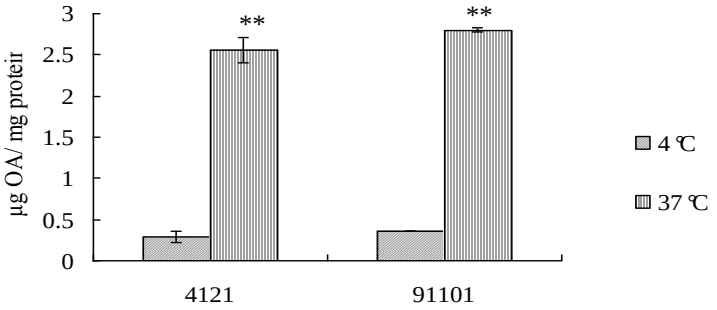
μg OA/ mg proteir
4121
91101
4 ℃
37 ℃

c

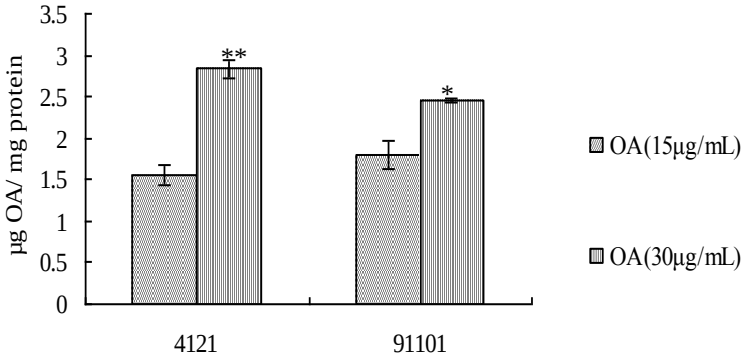
μg OA/ mg protein
4121
91101
OA(15μg/mL)
OA(30μg/mL)

d

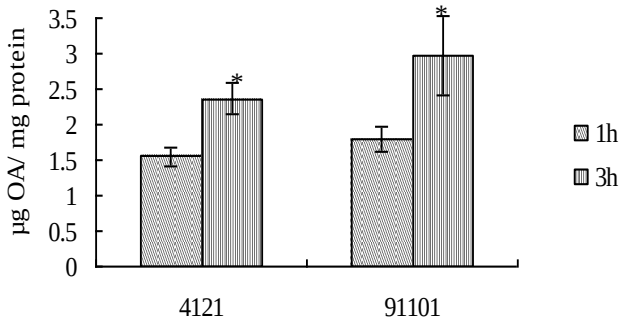
μg OA/ mg protein
4121
91101
1h
3h

Figure 2.9 Cellular uptake of SEOA NS. (a) Mass peak of OA by LCMS. The left peak is the internal standard and the right one is OA peak. Cellular uptake of SEOA NS is (b) temperature-dependent, (c) concentration-dependent, and (d) time-dependent. Data is presented as mean (μg/mg protein.mL) ± Std from three independent experiments repeated triplicate. *, *p<0.05*; **, *p<0.01*.

2.4.5 SEOA NS PHARMACOKINETICS PROFILE

2.4.5.1 RECOVERY, PRECISION AND ACCURACY IN ANALYSIS OF PLASMA SAMPLES

The LC-ESI-MS/MS system enabled a sensitive and well-defined separation between the drug, internal standard and endogenous components. LC-ESI-MS/MS peaks of OA and GA are shown in Figure 2.9a. The mass spectra of $[M-H]^-$ of OA and GA were indicated in Figures 2.10a and b, respectively. Figure 2.11 indicates the calibration standard cure of OA. It was linear ($R^2 = 0.9942$) within the range of 20–2,000 ng/mL. From Table 2.7, the absolute recoveries of OA from the plasma were more than 84.30 %, indicating that most of the OA introduced in the plasma samples were extracted. The within-day and between-day precision (R.S.D. %, n = 5) for the OA spiked control samples at 40, 100, and 800 ng/mL levels varied between 2.50 and 11.20. The corresponding within-day and between-day accuracy (bias %, n = 5) ranged between −12.00 and +6.50 (Table 2.7).

2.4.5.2 PHARMACOKINETICS RESULTS AFTER INTRAVENOUS ADMINISTRATION

Figure 2.12a shows the pharmacokinetics results of OA following single iv bolus dose (2 mg/kg) of NS (Group I). The findings demonstrated that the plasma concentration of OA declined rapidly over the first hour and was followed by a slower decline from 2 h onwards. The maximum plasma concentration (C_{max}) was high (21.98 ± 5.79 μg/mL) and plasma elimination half-life ($T_{1/2}$) was found to be 88.41 ± 16.15 min. AUC and Cl values were calculated as 121.49 ± 27.37 μg.min/mL and 17.11 ± 3.67 mL/min/kg, respectively.

2.4.5.3 PHARMACOKINETICS RESULTS AFTER ORAL ADMINISTRATION

The plasma pharmacokinetic profiles and the pharmacokinetic parameters following single oral dose of SEOA NS (10 and 20 mg/kg) and OA coarse suspensions (20 mg/kg) are shown in Figure 2.12b and Table 2.8.

Table 2.7 The recovery, precision and accuracy (n=5) of the assay method

Concentration	**Recovery**		**Within-day**		**Between-day**	
(ng/mL)	Mean (%)	R.S.D (%)	Precision (R.S.D %)	Accuracy (Bias %)	Precision (R.S.D %)	Accuracy (Bias %)
40	86.40	6.50	5.60	-8.30	11.20	-12.00
100	94.70	2.10	4.90	5.90	4.00	3.80
800	84.30	1.30	2.50	6.50	1.90	-5.80

Bias %=[(concentration added-concentration found)/concentration added]×100

Table 2.8 Oral pharmacokinetics profiles of SEOA NS and coarse suspension

Parameter	Group II	Group III	Group IV
Formulation	NS	NS	Suspension
Dose (mg/kg)	10.00	20.00	20.00
AUC (μg.min/mL)	21.35 ± 3.89 [a, c]	44.06 ± 7.25 [a, b]	6.74 ± 3.42 [b, c]
T_{max} (min)	13.00 ± 4.47	21.00 ± 8.22	13.00 ± 4.47
C_{max} (ng/mL)	397.35 ± 170.19 [a, c]	817.19 ± 255.21 [a, b]	69.95 ± 42.71 [b, c]
$T_{1/2}$ (min)	76.38 ± 38.19	78.06±29.21	102.10±16.56
F %	3.51 ± 0.64	3.63 ± 0.60	0.56 ± 0.28 [b, c]

Data is presented as Mean ± Std, N=5.[a], *p<0.05* between Group II and III; [b], *p<0.05* between III and IV; [c], *p<0.05* between II and IV

a.

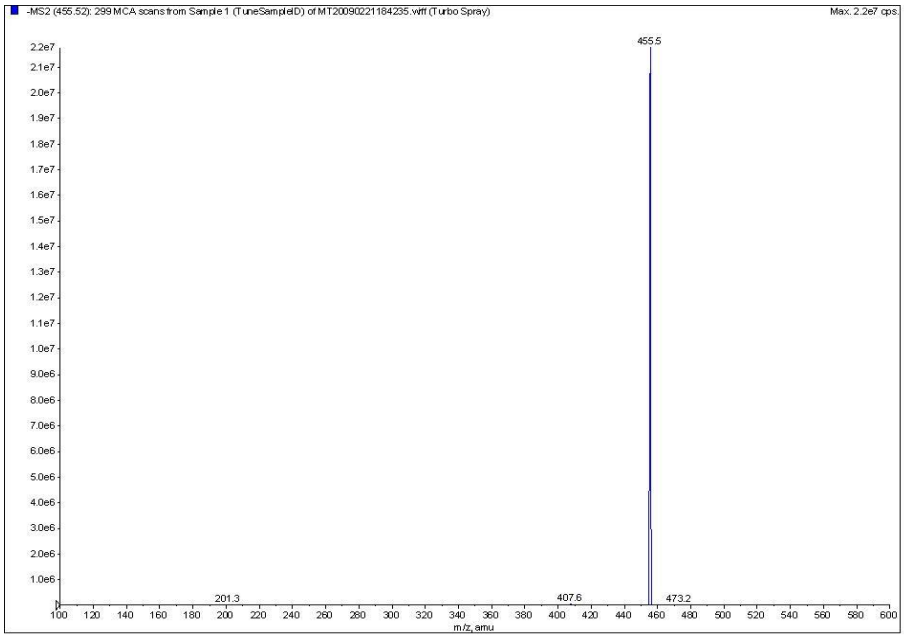

b.

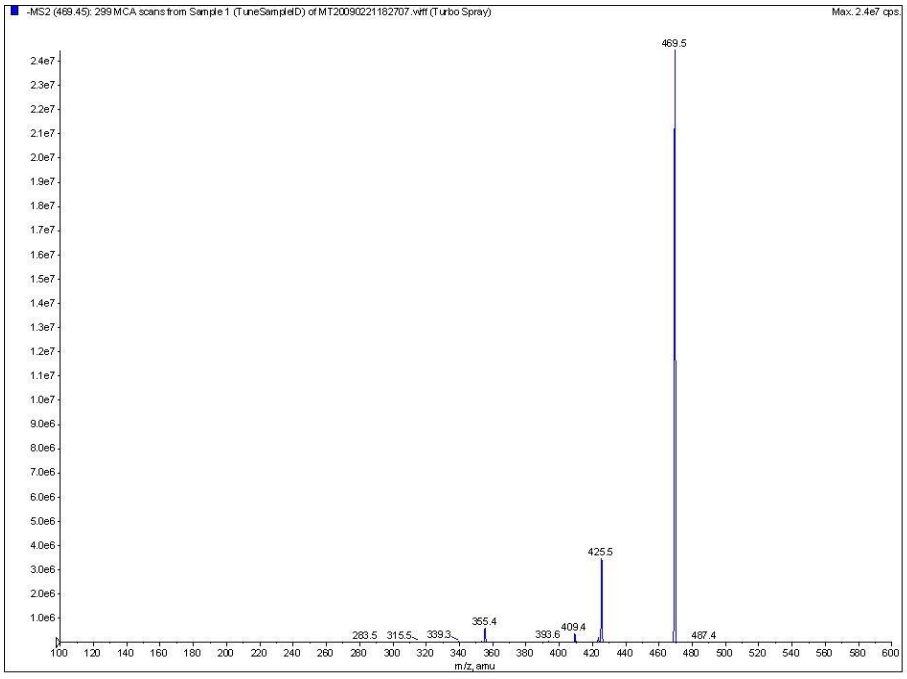

Figure 2.10 Mass spectra of $[M-H]^-$ of oleanolic acid (a, OA) and glycyrrhetinic acid (b, GA, internal standard)

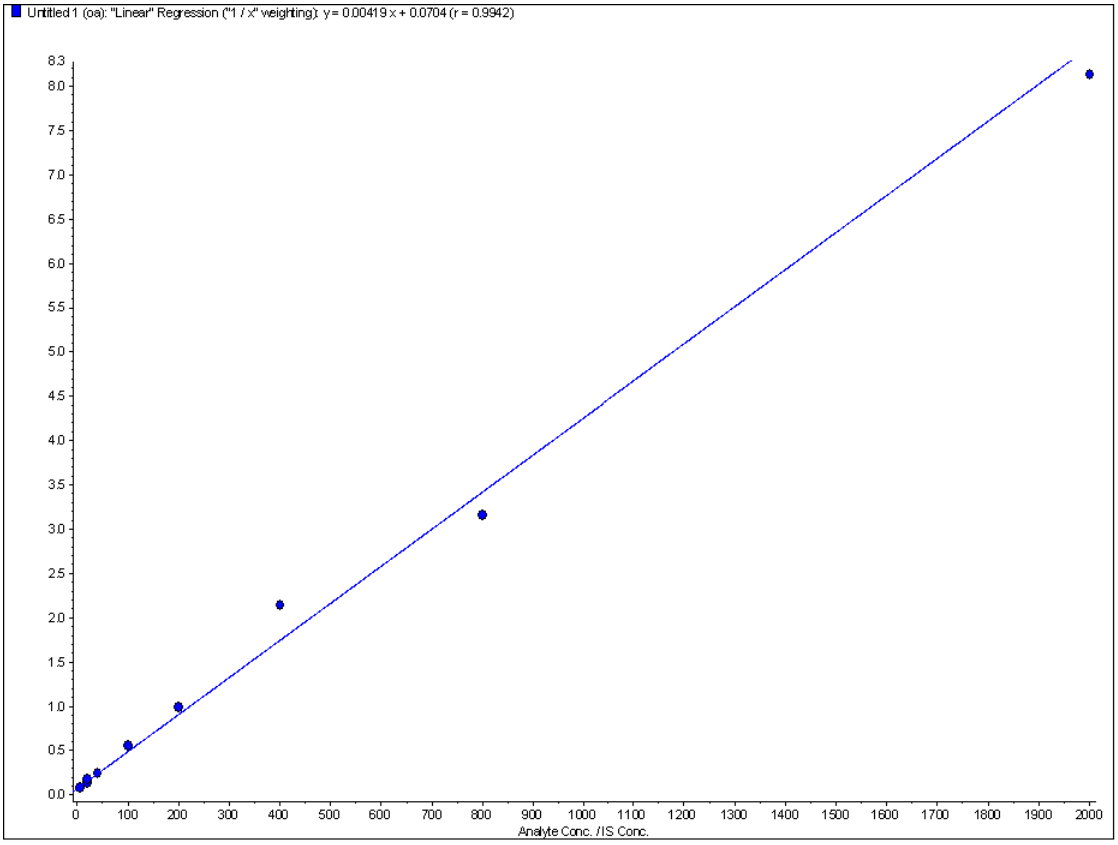

Figure 2.11 Calibration curve of OA standards ranged from 20-2000 ng/mL; R^2 =0.9942

In all cases, OA in NS groups resulted in a significantly (*p<0.05*) higher C_{max} than the suspension formulations. However, there were no significant differences (*p>0.05*) in T_{max} and $T_{1/2}$. In all groups, the NS group (Groups II and III) had a significantly higher bioavailability (F %) values (6 to 7 folds higher) than the suspension group (Group IV) (*p<0.05*) while for between 10 mg/kg and 20 mg/kg NS groups, there was no statistically significant differences (*p>0.05*). These findings indicated that the dosage form of OA affected the extent of its oral absorption. Figure 2.12b indicates that the plasma concentration of OA declined rapidly over the first stage and was followed by a second peak at 2 h, 3 h and 4 h for Group IV, Group III and Group II respectively, which was probably due to the enterohepatic recirculation of OA.

Oral bioavailability of a drug is dependent on various factors including the stability of the ingested drug in the gastrointestinal (GI) tract, its aqueous solubility, its permeability through the intestinal membrane and the first-pass elimination rate (134). A report by Jeong et al. (28) suggested that the low oral bioavailability of OA suspension may be due to its poor solubility, poor gastrointestinal absorption (by Caco-2 cell permeability model) and hepatic first-pass metabolism. However, in the present *in vivo* pharmacokinetic study, the findings indicated that the bioavailability of OA was highly enhanced by the NS formulation. Among all the NS formulations studies, the selected SEOA 4121 NS had encapsulated the highest amount of OA, demonstrated to possess relatively good *in vitro* stability in rats' plasma, SGF and SIF for 24 h, and shown to produce increased *in vitro* dissolution rate. The NS formulation produced could not only enhance the saturation solubility and dissolution rate of OA but also augmented its bioavailability and provided some protection against breakdown in various media.

a.

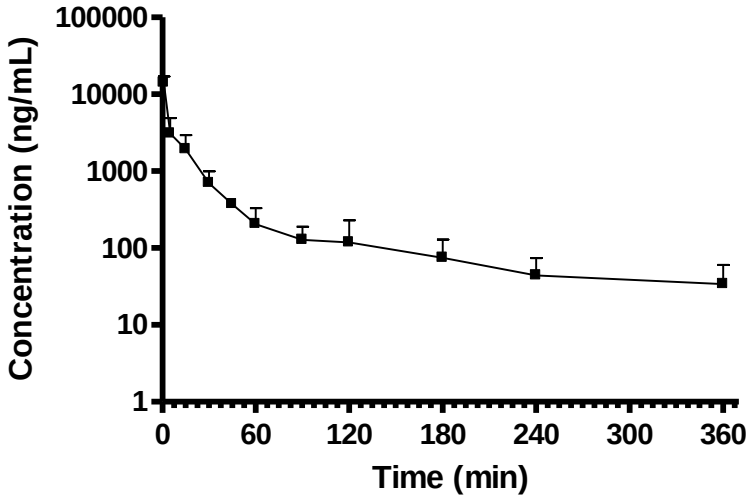

b

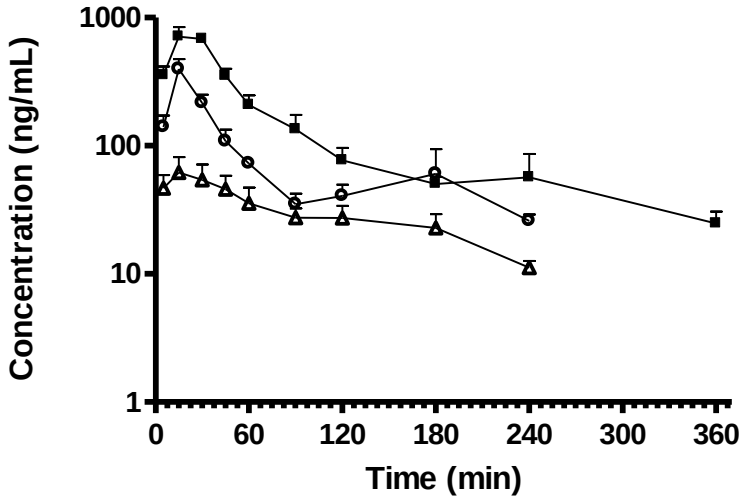

Figure 2.12 Mean plasma concentration-time profiles comparison of OA in rats after (a) IV injection at 2 mg/kg (■,n=5), (b) oral administration of OA NS at 10 mg/kg (○, n=5), 20 (■, n=5) mg/kg doses and oral administration of OA coarse suspension (△, n=5, control) at 20 mg/kg dose. Vertical bars represent standard deviation

2.5. CONCLUSION

NS of OA can be prepared by emulsion-organic solvent evaporation method using SEL and / or SEP as stabilizing surfactants. Mean particle sizes of most SEOA NS were around 100 nm. They were chemically and physically stable under short-term storage. The different weight ratios of SEL to SEP and SE to OA influenced the characteristics of SEOA NS. These NS particles were usually found to form clustered agglomerates and each sub-units were seen to be covered by distinct SE coating on the periphery. Preparation of OA as NS increased its saturation solubility considerably. With a huge surface area to volume ratio, the saturation solubility of resultant SEOA particles ranged from 0.66 mg/mL (SEOA91101 NS) to 1.89 mg/mL (SEOA4121 NS), which were of 191 to 550 folds increase over free OA. SEOA NS increased the OA dissolution rate markedly. Most of the dissolved OA existed in the NS particulates and not in the free dissolved molecular form. Formulation of OA as NS significantly and substantially increased the cytotoxicity of OA. Both SEOA91101 and SEOA4121 reduced the proliferation rate of A549 cell lines to a much greater extent than free OA. This increased activity was attributed to the nanonized drug and not the SE. Cellular uptake of SEOA NS by A549 cells was shown to be a temperature-, concentration- and time-dependent process. NS of OA not only increased its saturation solubility and dissolution rate to a great extent but also change the pharmacokinetic profile of OA after oral administration. Oral bioavailability of OA was enhanced by the NS formulation, which showed much higher C_{max} and F % (6 to 7 times increase) than the coarse suspension group. Dose-independent pharmacokinetics of OA was observed after oral administration in the range of 10 to 20

mg/kg. However, the cellular uptake mechanism and *in vivo* bioeffect of SEOA NS still needed further research.

CHAPTER 3. DEVELOPMENT AND EVALUATION OF SEOA NS VIA WET BALL MILLING OPTIMIZED BY DESIGN OF EXPERIMENTS (DOE)

CHAPTER 3. DEVELOPMENT AND EVALUATION OF SEOA NS VIA WET BALL MILLING OPTIMIZED BY DESIGN OF EXPERIMENTS (DOE)

3.1 INTRODUCTION

Design of experiments (DOE) was first exploited in 1958 by Fisher (135-137), and has since been used extensively in various fields including agriculture engineering food science and pharmacy. DOE is a methodology for studying any response that varies as a function of one or more independent variables. By observing the response under a planned matrix of settings, a statistically valid mathematical model for the responses within the designed space can be determined (138). The use of DOE is a revolutionary approach to optimization and a very useful tool for the screening of experimental parameters. Simple experimental designs and statistical tools for data analysis can provide much information about the system under scrutiny with the requirement of much less number of experiments to be carried out (139).

The experimental method of "changing one separate factor at a time" (COST) or also termed as studying "one variable at a time" (OVAT) is still commonly used. The aim of optimization does not easily lead to the real optimal set of conditions and may lead to different implications, depending on the starting point investigated (139). The approach also requires many experiments covering a range of possibilities. In contrast, the DOE approach is to use an essential tool for studying complex systems since it offers an organized approach that connects the various experiments in a rational manner, giving rise to more precise information that can be arrived from much fewer experiments (138).

When DOE is used, the following issues should be carefully considered (139) and they

are listed as follows.

a) **Factor:** Experimental variable, which can be quantitative (time, temperature, etc.) or qualitative (solvent, buffer, etc.)

b) **Response:** Property of the system that is being measured

c) **Interaction**: A state where two or more factors are dependent on each other

d) **Confounding:** Effects that cannot be estimated separately

Wet ball milling is one of the widely used top-down method to prepare of NS. Comparing with dry ball milling, the liquid in the wet method could help reduce and remove the heat generated by the strong impacts of the milling media and minimize the risk of chemical degradation due to heat-related instability. The use of DOE has been proven to be efficient in optimizing the formulation variables used in milling (140, 141).

The aim of this study was to optimize the operational parameters for preparing SEOA NS by wet ball milling with the help of the Minitab software (version 15, Minitab Inc. State College, Pennsylvania, USA) and to study the *in vivo* and *in vitro* properties of the optimized products produced.

3.2 MATERIALS

OA was purchased from Nanjing Qinze Pharmaceutics Ltd. Co. (Nanjing, China). SEL (batch M07A001, 90 % purity) and SEP (batch M07C003, 90 % purity) were obtained from Compass Foods Pte. Ltd. (Singapore). Methyl thiazolyl tetrazolium (MTT) and F12 Ham Kaighn's modification (F12K) medium were purchased from Sigma Aldrich Ltd. Co. (St.

Louis, MO, USA). A549 human non small cell lung cancer cell line (NSCLC) was purchased from American Type Culture Collection (Rockville, MD, USA). Fetal bovine serum (FBS) was purchased from Hyclone Laboratories Ltd. Co. (Logan, UT, USA). 4-(2-hydroxyethyl)-1-piperazineethanesulfonic acid (HEPES) was purchased from Applichem Ltd. Co. (Darmstadt, Germany). MilliQ water (18.2 MΩ cm at 25 ℃) was obtained from a Millipore Direct-Q ultra-pure water system (Billerica, MA, USA) and used throughout the study.

3.3 METHODS

3.3.1 PREPARATION OF SEOA NS BY WET BALL MILLING

SEOA NS formulations were prepared by the wet ball milling method using a laboratory scaled ball mill (S1, Retsch, Haan, Germany) (Figure 3.1) with 10 mm diameter stainless steel balls and the milling procedure adopted was according to the method described by the instrument manual. In brief, SEP and SEL were mixed with OA in a beaker at predetermined ratio and diluted with MilliQ water as the liquid medium to a final volume of 100 mL. The mixture was then poured into the stainless steel milling chamber containing stainless steel balls. The ball milling process was performed over 25 min followed by a 5 min break to allow for cooling before proceeding with milling again, repeating the cycle until completion of the proposed milling time. After a certain prescribed period of ball milling, the suspension was carefully extracted by pipettes, transferred to clean BD Falcon™ 50 mL conical tubes

(BD Bioscience, Mississauga, Canada), centrifuged at 13000 rpm for 10 min and filtered through 0.22 μm membranes to produce the clear NS.

Figure 3.1 Ball mill used for wet milling (Technical specifications: 220 V, 50 Hz, 75 W. Container dimensions (ø) x (H): 7.5 x 6.5 cm).

NS preparation was optimized with respect to milling time, rotational milling speed, ratio of SEP to SEL and ratio of SE (SEL and SEP) to OA with the help of the Minitab software by 4 factors and 2 levels factorial design analysis. Milling time was set as 1 h (low level) and 3 h (high level); rotational milling speed was set at 300 rpm (low level) and 600 rpm (high level); SEL : SEP was set at 1 : 1 (low level) and 9 : 1 (high level) and SE : OA

was set at 1 : 1 (low level) and 10 : 1 (high level). Detailed settings for the preparation of the various SEOA NS are shown in Table 3.1.

3.3.2 PARTICLE SIZE AND POLYDISPERSITY INDEX ANALYSIS

Dynamic light scattering (DLS) measurements were performed using the Zetasizer Nano-ZS90 (Malvern Instruments, Malvern, UK) at a wavelength of 532 nm. The scattering angle was fixed at 90° and the temperature of the sample was maintained at 25 ℃. Particle size and polydispersity index (PDI) determinations were carried out using diluted suspensions by adding 4 times of each volume with MilliQ water.

3.3.3 FT-IR MEASUREMENT

Pure OA, lyophilized SEOA-GBD NS and physical mixture of SEL and SEP at 9 : 1 (w/w) were analyzed using a FT-IR Spectrometer (PerkinElmer Spectrum 100 Series, Norwalk, CT, USA). Samples were mixed with anhydrous potassium bromide (1 : 100) and ground in a mortar and then pressed in a hydraulic press (14 tons) to small discs. The discs were placed under the infrared beam and the FT-IR spectra were collected in a spectral region between 4000 and 450 cm^{-1}.

3.3.4 TRANSMISSION ELECTRON MICROSCOPY (TEM)

The NS samples were applied onto copper grids for TEM observation. The cooper grids were first coated by 0.25 % Formvar film and then by carbon in a sequential order. The film face of the grid was applied with the NS sample and then stained with 5 % PTA. Excess applied liquids were carefully blotted off during each step. After drying for over 10 min under bench lamp, the sample was ready for examination. TEM micrographs were obtained using a JEOL JEM 2010 transmission electronic microscope (JEM 2010, JEOL Ltd. Co., Tokyo, Japan) operating at 200 kV.

Table 3.1 Detailed settings of SEOA NS made from wet ball milling

NS	Milling Speed (rpm)	Milling Time (h)	SEL to SEP ratio	SE to OA ratio
FBC	600	1	1 : 1 (5 g, 5 g)	10 : 1 (10 g, 1 g)
HAC	300	1	9 : 1 (9 g, 1 g)	10 : 1 (10 g, 1 g)
EAC	300	1	1 : 1 (0.5 g, 0.5 g)	1 : 1 (1 g, 1 g)
FBD	600	3	1 : 1 (5 g, 5 g)	10 : 1 (10 g, 1 g)
HAD	300	3	9 : 1 (9 g, 1 g)	10 : 1 (10 g, 1 g)
EAD	300	3	1 : 1 (0.5 g, 0.5 g)	1 : 1 (1 g, 1 g)
EBC	600	1	1 : 1 (0.5 g, 0.5 g)	1 : 1 (1 g, 1 g)
EBD	600	3	1 : 1 (0.5 g, 0.5 g)	1 : 1 (1 g, 1 g)
GAC	300	1	9 : 1 (0.9 g, 0.1 g)	1 : 1 (1 g, 1 g)
GAD	300	3	9 : 1 (0.9 g, 0.1 g)	1 : 1 (1 g, 1 g)
GBC	600	1	9 : 1 (0.9 g, 0.1 g)	1 : 1 (1 g, 1 g)
GBD	600	3	9 : 1 (0.9 g, 0.1 g)	1 : 1 (1 g, 1 g)
HBC	600	1	9 : 1 (9 g, 1 g)	10 : 1 (10 g, 1 g)
HBD	600	3	9 : 1 (9 g, 1 g)	10 : 1 (10 g, 1 g)
FAC	300	1	1 : 1 (5 g, 5 g)	10 : 1 (10 g, 1 g)
FAD	300	3	1 : 1 (5 g, 5 g)	10 : 1 (10 g, 1 g)

The first alphabets (E, F, G, H) encode the ratio between SEL to SEP and SE to OA, the middle (A or B) encode the milling speed, and the last (C or D) encode the milling time.

3.3.5 PERCENT ENCAPSULATION EFFICIENCY (EE %) AND SATURATION SOLUBILITY

EE % and OA saturation solubility of SEOA NS were measured and calculated by the results from HPLC analysis. HPLC analysis was carried out using an Aglient Model 1100 HPLC unit (Agilent, Palo Alto, CA, USA) with a C18 column (ODS 5 μm, 3.9 mm x 150 mm; Waters, Milford, MA, USA) and mobile phase of 65 % acetonitrile and 35 % MilliQ water. Column temperature was maintained at 24 ℃. Flow rate was 1 mL/min and uv detection wavelength was 210 nm. Standard samples were dissolved in methanol. The freshly prepared NS were dissolved in at least 5 x volumes of methanol to ensure that OA was fully dissolved and fell within the standard calibration curve concentration range. All samples were filtered through 0.22 μm membranes before measurements. The calibration curve over the concentration range of 0.02–0.20 mg/mL was constructed by plotting the peak area of the analyte against the concentration spiked for each media. Six independently weighed concentrations (0.02, 0.04, 0.06, 0.08, 0.10, 0.20 mg/mL) were used to obtain the calibration curve. The linearity of the assay procedure was determined by calculation of a regression line. Concentrations of OA in diluted SEOA NS samples were obtained from the resulting peak areas and the regression equation of the calibration curve. Saturation solubility of OA was calculated from the amount of OA dissolved in diluted sample multiplied by the dilution factor. For calculation of the EE % of OA, the following equation was used,

$$EE\ \% = OA_{NS}/OA_{T} \times 100\ \%$$

Where, OA_{NS} indicates amount of OA in NS and OA_{T} indicates the total amount of OA

added during preparation.

3.3.6 LYOPHILIZATION OF SEOA NS AND FREE OA SOLUTION

SEOA NS and free OA solution were frozen at -80 ℃ overnight and then freeze dried (Labconco Corp., Kansas City, MO, USA) for 24 h at -70 ℃ and 0.02 mbar.

3.3.7 *IN VITRO* DISSOLUTION TEST

Dissolution experiments were carried out using a dissolution apparatus (Model 2100c; Distek, North Brunswick, NJ, USA) according to the USP 29 Apparatus 2 (United States Pharmacopeia Convention, Inc., Rockville, MD, USA, 2006). The dissolution medium was 500 mL pH 7.4 phosphate buffer solution containing 1 % sodium dodecyl sulphate (SDS), thermostated at 37 ± 0.5 ℃ with paddles rotated at 100 rpm. SEOA-GBD NS, SEOA-GBD NS lyophilized powder, OA coarse suspension (suspended in N,N-DMAC : PEG400 : water in the ratio of 2 : 4 : 1, v/v/v) and SEOA-GBD NS in dialysis bags (MWCO 2,000; Spectrum Medical Industries Inc, Singapore) were all added into the dissolution media, each bag contained an estimated amount equivalent to 8 mg OA. Samples (3 mL) were withdrawn at predetermined time intervals and filtered through 0.22 μm filters. After each withdrawal, an equal volume of the dissolution medium was added to maintain the volume constant. The content of dissolved OA was determined using HPLC. All dissolution experiments were performed in triplicates, all sample analyses were carried out in triplicates and reported

results were the mean values.

3.3.8 STABILITY STUDY

The effect of storage time on the stability of SEOA NS was investigated at 4 ℃. Physical stability was measured as the percentage changes in particle size of SEOA NS after storage of 15 and 30 days. Chemical stability was measured as the relative concentration (percentage of original concentration) of OA in NS (after filtration) at the same time intervals. Each sample measurement was repeated thrice, and all studies were carried out by three independent experiments.

3.3.9 CYTOTOXICITY OF OA AND SEOA NS

A549 human NSCLC cells were cultured in F12 Ham Kaighn's modification (F12K) medium, supplemented with 10 % FBS, 10 mM HEPES, 100 U/mL penicillin G and 100 µg/mL streptomycin. The cells were maintained at 37 ℃ in a 5 % CO_2 humidified incubator. To determine cytotoxicity of OA and SEOA NS, A549 cells were seeded in 96-well plates at a density of 6 x 10^3 cells per well and incubated for 24 h at 37 ℃ in a 5 % CO_2 humidified incubator. Culture media were then removed and replaced with 100 µL fresh media (blank) or fresh media containing 0.5 % DMSO (control) or different concentrations of OA (in media with 0.5 % DMSO) or SEOA NS. After 24 and 72 h incubation, 10 µL MTT solution (5

mg/mL in PBS) was added to each well. After incubation at 37 ℃ for 4 h, the mixtures in the wells were removed, and 110 μL DMSO was added to each well and shaken at 100 rpm for 30 min. Absorbance was measured using a multiplate reader (Molecular Devices, Sunnyvale, CA, USA) at 590 nm. Proliferation rate (%) was calculated as ((sample reading-blank reading) / (control reading-blank reading)) × 100.

3.3.10 PHARMACOKINETICS STUDY

3.3.10.1 INTRAVENOUS AND ORAL ADMINISTRATION OF OA TO RATS

The study design and animal handling protocol of this pharmacokinetic study were followed the method described in Chapter 2. Adult male Sprague–Dawley rats (250 – 300 g) were purchased from the Laboratory Animal Center of the National University of Singapore. The rats were housed under temperature (22 ± 1 ℃) and relative humidity (60 – 70 %) controlled environment in Animal Holding Unit of the university operated at a 12-h light/dark cycle. The rats were given free access to food and water before surgery. On the day before the pharmacokinetic study, a polyethylene tube (i.d. 0.58 mm, o.d. 0.965 mm, Becton Dickinson, Sparks, MD, USA) was placed into the right jugular vein through surgical implant under anaesthesia. The intravenous (iv) drug administration and blood sample collection were performed through this cannula. The rats were randomly divided into four groups (n = 5 per group). Group I received iv administration of OA while three other groups received oral doses through gavage. It is known that oral absorption may be influenced by different dietary

regimens and the inherent bile salt solubilisation capacity in the intestine. Hence, the rats for oral administration (Groups IIb, IIIb and IV) were kept in fasting condition overnight prior to the oral gavage and during blood collection but free access to water were allowed. However, such restriction was not applied to the rats that received iv administration. Rats in groups IIb and IIIb were administered single doses of SEOA-GBD NS by oral gavage at the doses of 10 and 20 mg/kg were given, respectively. As controls and comparators, rats in groups I and IV would receive either SEOA4121 NS by iv administration (2 mg/kg) or oral administration of coarse OA suspension in N, N-DMAC : PEG400 : water (2 : 4 : 1, v/v/v) at the dose of 20 mg/kg. Serial blood samples (200 μL) were collected from each animal at 1, 5, 15, 30, and 45 min, and 1, 1.5, 2, 3, 4, 6, 8, 10 and 12 h after iv administration and at 5, 15, and 30 min, and 1, 1.5, 2, 3, 4, 6, 8, 10 and 12 h after oral administration. The cannula was flushed and blood was replaced by an equivalent volume of heparin–saline (20 IU/mL heparin in normal saline) after each draw of blood sample. Plasma samples were collected after centrifugation (3,000 g x 5 min) of the blood samples and stored at −80 ℃ until LC-ESI-MS/MS analysis.

3.3.10.2 SAMPLE PREPARATION AND CALIBRATION

The sample preparation method (liquid-liquid extraction) was adopted from a previous study with minor modification (131). The plasma sample (100 μL) was spiked with a methanol solution (5 μL) of GA (20 μg/mL) as IS and mixed briefly in a clean 2 mL centrifuge tube. Next, ethyl acetate (300 μL) was added to the tube and mixed for 1 min to facilitate extraction. After this liquid-liquid extraction step, the tube was centrifuged (13,000

g x 10 min) and the ethyl acetate layer was carefully transferred to another clean tube. The extraction procedure was repeated for two additional aliquots of ethyl acetate and the cumulated ethyl acetate layers were collected in the same tube. The ethyl acetate sample was then dried under nitrogen flow at 40 ℃. The residue was reconstituted with methanol (75 μL) and centrifuged (13,000 g x 5 min). The supernatant was injected (10 μL) into the HPLC to determine OA content. Calibration standards were prepared with 100 μL blank plasma samples, adopting the same preparation procedure. The calibration curve was obtained using blank plasma samples spiked with OA and internal standard. The blank plasma samples were obtained from pooled rat plasma. The calibration curve for OA was linear (r^2 = 0.9907) within the range of 20–2,000 ng/mL of OA.

3.3.10.3 CHROMATOGRAPHY AND TANDEM MASS SPECTROMETRY ANALYSIS

The concentrations of OA in plasma were determined by the same method as described in Chapter 2. Briefly, the HPLC system was an Agilent 1100 equipped with the G1312A binary pump and a G1379A degasser (Agilent, Palo Alto, CA, USA). The HPLC column was a C18 column (300 mm × 2. mm i.d.) packed with 3 μm ODS stationary phase (Hypersil Aquasil, Thermo Scientific, Waltham, MA, USA) which was protected with a guard column (Inertsil ODS-3; GL Sciences, Tokyo, Japan). The HPLC mobile phase consisted of acetonitrile/10 mM ammonium acetate buffer pH 6.5 (15 : 85, v/v). The flow rate was set at 0.30 mL/min and analysis was performed in an isocratic mode. The mass spectrometer was

the Qtrap 3000 model with an electrospray ionization (ESI) interface (Applied Biosystems, Toronto, Canada). Negative ion ESI with the collision energy -30 V, curtain gas 10 psi and ion source temperature 200 ℃ were used. Quantification was performed with multiple selected reaction monitoring (MRM) mode. The transition of OA is 455.5/455.5 (m/z) and GA (IS) is 469.5/425.5 (m/z) with a scan time of 100 ms per transition.

3.3.10.4 RESULTS ANALYSIS

WinNonlin standard Version 5.01 (Scientific Consulting Inc., Apex, NC, USA) was used to analyze the pharmacokinetic parameters and a non-compartmental model was adopted for the analysis. The area under the plasma concentration (AUC) versus time curve ($AUC_{0\rightarrow t}$) in rats that received oral administration (Groups IIb, IIIb and IV) was calculated by the linear trapezoidal rule with the time point from 0 to the last detectable time point, whereas the $AUC_{0\rightarrow t}$ in rats that received iv dosing (Group I) was calculated through the same rule except the logarithmic scale was taken. Clearance (Cl) values were calculated using the equation: $Cl = \frac{Dose}{AUC_{0\rightarrow t}}$. Absolute bioavailability (F %) of OA after oral administration (Groups 2 - 4) was calculated using the following equation:

$$F\% = \frac{\frac{AUC_{0\rightarrow t}(Group\,2,3\,or\,4)}{Dose(Group\,2,3\,or\,4)}}{\frac{AUC_{0\rightarrow t}(Group\,1)}{2mg/kg}} \times 100$$

Relative bioavailability (rF %) between oral administration groups was calculated as:

$$rF\% = \frac{\frac{AUC_{0 \to t}(GroupA)}{Dose(GroupA)}}{\frac{AUC_{0 \to t}(GroupB)}{Dose(GroupB)}} \times 100 = (F_A/F_B) \times 100$$

3.3.11 STATISTICAL ANALYSIS

Results were presented as mean ± standard deviation (Std). Statistical significance of the results was analyzed using two-tail independent sample t test or one-way ANOVA. Values of $p<0.05$ were considered statistically significant. Minitab software (version 15, Minitab Inc. State College, Pennsylvania, USA) was used to perform factorial design analysis.

3.4 RESULTS AND DISCUSSIONS

3.4.1 CHARACTER OF SEOA NS

3.4.1.1 PARTICLE SIZE AND POLYDISPERSE INDEX (PDI) OF DIFFERENT SEOA NS FORMULATIONS

The particle size and polydispersity index (PDI) of SE-OA NS were measured by the dynamic light scattering (DLS). Figure 3.2a shows a SEOA NS typical size normal distribution curve by volume (%) and the measured particle size was below 100 nm. Figure 3.2b gives the comparison chart of all the 16 formulations studied. Table 3.2 indicates the detailed size data and statistical analysis by one-way ANOVA. The mean particle sizes of the 16 formulations distributed widely, and the overall averaged size was 93.67 ± 53.53

(nm).With the exception of FBC (252.53 nm), FBD (156.87 nm) and HBD (146.70 nm), other particle sizes were all below 100 nm (see Table 3.2) and the averaged size, without the three NS mentioned, decreased to 72.51 ± 17.66 (nm).

The PDI of 16 formulations also varied considerably, from the lowest at 0.21 to biggest value of 1.0. The overall averaged PDI was 0.53 ± 0.29, but if the five formulations with largest PDI (FBC, HAD, HBC, FBD, and FAD) values were excluded in the calculations, the averaged PDI of the rest would drop to 0.34 ± 0.08.

The above observations had indicated that some NS formulations "*impaired*" the overall property of the 16 SEOA NS formulations that were prepared by wet ball milling. To obtain a better understanding of the operational mechanisms in the milling process, the influence of the four major preparation parameters will be elaborated later, with the help of the analysis provided by Minitab software.

a

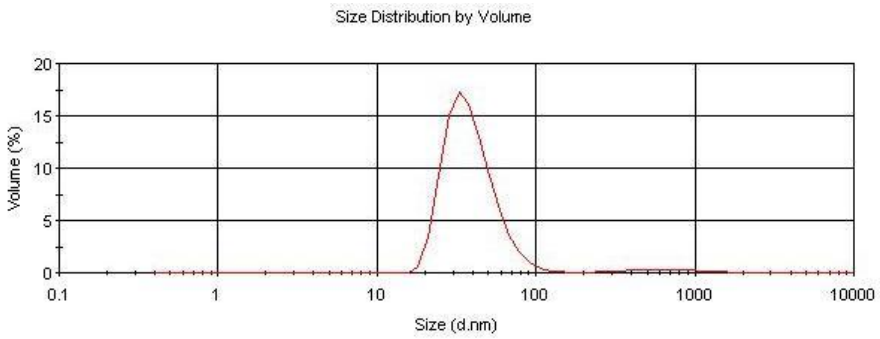

b

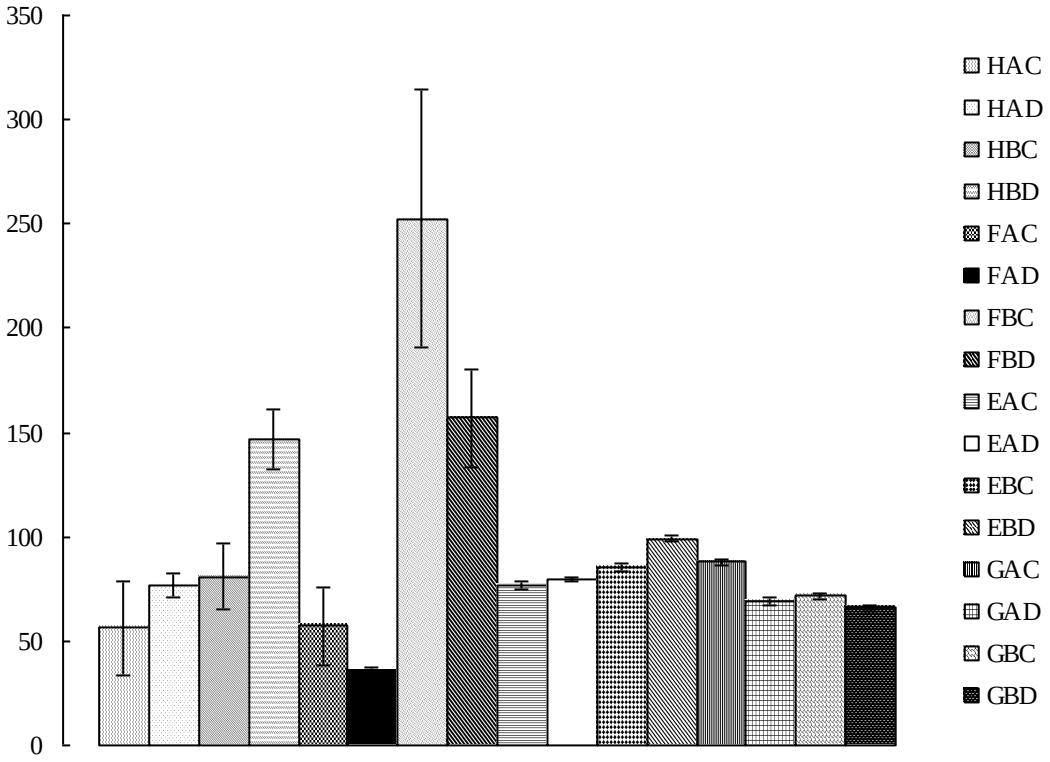

Figure 3.2a Representative particle size distribution data obtained from Zetasizer (Nano-ZS90) Instrument by the intensity of volume. Figure 3.2b Particle size of different SEOA NS. Data is presented as mean (nm) ± Std from three independent experiments repeated triplicate.

Table 3.2 Comparison of size and PDI

NS	Size (nm)	PDI
1.FBC	$252.53 \pm 62.12^{2,3,4,5,6,7,8,9,10,11,12,13,14,15,16}$	$0.96 \pm 0.07^{2,3,7,9,10,11,12,13,14,15,16}$
2.HBD	$146.70 \pm 13.98^{1,3,4,5,7,8,9,10,11,13,14,15,16}$	$0.46 \pm 0.02^{1,3,4,5,6,7,8,9,15}$
3.HAC	$56.35 \pm 22.71^{1,2,6}$	$0.24 \pm 0.02^{1,2,4,5,6,8,12,13}$
4.HAD	$76.74 \pm 5.85^{1,2,6}$	$0.85 \pm 0.04^{2,3,6,7,9,10,11,12,13,14,15,16}$
5.HBC	$80.78 \pm 15.62^{1,2,6}$	$0.90 \pm 0.11^{2,3,7,9,10,11,12,13,14,15,16}$
6.FBD	$156.87 \pm 23.72^{1,3,4,5,7,8,9,10,11,12,13,14,15,16}$	$1.00 \pm 0.00^{2,3,4,7,9,10,11,12,13,14,15,16}$
7.FAC	$57.25 \pm 18.73^{1,2,6}$	$0.21 \pm 0.05^{1,2,4,5,6,8,11,12,13,14}$
8.FAD	$35.83 \pm 1.11^{1,2,6,12}$	$0.96 \pm 0.04^{2,3,7,9,10,11,12,13,14,15,16}$
9.EAC	$77.09 \pm 1.93^{1,2,6}$	$0.31 \pm 0.02^{1,2,4,5,6,8}$
10.EAD	$79.84 \pm 0.95^{1,2,6}$	$0.33 \pm 0.05^{1,4,5,6,8}$
11.EBC	$85.46 \pm 2.08^{1,2,6}$	$0.35 \pm 0.04^{1,4,5,6,7,8}$
12.EBD	$99.20 \pm 1.49^{1,6,8}$	$0.44 \pm 0.03^{1,3,4,5,6,7,8,15}$
13.GAC	$87.77 \pm 1.35^{1,2,6}$	$0.41 \pm 0.02^{1,3,4,5,6,7,8}$
14.GAD	$68.99 \pm 1.51^{1,2,6}$	$0.35 \pm 0.03^{1,4,5,6,7,8}$
15.GBC	$71.52 \pm 1.19^{1,2,6}$	$0.31 \pm 0.01^{1,2,4,5,6,8,12}$
16.GBD	$65.73 \pm 1.71^{1,2,6}$	$0.34 \pm 0.04^{1,4,5,6,8}$

Data represent 3 independent experiments repeated in triplicate. Values are presented as means $\pm$ std. [1], significantly different compared with FBC. [2], significantly different compared with HBD. [3], significantly different compared with HAC. [4], significantly different compared with HAD. [5], significantly different compared with HBC. [6], significantly different compared with FBD. [7], significantly different compared with FAC. [8], significantly different compared with FAD. [9], significantly different compared with EAC, [10], significantly different compared with EAD. [11], significantly different compared with EBC, [12], significantly different compared with EBD.[13], significantly different compared with GAC, [14], significantly different compared with GAD. [15], significantly different compared with GBC. [16], significantly different compared with GBD ($p<0.05$). Statistics were carried out by one- way ANOVA.

3.4.1.2 MORPHOLOGY OF MILLED NS DETERMINED BY TEM

Determination of the morphology and particle size of SEOA NS were carried out by imaging using the transmission electron microscopic (TEM). Figure 3.3 shows the representative TEM photomicrographs of SEOA NS prepared by wet ball milling. In Figure 3.3a, with the magnification of 15,000 times, the particles of NS can be found scattering widely on the cooper grid (the small black dots). In Figure 3.3b, the particles of SEOA NS can be observed clearer with a magnification of 40,000 times. The NS particles were generally spherical in shape and with a mean diameter of around 20 nm. The smaller particle sizes observed as compared to the result of DLS may be attributed to the nano-aggregation effect in free liquid media of the high energy free NS particles. Free single particles of NS tended to aggregate together and DLS method could only provide sizes by the overall Brownian effect of the aggregates, thus only giving the aggregates' size distribution. The less opaque outer shells of each separate particle were likely to be constituted layers of the surfactants, SEL and / or SEP. The surfactant layers around the NS particles were most likely important to the formation of NS as they were believed to act as barriers preventing constituent particles from aggregation in the NS suspension.

a b

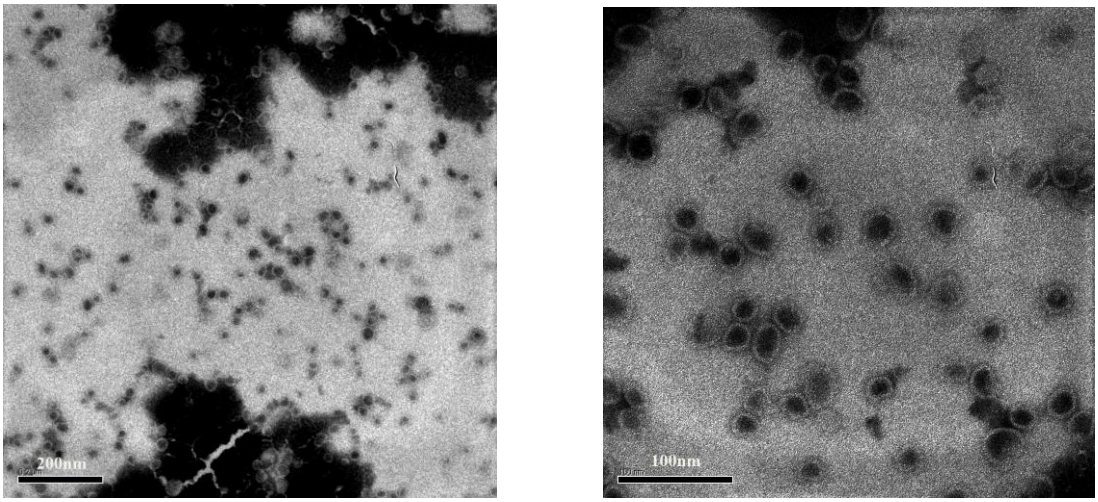

Figure 3.3 Representative TEM of SEOA NS produced by wet ball milling method. In Figure 3.3a, bar = 200 nm, magnification 15,000 times. In Figure 3.3b, bar = 100 nm, magnification 40,000 times.

3.4.1.3 SEOA NS ENCAPSULATION EFFICIENCY (EE %) AND SATURATION SOLUBILITY

Saturation solubility and EE % results are shown in Figure 3.4 and Table 3.3. The saturation solubility of OA obtained ranged from 2.08 to 5.49 mg/mL, which were much higher than free OA, and also higher than the previously reported SEOA NS prepared using the emulsion solvent evaporation method. Of all the formulations studied, HBD (5.49 mg/mL, 54.88 %) and FAD (5.36 mg/mL, 53.63 %) had the highest results. A further study on the influencing factors contributing to the alterations in solubility and EE % will be discussed later.

3.4.1.4 FT-IR

The FT-IR measurement was carried out to verify the existence of possible structure interactions between surfactants and OA. Figure 3.5 shows that all major peaks of free OA were still present in the lyophilized SEOA NS. This observation indicated that OA was not chemically modified when formulated as SEOA NS.

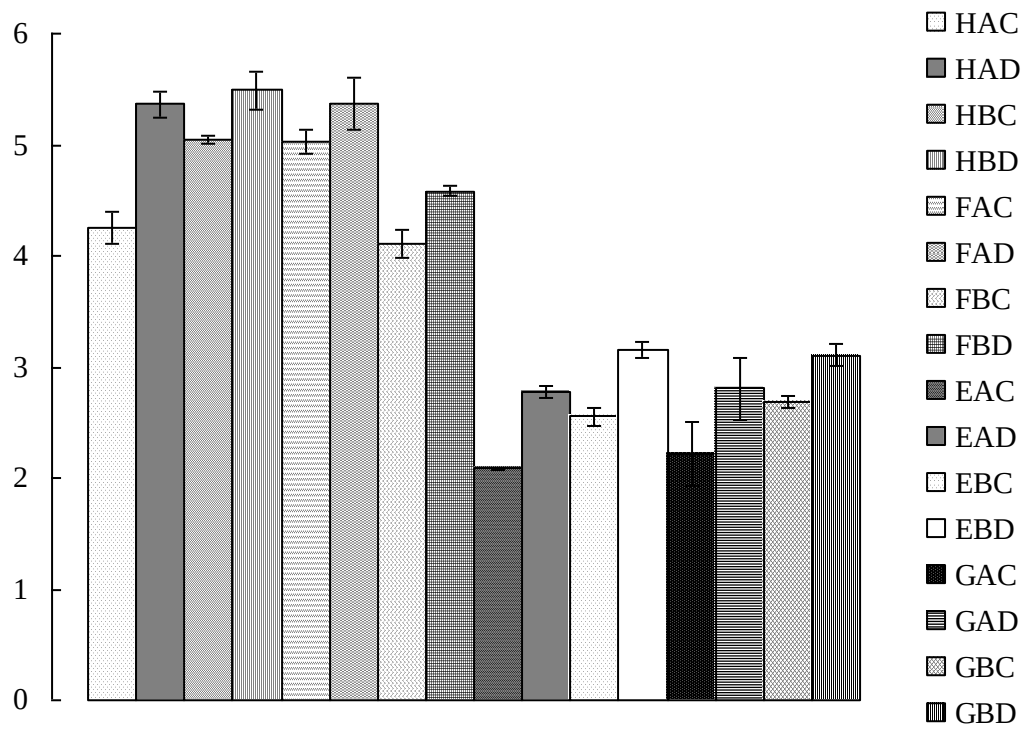

Figure 3.4 OA saturation solubility in SEOA NS. Data is presented as mean (mg/mL) ± Std from three independent experiments repeated triplicate.

Table 3.3 Comparison of OA saturation solubility and EE %

NS	Saturation Solubility (mg/mL)	EE %
1.FBC	$4.10 \pm 0.13^{3,4,5,6,7,8,9,10,11,12,13,14,15,16}$	$41.03 \pm 1.26^{3,4,5,6,7,8,9,10,11,12,13,14,15,16}$
2.HAC	$4.25 \pm 0.14^{3,5,6,7,8,9,10,11,12,13,14,15,16}$	$42.49 \pm 1.45^{3,5,6,7,8,9,10,11,12,13,14,15,16}$
3.EAC	$2.08 \pm 0.00^{1,2,4,5,6,7,8,10,11,12,13,14,15,16}$	$20.82 \pm 0.04^{1,2,4,5,6,7,8,10,11,12,13,14,15,16}$
4.FBD	$4.58 \pm 0.04^{1,3,5,6,7,8,9,\ 10,11,12,13,14,15,16}$	$45.79 \pm 0.43^{1,3,5,6,7,8,9,\ 10,11,12,13,14,15,16}$
5.HAD	$5.36 \pm 0.12^{1,2,3,4,\ 6,7,8,9,\ 10,11,12}$	$53.63 \pm 1.17^{1,2,3,4,\ 6,7,8,9,\ 10,11,12}$
6.EAD	$2.77 \pm 0.05^{1,2,3,4,5,9,13,14,15,16}$	$27.70 \pm 0.54^{1,2,3,4,5,9,13,14,15,16}$
7.EBC	$2.55 \pm 0.08^{1,2,3,4,5,,8,12,13,14,15,16}$	$25.51 \pm 0.77^{1,2,3,4,5,,8,12,13,14,15,16}$
8.EBD	$3.15 \pm 0.07^{1,2,3,4,5,7,9,11,13,14,15,16}$	$31.51 \pm 0.71^{1,2,3,4,5,7,9,11,13,14,15,16}$
9.GAC	$2.22 \pm 0.29^{1,2,4,5,6,8,10,11,12,13,14,15,16}$	$22.17 \pm 2.93^{1,2,4,5,6,8,10,11,12,13,14,15,16}$
10.GAD	$2.81 \pm 0.28^{1,2,3,4,5,9,13,14,15,16}$	$28.11 \pm 2.79^{1,2,3,4,5,9,13,14,15,16}$
11.GBC	$2.68 \pm 0.06^{1,2,3,4,5,8,9,13,14,15,16}$	$26.83 \pm 0.60^{1,2,3,4,5,8,9,13,14,15,16}$
12.GBD	$3.11 \pm 0.10^{1,2,3,4,5,7,9,\ 13,14,15,16}$	$31.08 \pm 0.96^{1,2,3,4,5,7,9,\ 13,14,15,16}$
13.HBC	$5.04 \pm 0.03^{1,2,3,4,6,7,8,9,10,11,12,14}$	$50.41 \pm 0.34^{1,2,3,4,6,7,8,9,10,11,12,14}$
14.HBD	$5.49 \pm 0.16^{1,2,3,4,6,7,8,9,10,11,12,13,15}$	$54.88 \pm 1.64^{1,2,3,4,6,7,8,9,10,11,12,13,15}$
15.FAC	$5.03 \pm 0.11^{1,2,3,4,6,7,8,9,10,11,12,14}$	$50.35 \pm 1.08^{1,2,3,4,6,7,8,9,10,11,12,14}$
16.FAD	$5.36 \pm 0.23^{1,2,3,4,6,7,8,9,10,11,12}$	$53.63 \pm 2.32^{1,2,3,4,6,7,8,9,10,11,12}$

Data represent 3 independent experiments repeated in triplicate. Values are presented as means $\pm$ std. [1], significantly different compared with FBC. [2], significantly different compared with HAC. [3], significantly different compared with EAC. [4], significantly different compared with FBD. [5], significantly different compared with HAD. [6], significantly different compared with EAD. [7], significantly different compared with EBC. [8], significantly different compared with EBD. [9], significantly different compared with GAC, [10], significantly different compared with GAD. [11], significantly different compared with GBC, [12], significantly different compared with GBD.[13], significantly different compared with HBC, [14], significantly different compared with HBD. [15], significantly different compared with FAC. [16], significantly different compared with FAD ($p<0.05$) Statistics were carried out by one- way ANOVA.

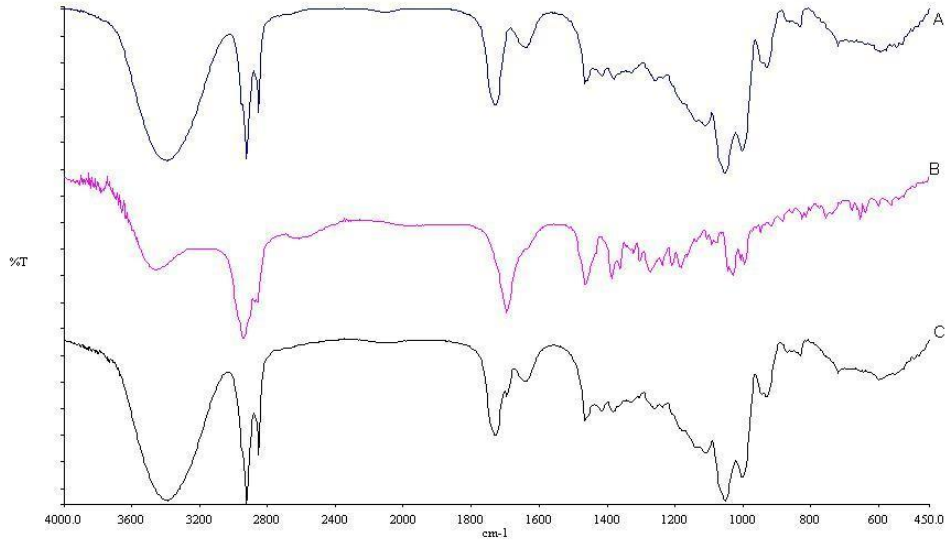

Figure 3.5 FTIR spectra of lyophilized SEOA-GBD NS (A), free OA (B) and physical mixture of SEL and SEP at 9 : 1 (w/w) (C).

3.4.1.5 STABILITY OF SEOA NS

Physical stability of SEOA NS can be elucidated from the data shown in Table 3.4. Although the initial particle size was very small upon manufacture, most of the particles tended to aggregate together with time and grow to much larger entities after prolonged storage. After storage for 15 days, size change found ranged from 15.9 % to 3510.6 % and 30 days storage produced growth ranged from 37.4 % to 4467.4 %. Among the products prepared, GBD (23.5 % for 15 days, and 37.4 % for 30 days) and GAD (15.9 % for 15 days, and 47.0 % for 30 days) were the more stable SEOA NS products.

Table 3.5 demonstrates the chemical stability of SEOA NS. During the first 15 days storage, most of the NS products were relatively stable (>80 % relative concentration). The chemical stability after 30 days storage varied from 68.7 % to 93.7 %. GBD (103.5 % for 15 days, and 93.7 % for 30 days) was the most stable formulation among all the products produced.

Table 3.4 Physical stability of SEOA NS

	NS	15-day size change (%)	30-day size change (%)
1	FBC	1230.91 ± 774.40 [2,3,7,9.10,11,12,13,14,15,16]	1405.94 ± 400.95 [2,3,7,9,10,11,12,13,14,15,16]
2	HBD	227.65 ± 36.78 [1,3,4,6,7,8]	272.71 ± 212.84 [1,3,4,6,7,8]
3	HAC	3510.55 ± 1017.02 [1,2,4,5,6,7,8,9,10,11,12,13,14,15,16]	4705.99 ± 1354.43 [1,2,4,5,6,8,9,10,11,12,13,14,15,16]
4	HAD	1062.11 ± 181.51 [2,3,7,8,9, 10,11,12,13,14,15,16]	1989.83 ± 768.56 [2,3,7,9, 10,11,12,13,14,15,16]
5	HBC	532.32 ± 182.68 [3,7,8]	1294.42 ± 282.78 [3,7,9, 10,11,12,13,14,15,16]
6	FBD	1074.16 ± 520.54 [2,3,7,8,9, 10,11,12,13,14,15,16]	1868.55 ± 960.09 [2, 3,7,9, 10,11,12,13,14,15,16]
7	FAC	2321.58 ± 861.31 [1,2,3,4,5,6,9,10,11,12,13,14,15,16]	4467.42 ± 1481.09 [1,2,4,5,6,8, 9, 10,11,12,13,14,15,16]
8	FAD	1877.58 ± 813.64 [2,3,4,5,6, 9,10,11,12,13,14,15,16]	1882.04 ± 571.84 [2,3,7, 9, 10,11,12,13,14,15,16]
9	EAC	127.13 ± 6.48 [1,3,4,6,7,8]	245.30 ± 5.15 [1,3,4,5,6,7,8]
10	EAD	97.09 ± 5.97 [1,3,4,6,7,8]	101.85 ± 3.10 [1,3,4,5,6,7,8]
11	EBC	45.92 ± 1.88 [1,3,4,6,7,8]	140.82 ± 8.61 [1,3,4,5,6,7,8]
12	EBD	27.58 ± 2.37 [1,3,4,6,7,8]	126.64 ± 12.93 [1,3,4,5,6,7,8]
13	GAC	37.32 ±2.75 [1,3,4,6,7,8]	79.82 ± 12.82 [1,3,4,5,6,7,8]
14	GAD	15.87 ± 2.96 [1,3,4,6,7,8]	46.98 ± 7.90 [1,3,4,5,6,7,8]
15	GBC	31.16 ± 3.55 [1,3,4,6,7,8]	105.81 ± 11.42 [1,3,4,5,6,7,8]
16	GBD	23.45 ± 2.04 [1,3,4,6,7,8]	37.41 ± 4.06 [1,3,4,5,6,7,8]

Data represent 3 independent experiments repeated in triplicate. Original particle sizes of NS were set as 100. Values are presented as means ± std. [1], significantly different compared with FBC. [2], significantly different compared with HBD. [3], significantly different compared with HAC. [4], significantly different compared with HAD. [5], significantly different compared with HBC. [6], significantly different compared with FBD. [7], significantly different compared with FAC. [8], significantly different compared with FAD. [9], significantly different compared with EAC, [10], significantly different compared with EAD. [11], significantly different compared with EBC, [12], significantly different compared with EBD.[13], significantly different compared with GAC, [14], significantly different compared with GAD. [15], significantly different compared with GBC. [16], significantly different compared with GBD ($p<0.05$). Statistics were carried out by one- way ANOVA.

Table 3.5 Chemical stability of SEOA NS

NS		15-day relative concentration (%)	30-day relative concentration (%)
1	FBC	$99.66 \pm 0.74^{4,5,7,8,13}$	$84.78 \pm 2.92^{4,5,8,14}$
2	HAC	$87.42 \pm 0.47^{3,9,11,12}$	$80.85 \pm 5.20^{5,12,14}$
3	EAC	$101.55 \pm 4.26^{2,4,5,6,7,8,13}$	$87.23 \pm 2.14^{4,5,8,14}$
4	FBD	$83.35 \pm 1.68^{1,3,9,10,11,12}$	$74.79 \pm 5.29^{1,3,9,10,12,16}$
5	HAD	$83.46 \pm 6.83^{1,3,9,10,11,12}$	$68.68 \pm 4.96^{1,2,3,6,7,9,10,11,12,13,15,16}$
6	EAD	$87.01 \pm 8.10^{3,9,11,12}$	$80.81 \pm 6.89^{5,12,14}$
7	EBC	$80.71 \pm 0.44^{1,3,9,10,11,12}$	$79.95 \pm 9.05^{5,9,12}$
8	EBD	$80.01 \pm 1.07^{1,3,9,10,11,12}$	$75.73 \pm 5.06^{1,3,9,10,12,16}$
9	GAC	$107.24 \pm 11.86^{2,4,5,6,7,8,13,14,15,16}$	$88.98 \pm 1.58^{4,5,7,8,13,14}$
10	GAD	$99.24 \pm 9.57^{4,5,7,8,13}$	$85.55 \pm 0.30^{4,5,8,14}$
11	GBC	$101.87 \pm 18.30^{2,4,5,6,7,8,13}$	$82.89 \pm 0.34^{5,12,14}$
12	GBD	$103.50 \pm 9.74^{2,4,5,6,7,8,13,15}$	$93.68 \pm 3.70^{2,4,5,6,7,8,11,13,14,15}$
13	HBC	$84.98 \pm 5.37^{1,3,9,10,11,12}$	$78.43 \pm 11.69^{5,9,12}$
14	HBD	91.09 ± 5.43^{9}	$71.12 \pm 0.70^{1,2,3,6,9,10,11,12,15,16}$
15	FAC	$89.36 \pm 6.92^{9,12}$	$81.42 \pm 6.39^{5,12,14}$
16	FAD	91.52 ± 6.56^{9}	$86.23 \pm 5.36^{4,5,8,14}$

Data represent 3 independent experiments repeated in triplicate. Original OA concentrations in NS were set as 100. Values are presented as means $\pm$ std. [1], significantly different compared with FBC. [2], significantly different compared with HAC. [3], significantly different compared with EAC. [4], significantly different compared with FBD. [5], significantly different compared with HAD. [6], significantly different compared with EAD. [7], significantly different compared with EBC. [8], significantly different compared with EBD. [9], significantly different compared with GAC, [10], significantly different compared with GAD. [11], significantly different compared with GBC, [12], significantly different compared with GBD.[13], significantly different compared with HBC, [14], significantly different compared with HBD. [15], significantly different compared with FAC. [16], significantly different compared with FAD ($p<0.05$). Statistics were carried out by one- way ANOVA.

3.4.1.6 ANALYSIS OF THE INFLUENCE OF PROCESS VARIABLES ON NS PROPERTIES

3.4.1.6.1. ANALYSIS OF PARTICLE SIZE INFLUENCING FACTORS

To find out how the four main production parameters (milling speed, milling time, SEL : SEP ratio and SE : OA ratio) influenced the particle size of SEOA NS, a factorial design was planned and results analysed by the use of the Minitab software (version 15, Minitab Inc. State College, Pennsylvania, USA).

From Figures 3.6a and b, most of the main parameters and their interactions had significant relationship with the resultant particle size ($p<0.05$) but not including milling time and its interactions (the standardized effect value below 2.04, $p>0.05$, Figure 3.6b). To further analysis the main effects, the three main parameters with significant effects were compared together (Figure 3.6c). Among them, RPM (milling speed) had the steepest slope, which meant that it had the largest impact. Relatively slower milling speed tended to yield smaller particle size NS. This finding may be attributed to the high milling speed which had produced more heat-related effects due to impact energy generated during ball milling preparation process. The NS products were hence more likely aggregated together, to form larger entities and hence reduced the surface free energy. Higher SEL to SEP ratio led to smaller particle size products and this was due to better stabilization effects of surfactant ratio. Lower SE : OA ratio produced lower drug encapsulation by surfactants and hence, also smaller particle sized products.

Interactive effect analysis was carried out to study the interactions between the three

main factors and findings are shown in Figures 3.6d1, d2 and d3. From Figure 3.6d1, in the study on the relationship between milling speed and SE : OA ratio, a lower milling speed (300 rpm) and higher SE : OA ratio (10 : 1) produced NS with smaller particle sizes. With a higher milling speed (600 rpm) and higher SE : OA ratio (10 : 1), the NS products were found to be of bigger particle size.

Figure 3.6d2 illustrates the correlation between SE : OA and SEL : SEP ratio. It was shown that with a lower SE : OA ratio (1 : 1) and bigger SEL : SEP ratio (9 : 1), the product's particle size was smaller. On the contrary, bigger particles were produced with a higher SE : OA ratio (10 : 1) and smaller SEL : SEP ratio (1 : 1).

In Figure 3.6d3, the relationship between milling speed and SEL : SEP ratio showed that smaller particles were produced when a lower milling speed (300 rpm) and smaller SEL : SEP ratio (1 : 1) were used whilst bigger sized products were produced by higher milling speed (600 rpm) and smaller SEL to SEP ratio (1 : 1).

a.

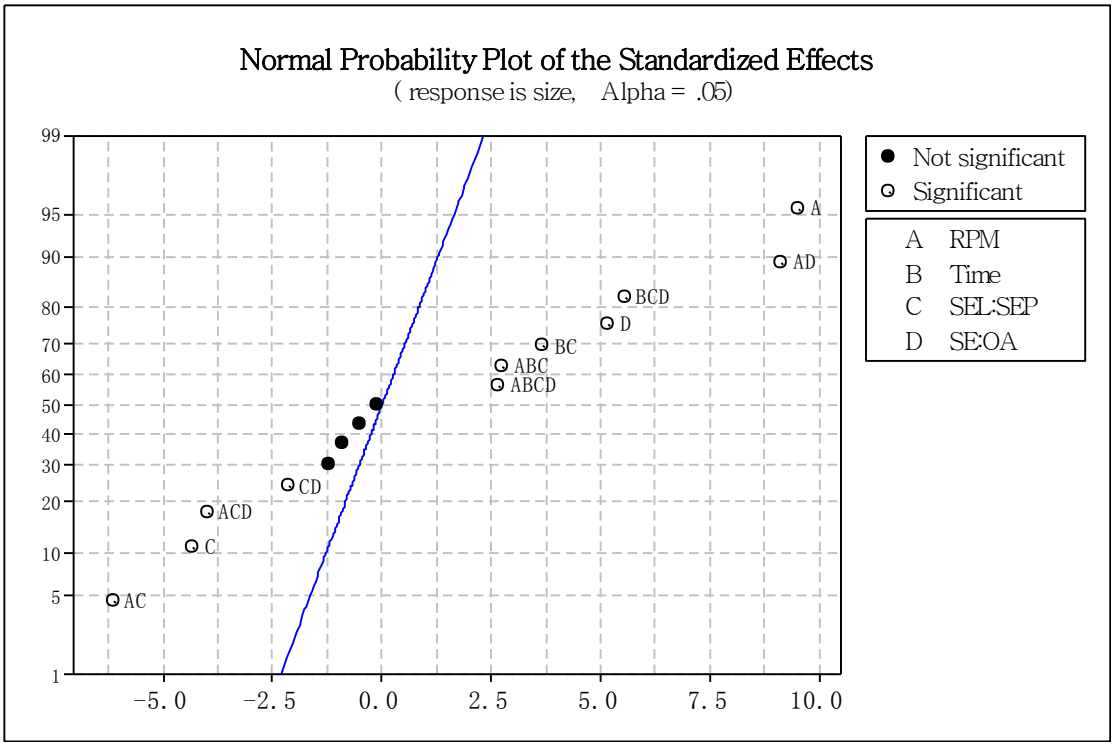
Normal Probability Plot of the Standardized Effects
(response is size, Alpha = .05)
Not significant
Significant
A RPM
B Time
C SEL:SEP
D SE:OA
A
AD
BCD
D
BC
ABC
ABCD
CD
ACD
C
AC
99
95
90
80
70
60
50
40
30
20
10
5
1
-5.0
-2.5
0.0
2.5
5.0
7.5
10.0

b.

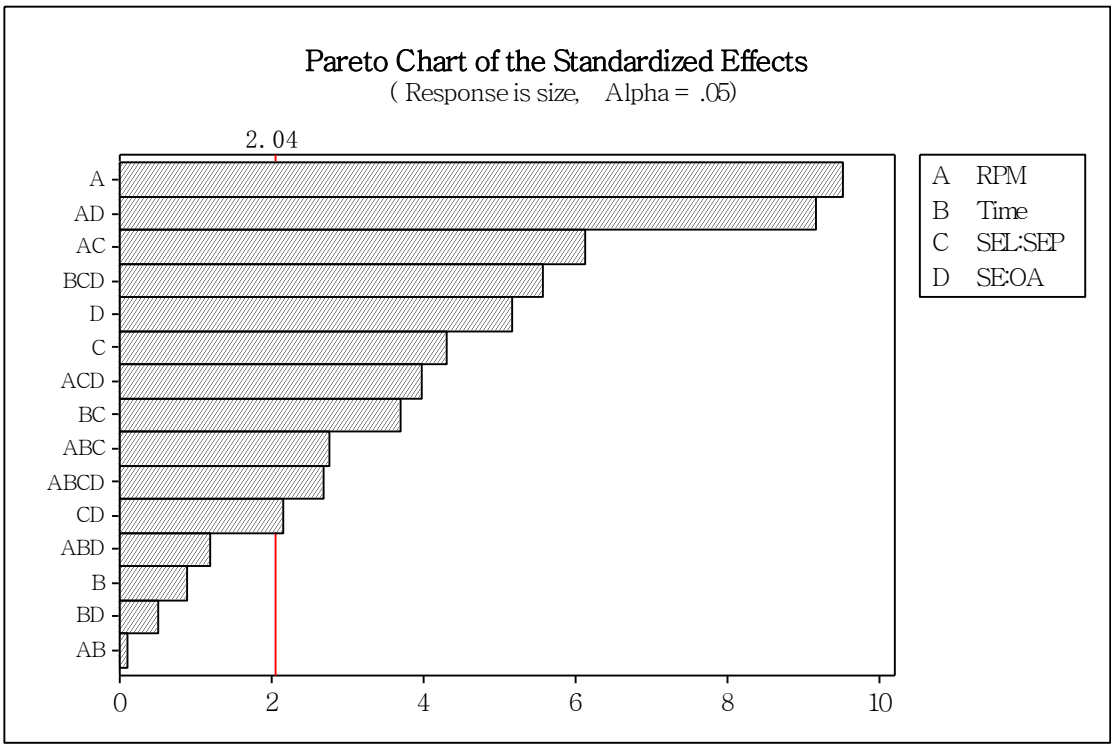
Pareto Chart of the Standardized Effects
(Response is size, Alpha = .05)
2.04
A RPM
B Time
C SEL:SEP
D SE:OA
A
AD
AC
BCD
D
C
ACD
BC
ABC
ABCD
CD
ABD
B
BD
AB
0
2
4
6
8
10

c.

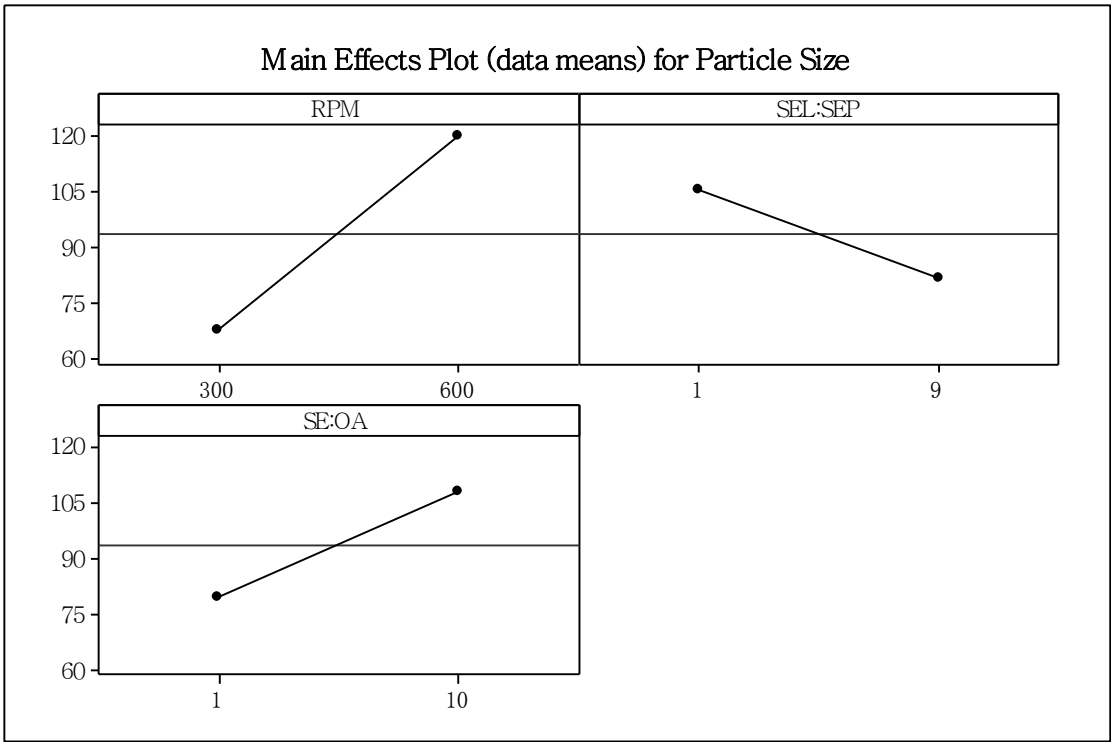
Main Effects Plot (data means) for Particle Size
RPM
SEL:SEP
SE:OA
120
105
90
75
60
300
600
1
9
1
10

d1

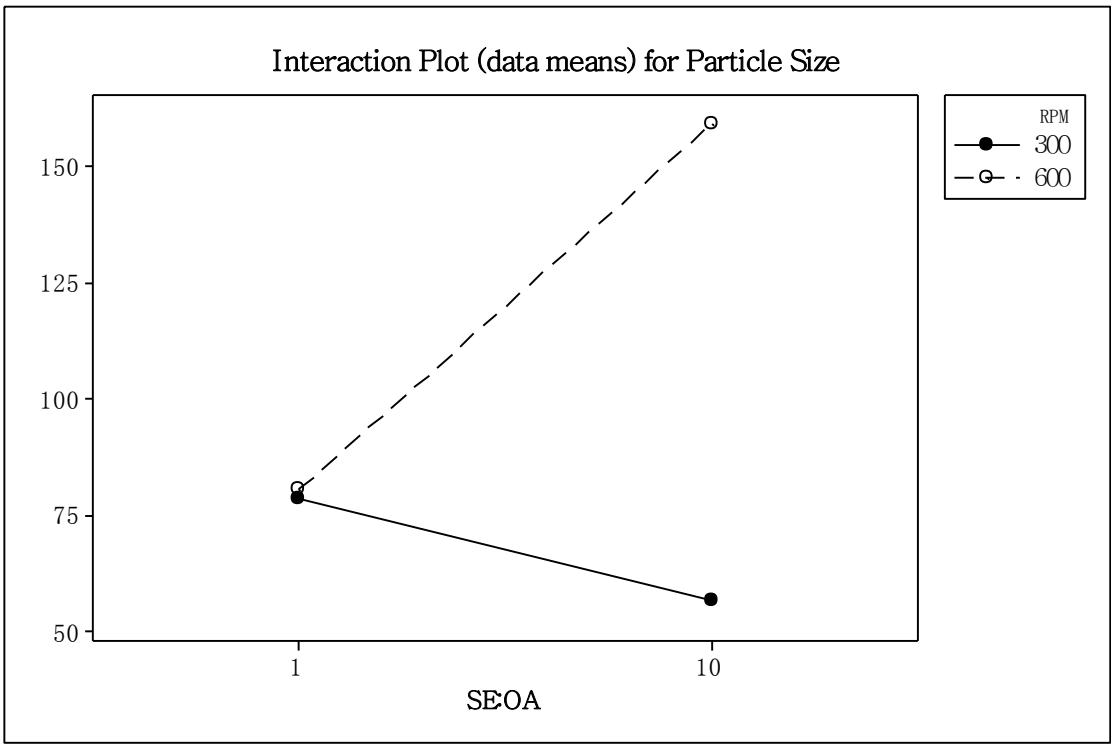
Interaction Plot (data means) for Particle Size
RPM
300
600
150
125
100
75
50
1
10
SE:OA

d2

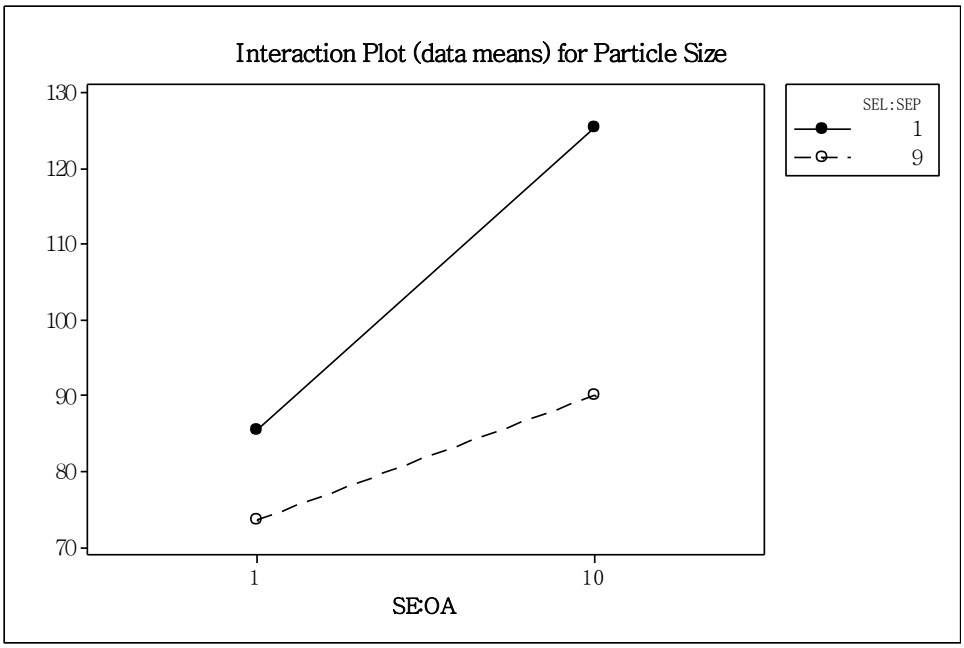

d3

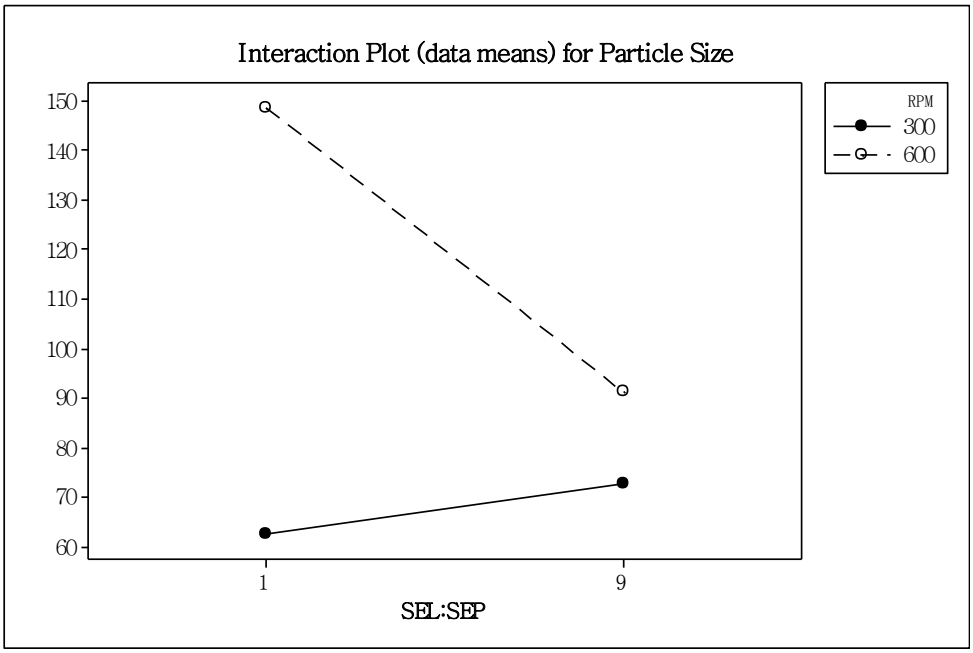

Figure 3.6 Minitab analysis of Particle Size influence factors. Normal Probability Plot of the Standardized Effects (3.6a), Pareto Chart of the Standardized Effects (3.6b), Main Effects Plot (data means) for Particle Sizes (3.6c), Interaction Plot (data means) for Particle sizes between milling speed and SE : OA (3.6d1),. Interaction Plot (data means) for Particle sizes between SE : OA and SEL : SEP (3.6d2), and Interaction Plot (data means) for Particle sizes between milling speed and SEL : SEP (3.6d3).

3.4.1.6.2. ANALYSIS THE FACTORS INFLUENCING THE PDI OF NS PRODUCTS

The four main production parameters (milling speed, milling time, SEL : SEP ratio and SE : OA ratio) were studied for their impact on the PDI of SEOA NS by the use of a factorial design.

From Figures 3.7a and b, all of the four parameters and their interactions had significant relationship with the PDI value ($p<0.05$) and SE : OA ratio had the highest effects (Figure 3.7b). For further analysis of the main effects, the four main production parameters were compared with one another (Figure 3.7c). Amongst the parameters, SE : OA ratio was found to possess the largest slope, which meant that it had the strongest influencing effect. Although higher SE : OA ratio showed higher drug encapsulation efficiency and higher saturation solubility, it was also found to be associated with resulting in larger particle sizes (Figure 3.6c) and wider PDI distributions and may had implied reduced stability of the production process. Faster milling speed and longer milling time had resulted in encapsulating more drug with the higher energy and heat input but the PDI became broader. It was evident that with higher SEL : SEP ratio, the particle size (Figure 3.6c) and PDI were both lower, suggesting that a high SEL : SEP ratio value had a close relationship with the optimized structure of SEOA NS produced and conferred better product stability.

Interaction effects analysis was carried out to study possible interactions between SE : OA ratio and the three other factors (Figures 3.7d1, d2 and d3). From Figure 3.7d1, the relationship between milling time and SE : OA ratio shows that with higher SE : OA ratio (10 : 1) and longer milling time (3 h), the prepared NS had a larger PDI. With a lower SE :

OA ratio (1 : 1) and shorter milling time (1 h), the distribution was relatively smaller.

Figure 3.7d2 illustrates the correlation between SE : OA and milling speed. It was found that with smaller SE : OA ratio (1 : 1), irrespective of the milling speed being slow (300 rpm) or fast (600 rpm), the particle size distributions were narrower. On the contrary, broader particle size distribution was observed with the use of higher SE : OA ratio (10 : 1) at a high milling speed (600 rpm).

Figure 3.7d3 shows the relationship between SE : OA ratio and SEL : SEP ratio and it is noted that when SE : OA was low (l : 1), regardless of the rations of SEL : SEP, low (1 : 1) or high (9 : 1), the PDI remained small. Large PDI values were produced by a low SEL : SEP (1 : 1) ratio when a high SE : OA (10 : 1) ratio was employed.

a

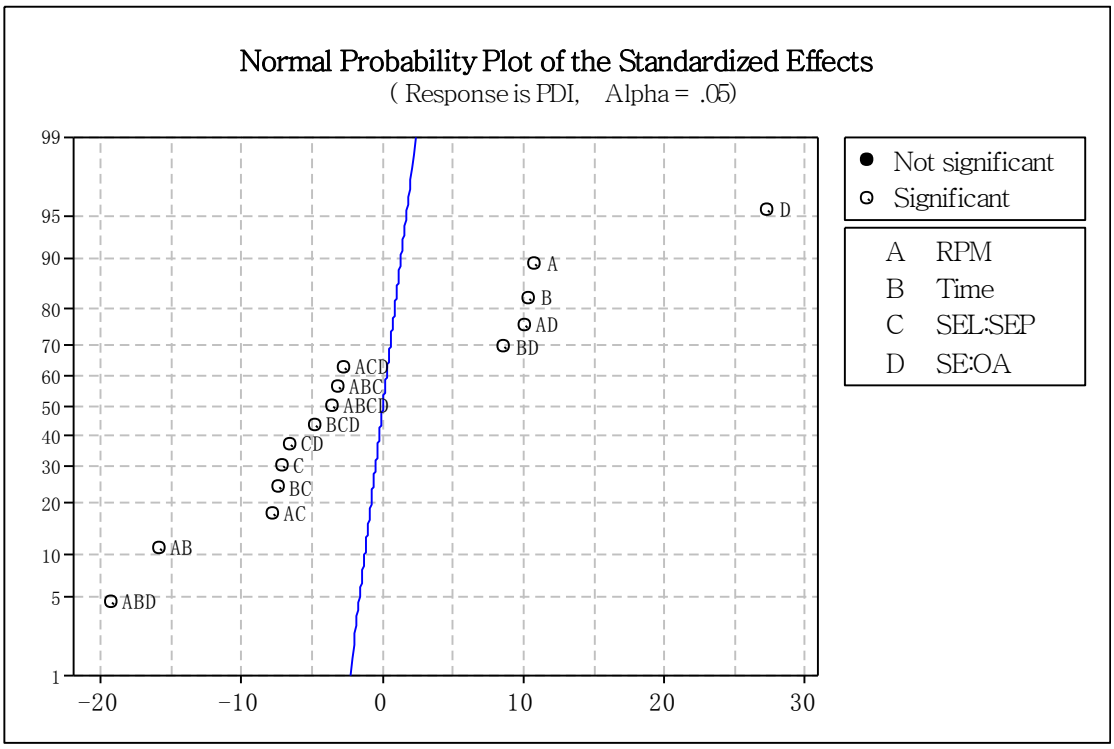
Normal Probability Plot of the Standardized Effects
(Response is PDI, Alpha = .05)
Not significant
Significant
A RPM
B Time
C SEL:SEP
D SE:OA
D
A
B
AD
BD
ACD
ABC
ABCD
BCD
CD
C
BC
AC
AB
ABD
99
95
90
80
70
60
50
40
30
20
10
5
1
−20
−10
0
10
20
30

b

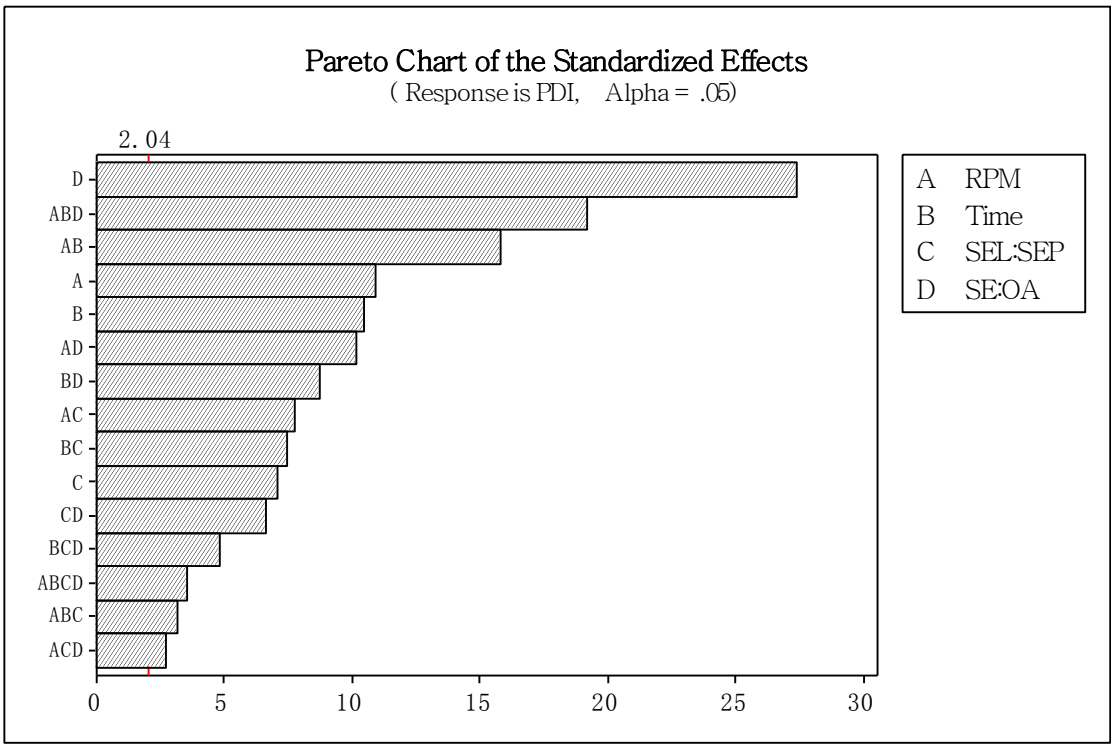
Pareto Chart of the Standardized Effects
(Response is PDI, Alpha = .05)
2.04
A RPM
B Time
C SEL:SEP
D SE:OA
D
ABD
AB
A
B
AD
BD
AC
BC
C
CD
BCD
ABCD
ABC
ACD
0
5
10
15
20
25
30

c

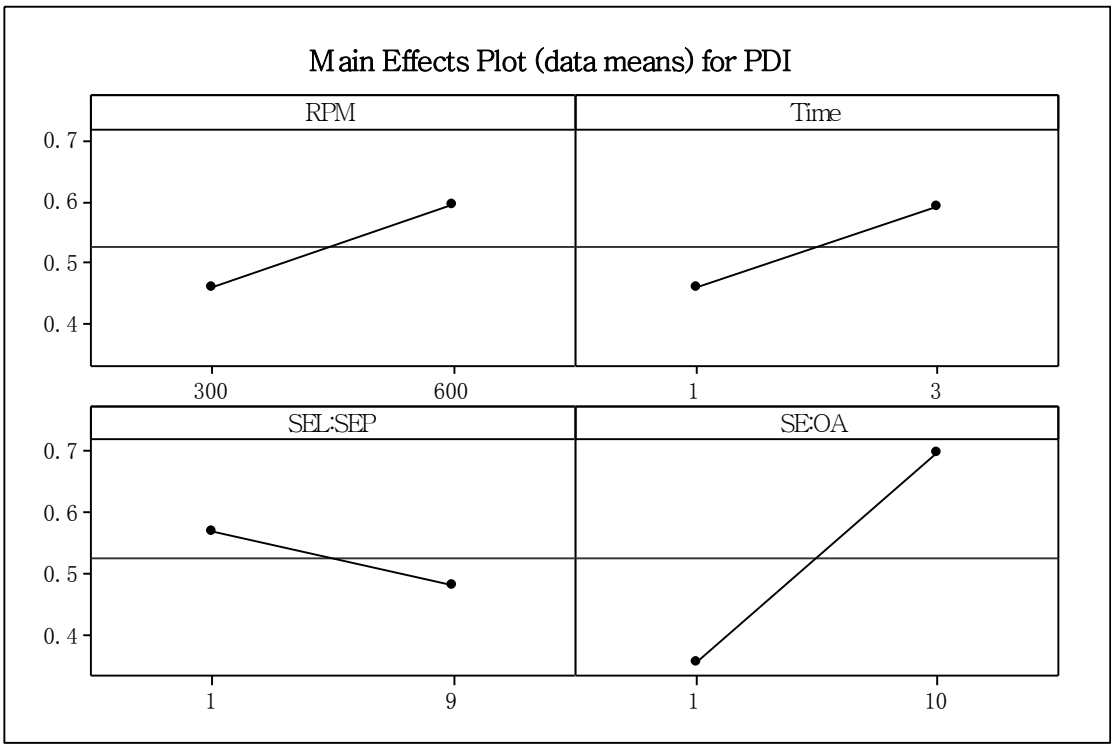
Main Effects Plot (data means) for PDI
RPM
Time
SEL:SEP
SE:OA
0.7
0.6
0.5
0.4
300
600
1
3
1
9
1
10

d1

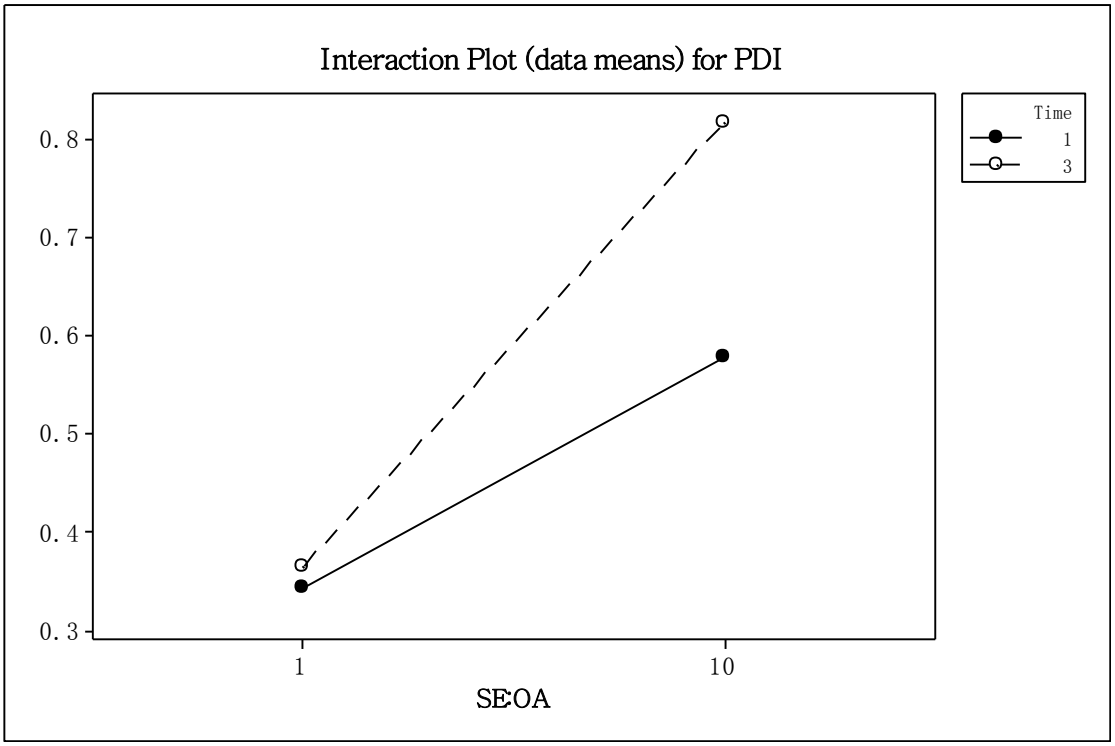
Interaction Plot (data means) for PDI
Time
1
3
0.8
0.7
0.6
0.5
0.4
0.3
1
10
SE:OA

d2

d3

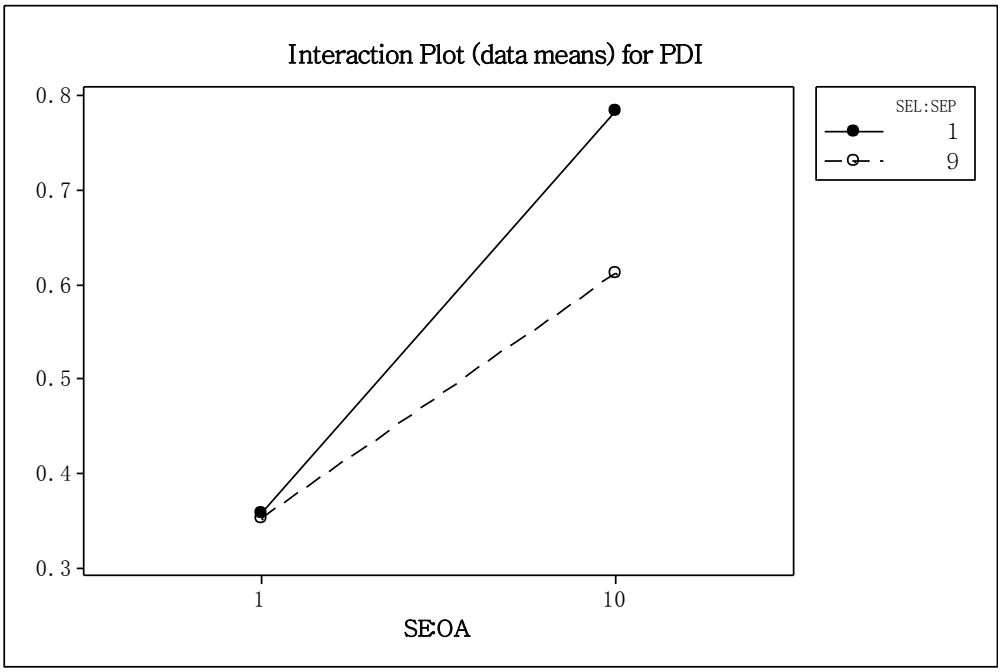

Figure 3.7 Minitab analysis of PDI influence factors. Normal Probability Plot of the Standardized Effects (3.7a), Pareto Chart of the Standardized Effects (3.7b), Main Effects Plot (data means) for PDI (3.7c), Interaction Plot (data means) for PDI between milling time and SE : OA (3.7d1),. Interaction Plot (data means) for PDI between SE : OA and milling speed (3.7d2), and Interaction Plot (data means) for PDI between SE : OA and SEL : SEP (3.7d3).

3.4.1.6.3 ANALYSIS OF THE SATURATION SOLUBILITY INFLUENCING FACTORS

As the initial total amount of OA used was same (1 g) for all formulations studied, the EE % value could be relevant as a determinant parameter to reflect saturation solubility. The examination of how the four production parameters had influenced the final OA saturation solubility in SEOA NS and the results of the factorial design analysis were critically examined.

From Figures 3.8a and b, most of the production parameters (including SE : OA ratio, milling time, interaction between milling speed and SEL to SEP ratio) are shown to have significant relationships with the saturation solubility ($p<0.05$). To further analysis this relationship, the four main production parameters were compared together (Figure 3.8c). Among the parameters, milling time and SE to OA ratio showed steeper slopes, which meant their higher influences. The two factors were selected for further interactive effect analysis (Figures 3.8d and e). The results showed that SE : OA ratio had a stronger influence on saturation solubility than time (a steeper slope) and hence, it was considered as the most important factor associated with saturation solubility. A possible reason for this was that the presence of a higher concentration of surfactant could have brought about better encapsulation, and more drugs were encapsulated. Prolonging the milling time was also seen to help to encapsulate more drugs. The interaction effect shown in Figure 3.8e indicates that with a high SE : OA ratio (10:1) and 3 h milling improved the yield SEOA NS by generating products with the highest saturation solubility.

a

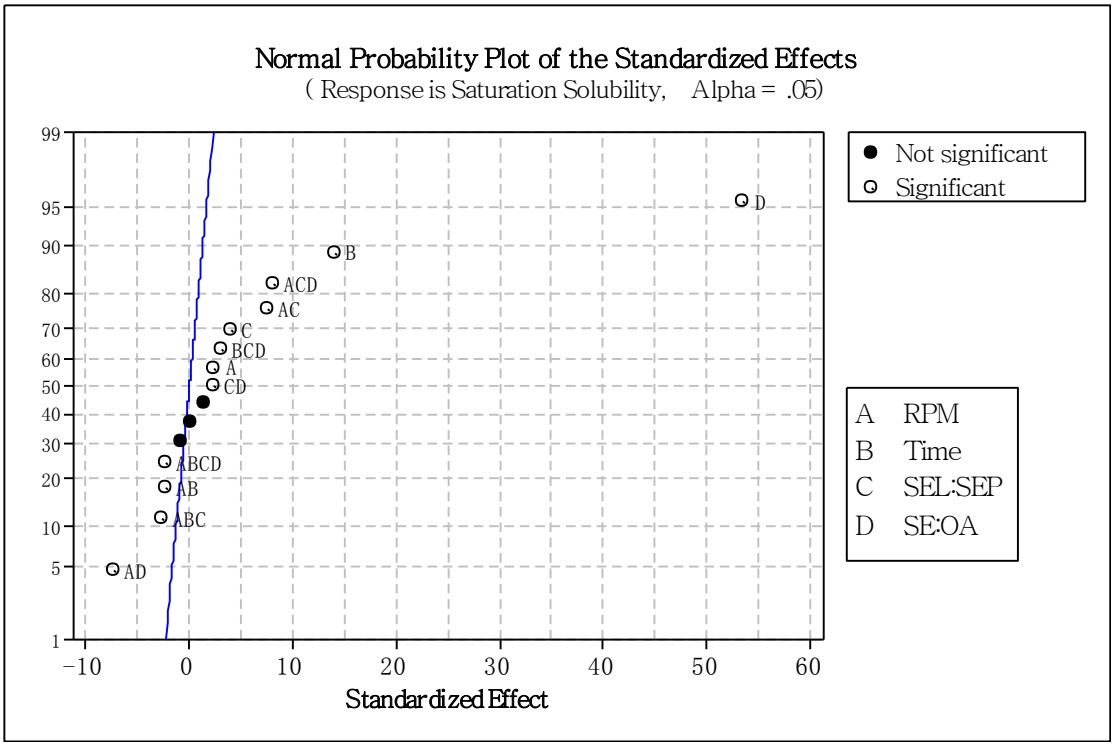
Normal Probability Plot of the Standardized Effects
(Response is Saturation Solubility, Alpha = .05)
Not significant
Significant
A RPM
B Time
C SEL:SEP
D SE:OA
D
B
ACD
AC
C
BCD
A
CD
ABCD
AB
ABC
AD
99
95
90
80
70
60
50
40
30
20
10
5
1
−10
0
10
20
30
40
50
60
Standardized Effect

b.

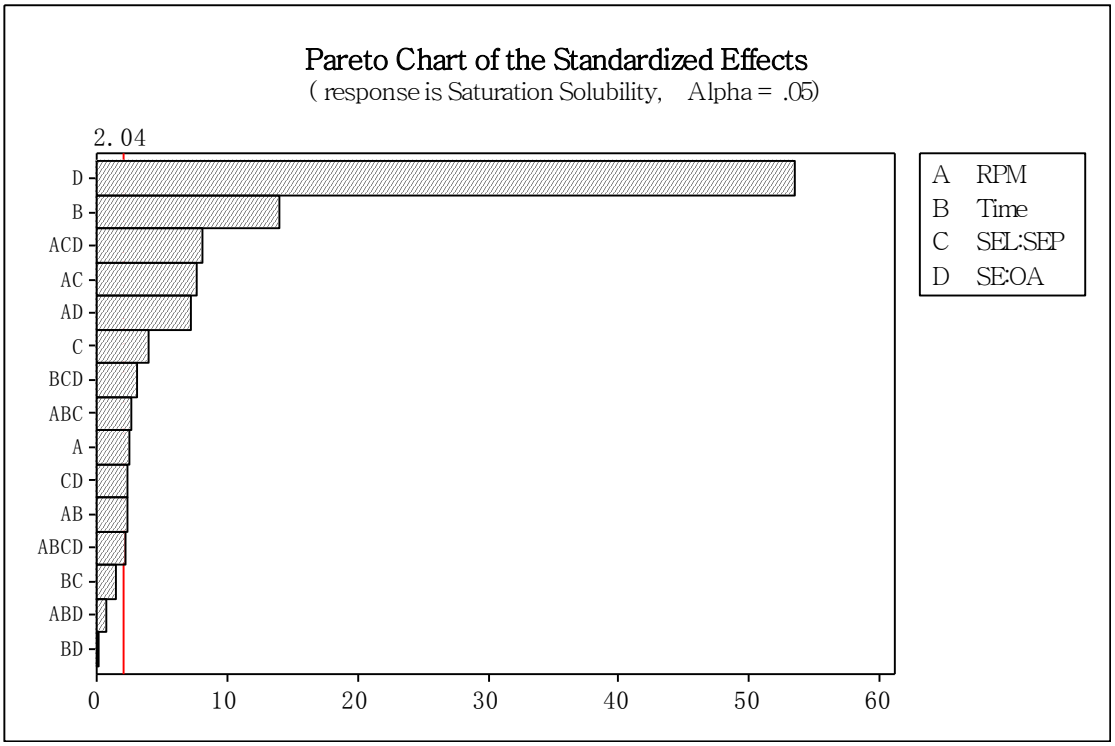
Pareto Chart of the Standardized Effects
(response is Saturation Solubility, Alpha = .05)
2.04
A RPM
B Time
C SEL:SEP
D SE:OA
D
B
ACD
AC
AD
C
BCD
ABC
A
CD
AB
ABCD
BC
ABD
BD
0
10
20
30
40
50
60

c

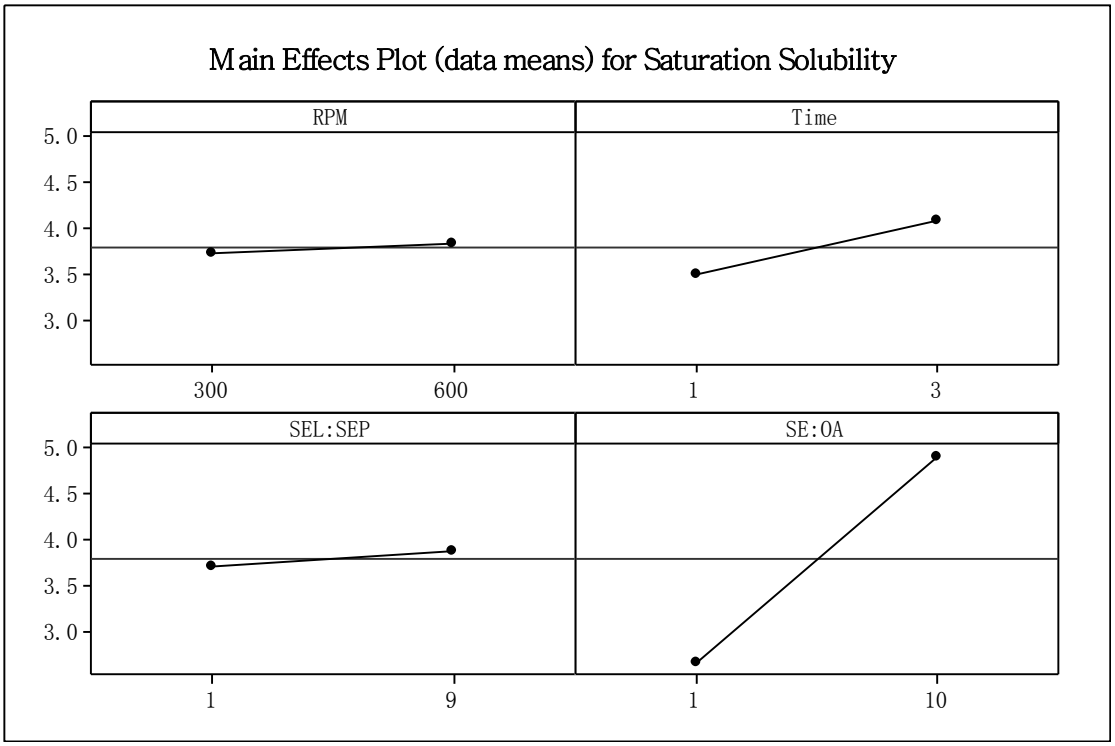
Main Effects Plot (data means) for Saturation Solubility
RPM
Time
SEL:SEP
SE:OA
5.0
4.5
4.0
3.5
3.0
300
600
1
3
1
9
1
10

d

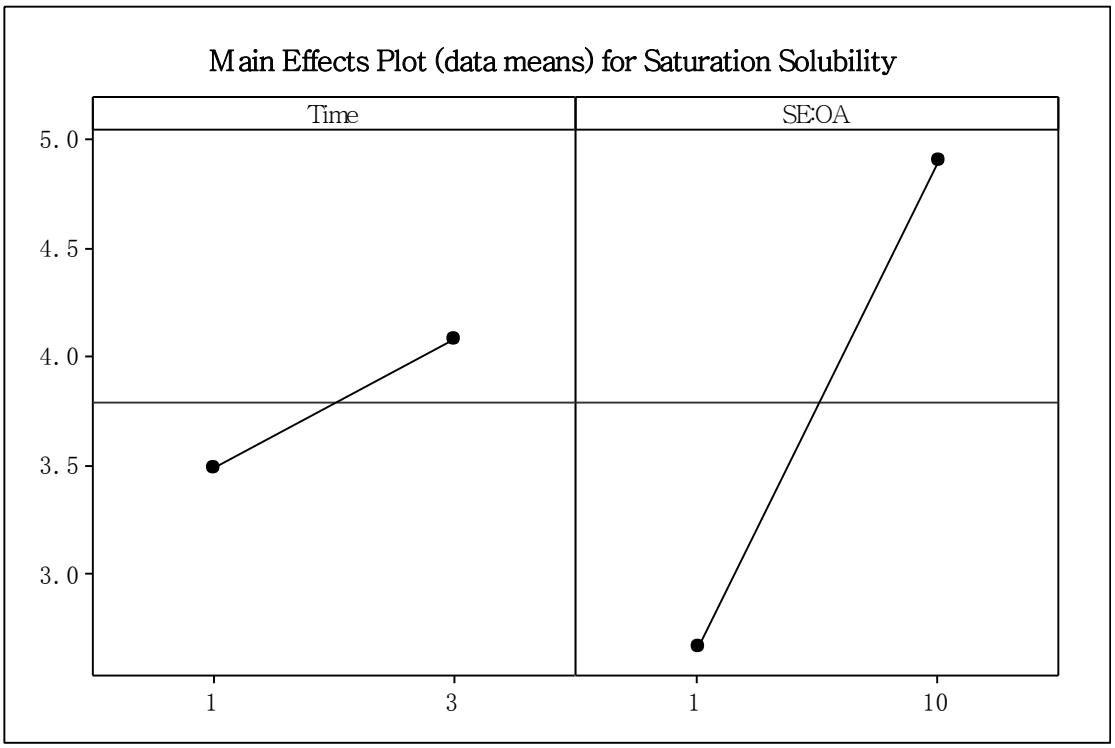
Main Effects Plot (data means) for Saturation Solubility
Time
SE:OA
5.0
4.5
4.0
3.5
3.0
1
3
1
10

e

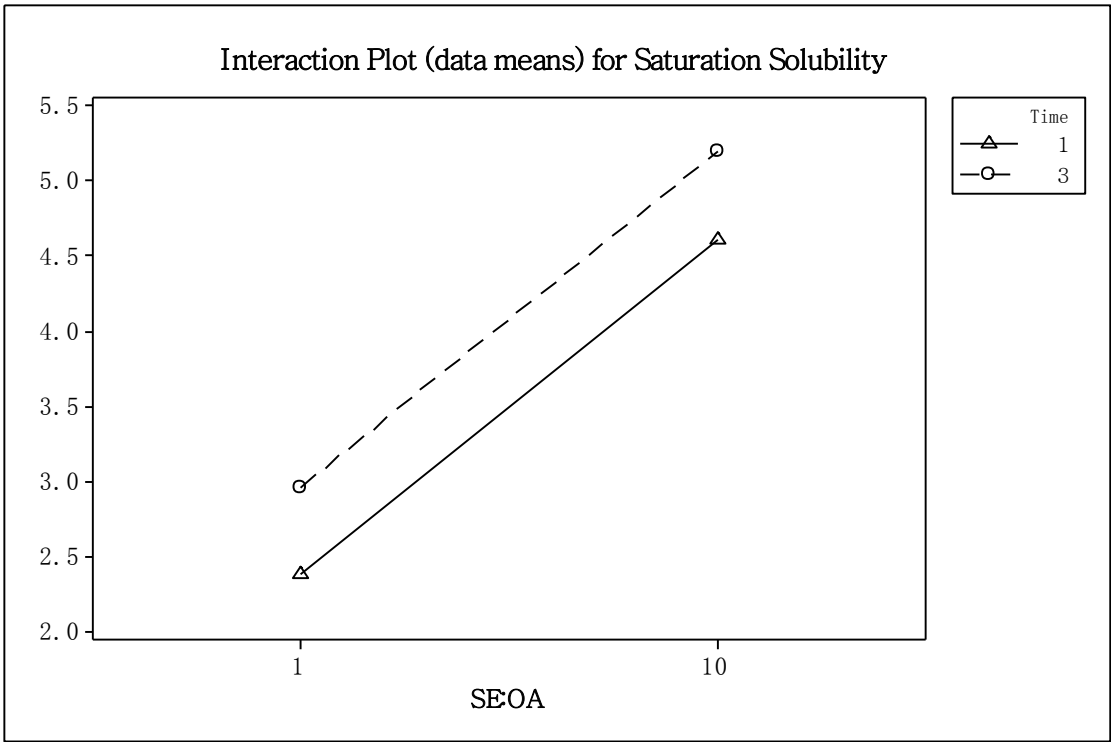

Figure 3.8 Minitab analysis of Saturation Solubility influence factors. Normal Probability Plot of the Standardized Effects (3.8a), Pareto Chart of the Standardized Effects (3.8b), Main Effects Plot (data means) for Saturation Solubility(four parameters) (3.8c), Main Effects Plot (data means) for Saturation Solubility (two major parameters) (3.8d), and Interaction Plot (data means) for Saturation Solubility (3.8e).

3.4.1.6.4 ANALYSIS OF PHYSICAL STABILITY INFLUENCING FACTORS

The effects of the four production parameters influencing the physical stability of SEOA NS were studied by the determination of the differences between the groups through a factorial design analysis on percent particle size change after 30 days of storage.

From Figures 3.9a and b, the main production parameters, SE : OA ratio, milling speed, interaction between milling speed and SE : OA ratio, and their interactions are shown to have significant relationships with the resultant physical stability ($p<0.05$) but not SEL : SEP ratio (the standardized effect value below 2.04, $p>0.05$, Figure 3.9 b). To further study the main effects of influence, the three production parameters with significant effects were compared together (Figure 3.9c). Among them, SE : OA ratio showed the steepest slope, which meant that it had the largest influence effect. Relatively higher SE : OA ratio yielded higher saturation solubility, EE % (discussed in Section 3.4.1.6.3) and hence, higher concentration of SEOA NS. According to Lifshitz–Slesov–Wagner (LSW) theory (77, 78),

$\omega = \frac{dr_N^3}{dt} = \frac{8}{9}[C(\infty)\gamma V_m D/\rho RT]$, Ostwald ripening rate ω (indicating as change rate of particle size) correlates with the saturation solubility C(∞) and interfacial tension γ. More SE could reduce interfacial tension γ and hence slow down the Ostwald ripening process (reducing ripening rate ω). However, it can also increase solubility of OA, which enhance saturation solubility C (∞) and could fasten the Ostwald ripening process (increasing ripening rate ω). If too much SE were used, the fast Ostwald ripening process derived from increased saturation solubility may override the slow down effect and may result in worse physical stability. Longer milling time (3 h) and higher milling speed (600 rpm) may had also helped

to reduce the percent size change and improved the physical stability of NS produced.

Interaction effects analysis was carried out to study the interactive relationships between the production three parameters (Figures 3.9d1, d2 and d3). From Figure 3.9d1, the relationship between milling time and SE : OA ratio shows that with a lower SE : OA ratio (1 : 1), immaterial if the milling time was long (3h) or short (1 h), the percent size change had always remained smaller (i.e. physically more stable). On the other hand, the higher percent size change (less stable) was produced by formulations with a higher SE : OA ratio (10 : 1) with a shorter milling time (1 h).

Figure 3.9d2 illustrates the relationship between SE : OA ratio and milling speed (RPM). It was found that with a smaller SE : OA ratio (1 : 1), regardless whether the milling speed was faster (300 rpm) or slower (600 rpm), the percent size change after 30 days was smaller. Thus, less physically stable NS particles were produced with higher SE : OA ratio (10 : 1) and slower milling speed (300 rpm).

The relationship between milling time and milling speed was studied. More stable SEOA NS were produced by the use of a faster milling speed (600 rpm) and a longer milling time (3 h). The shorter milling time (1 h) and with a slower milling speed often yielded less stable SEOA NS (Figure 3.9d3).

a.

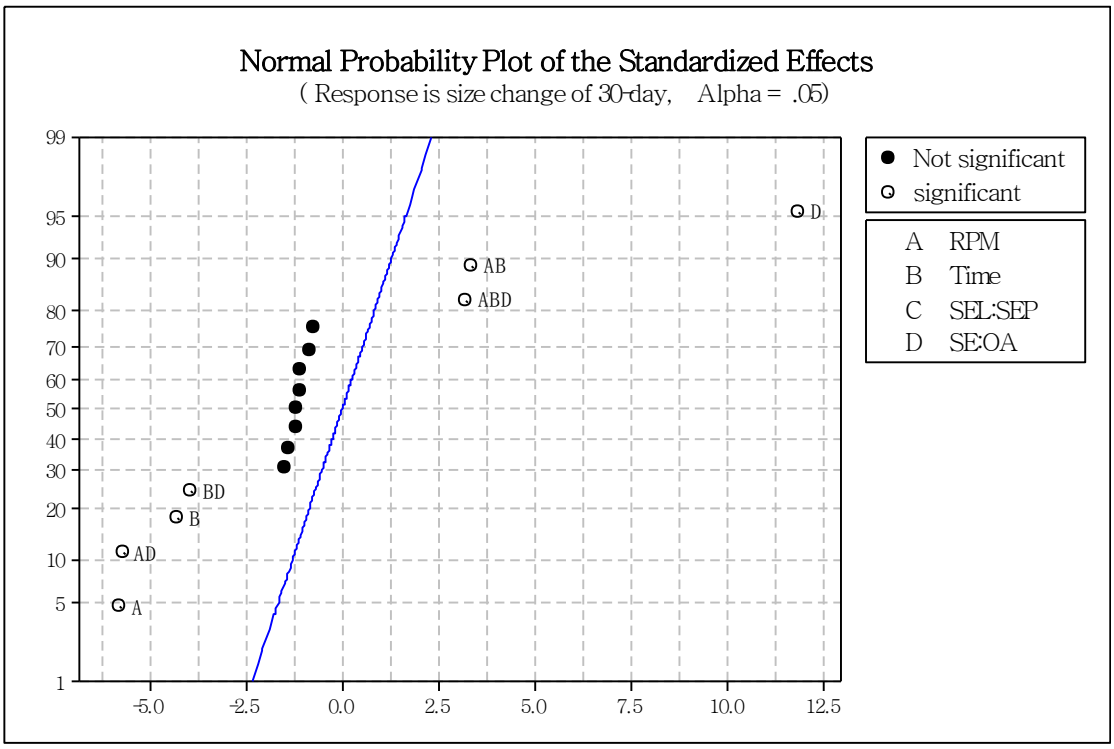
Normal Probability Plot of the Standardized Effects
(Response is size change of 30-day, Alpha = .05)
Not significant
significant
A RPM
B Time
C SEL:SEP
D SE:OA
D
AB
ABD
BD
B
AD
A
99
95
90
80
70
60
50
40
30
20
10
5
1
-5.0
-2.5
0.0
2.5
5.0
7.5
10.0
12.5

b.

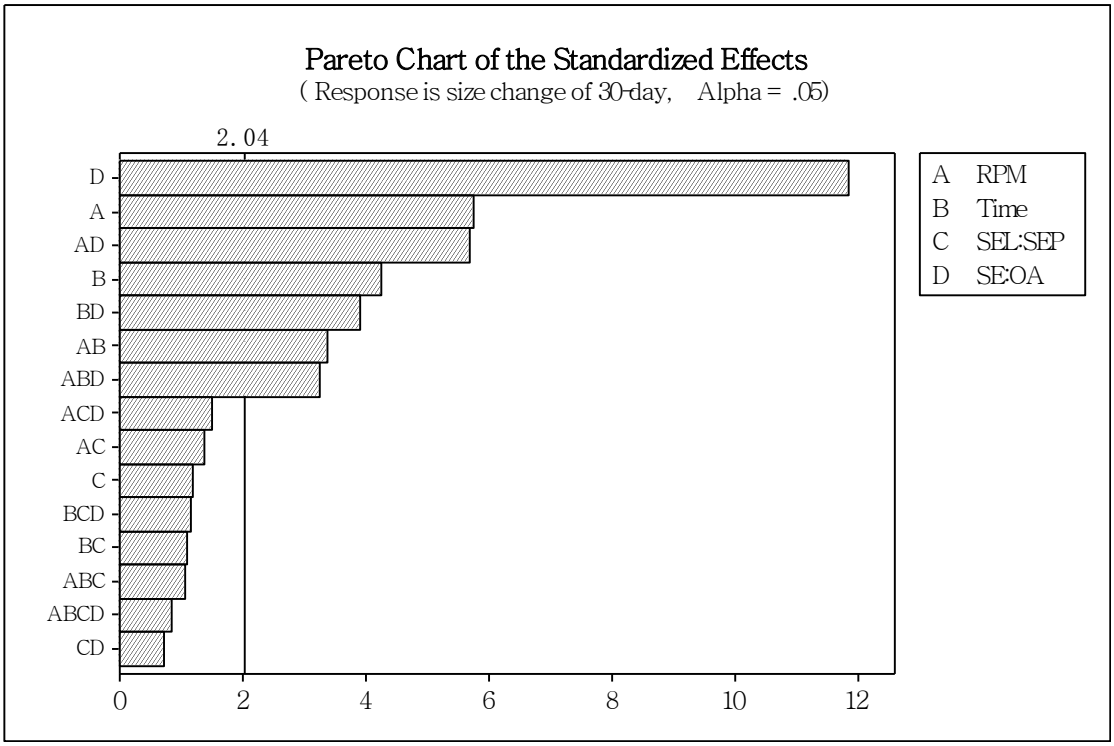
Pareto Chart of the Standardized Effects
(Response is size change of 30-day, Alpha = .05)
2.04
D
A
AD
B
BD
AB
ABD
ACD
AC
C
BCD
BC
ABC
ABCD
CD
A RPM
B Time
C SEL:SEP
D SE:OA
0
2
4
6
8
10
12

c.

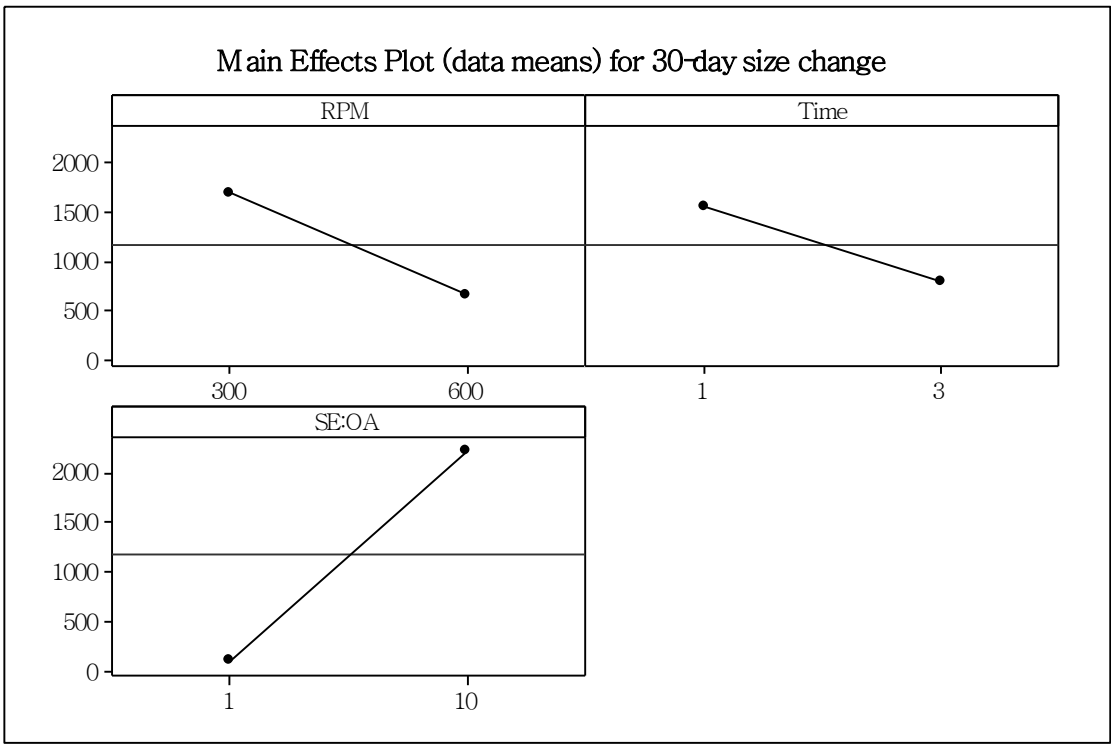
Main Effects Plot (data means) for 30-day size change
RPM
Time
SE:OA
2000
1500
1000
500
0
300
600
1
3
1
10

d1

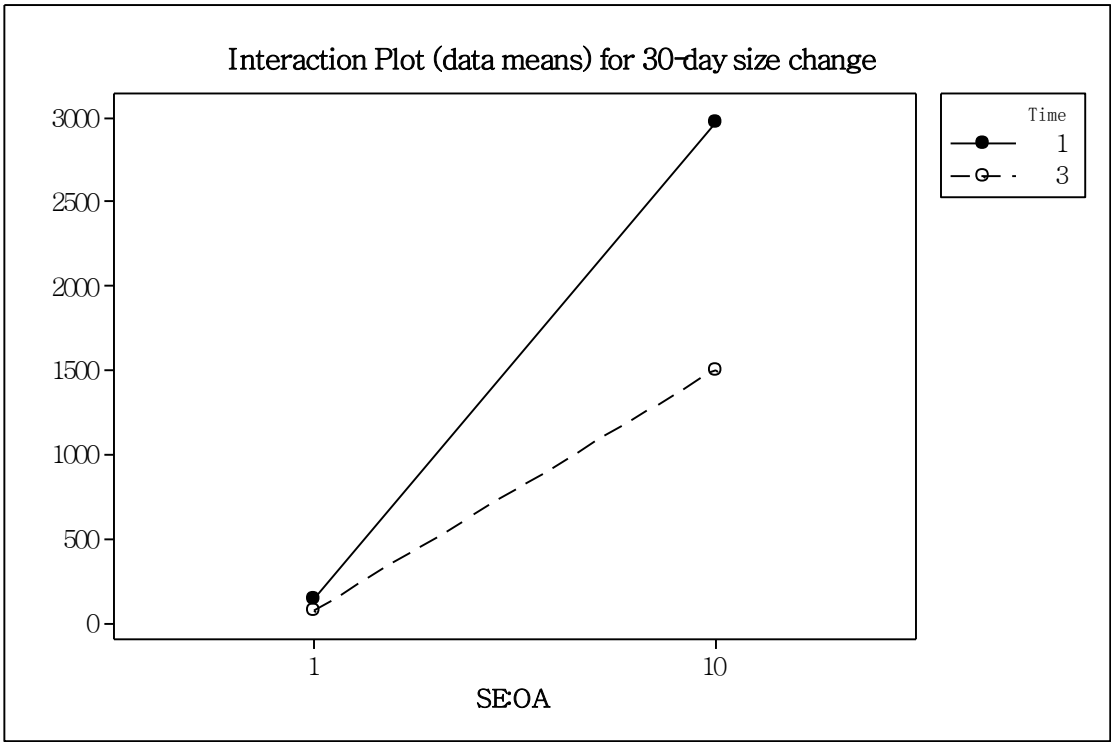
Interaction Plot (data means) for 30-day size change
Time
1
3
3000
2500
2000
1500
1000
500
0
1
10
SE:OA

d2

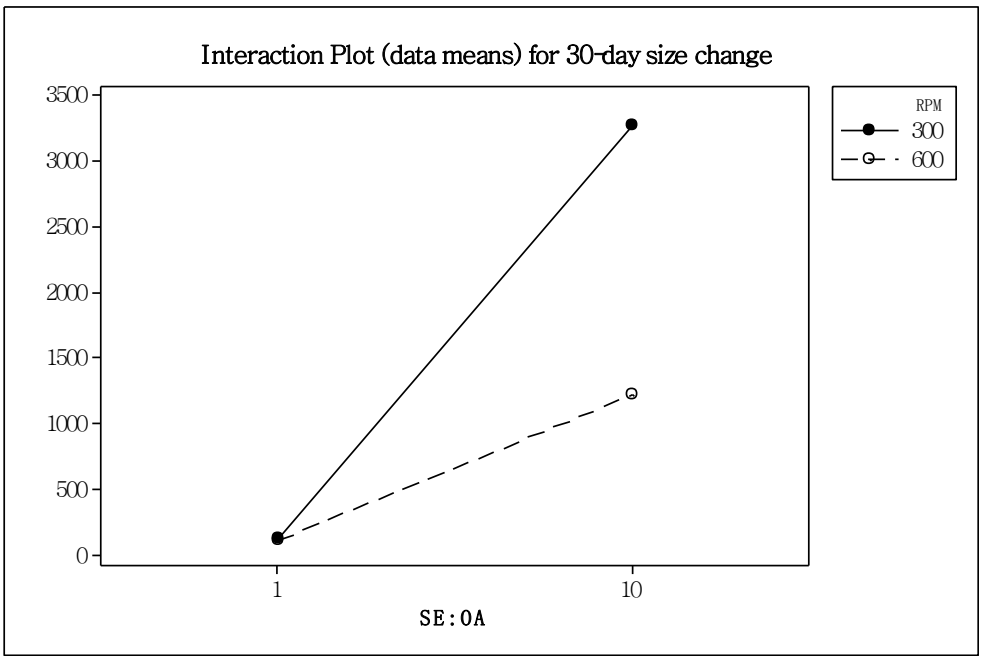

d3

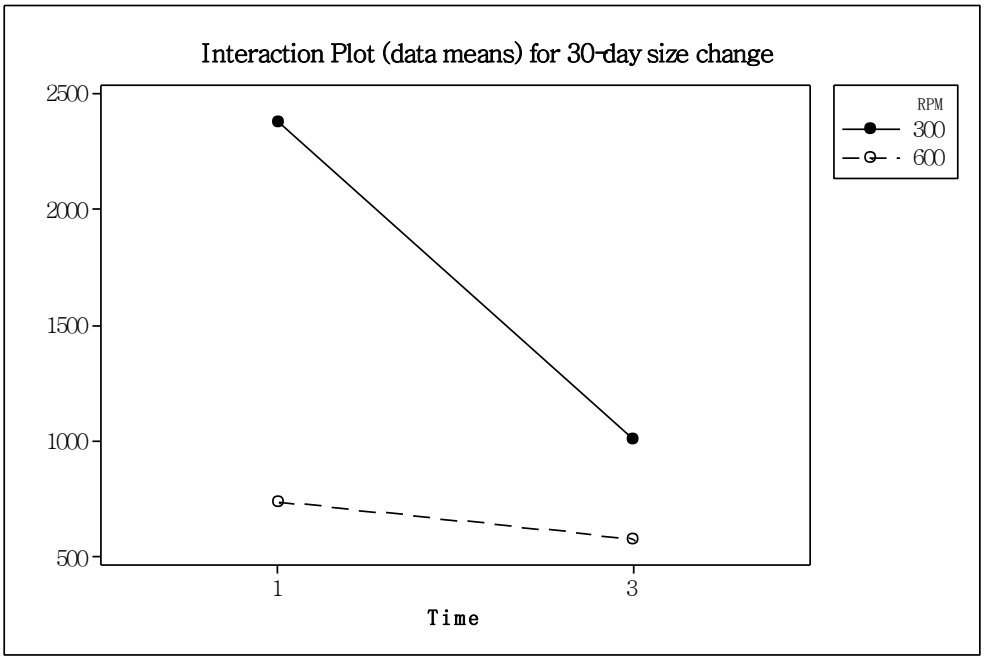

Figure 3.9 Minitab analysis of Physical Stability influence factors. Normal Probability Plot of the Standardized Effects (3.9a), Pareto Chart of the Standardized Effects (3.9b), Main Effects Plot (data means) for 30-day size change (3.9c), Interaction Plot (data means) for 30-day size change between milling time and SE : OA (3.9d1),. Interaction Plot (data means) between SE : OA and milling speed (3.9d2), and Interaction Plot (data means) between milling speed and milling time (3.9d3).

3.4.1.6.5 ANALYSIS OF CHEMICAL STABILITY INFLUENCING FACTORS

The four main production parameters influencing the chemical stability of SEOA NS were studied comparatively by the use of a factorial design on relative concentration change after 30 days of product storage after manufacture.

From Figures 3.10a and b, the main production parameters (SE : OA ratio, milling time) and their interactions showed significant relationships to the resultant chemical stability ($p<0.05$). However, other product parameters such as milling speed and SEL : SEP ratio showed much less influence, the standardized effect value was found to be below 2.037, $p>0.05$ (Figure 3.10b). The two main production parameters with significant effects were compared together (Figure 3.10c). Between them, SE : OA ratio showed a steeper slope, suggesting more a marked influence effect. Lower SE : OA ratio (1 : 1) led to higher chemical stability. Relatively higher SE : OA ratio increased the solubilised OA in SEOA NS, but if the solubility increased too high and beyond the surfactants' stabilization ability, lower product stability was encountered. The tendencies seen were rather similar to those observed for physical stability, as discussed earlier. Shorter milling time (1 h) produced better chemical stability since the lower energy input energy was less detrimental to the constituents present. Interaction effects analysis was carried out to study the interactionships between these two parameters (Figure 3.10d1). From Figure 3.10b, the interaction between SEL : SEP and SE : OA ratios were found to be the highest standardized effect and above others. This observation will be discussed later when explaining the findings shown in Figure 3.10d2.

From Figure 3.10d1 showing the relationship between milling time and SE : OA ratio, it

can be seen that with a lower SE : OA ratio (1 : 1) and shorter milling time (1 h) produced SEOA NS that was more chemically stable. Differences between a longer milling time (3 h) and shorter milling time (1 h) were found to be rather small. In addition, with a higher SE : OA ratio (10 : 1) and a longer milling time (3 h), the SEOA NS prepared tended to be less chemically stable.

Figure 3.10d2 illustrates the relationship between SE : OA ratio and SEL : SEP. It was found that a higher SEL : SEP ratio (9 : 1) and smaller SE : OA ratio (1 : 1) had caused the relative concentration of SEOA NS (i.e. chemical stability) after 30 days to be higher. Lower chemically stable particles were produced at a higher SE : OA ratio (10 : 1) and higher SEL : SEP ratio (9 : 1).

From the findings and discussion above, the production parameter, SE : OA ratio had consistently found to play an important role when considering all the four major production parameters in the production of SEOA NS. The optimal SE : OA ratio of 1 : 1 yielded smaller particle sizes and higher physical and chemical stability. Although the higher SE : OA ratio of 10 : 1 brought about higher saturation solubility and EE %, the overall stability would be sacrificed and hence not desirable for further studies. Among all the formulations to prepare NS with SE : OA ratio of 1 : 1, SEOA-GBD NS (600 rpm, 3 h, SEL : SEP at 9 : 1, w/w; SE : OA at 1 : 1, w/w) was found to be the optimal formulation as it had the highest stability, relatively high saturation solubility of OA (3.11 mg/mL) and small particle size with relatively low PDI (65.73 nm and 0.34).Further confirmation of the assumption was made by viewing the response optimization results derived from the factorial design study (Figure 3.11). Three production parameters were investigated by setting them for minimum outcomes.

The upper limits of 30-day particle size change (%), PDI and particle size were set at 100, 0.5, and 100 respectively. Saturation solubility and 30-day relative concentration (%) (representing chemical stability) were sought for maximum outcomes. Their lower limits were set as 1 and 80 respectively. After response optimization, SE-OA-GBD NS was found to be at the optimal formulation conditions and it was hence selected for further *in vitro* and *in vivo* studies.

a.

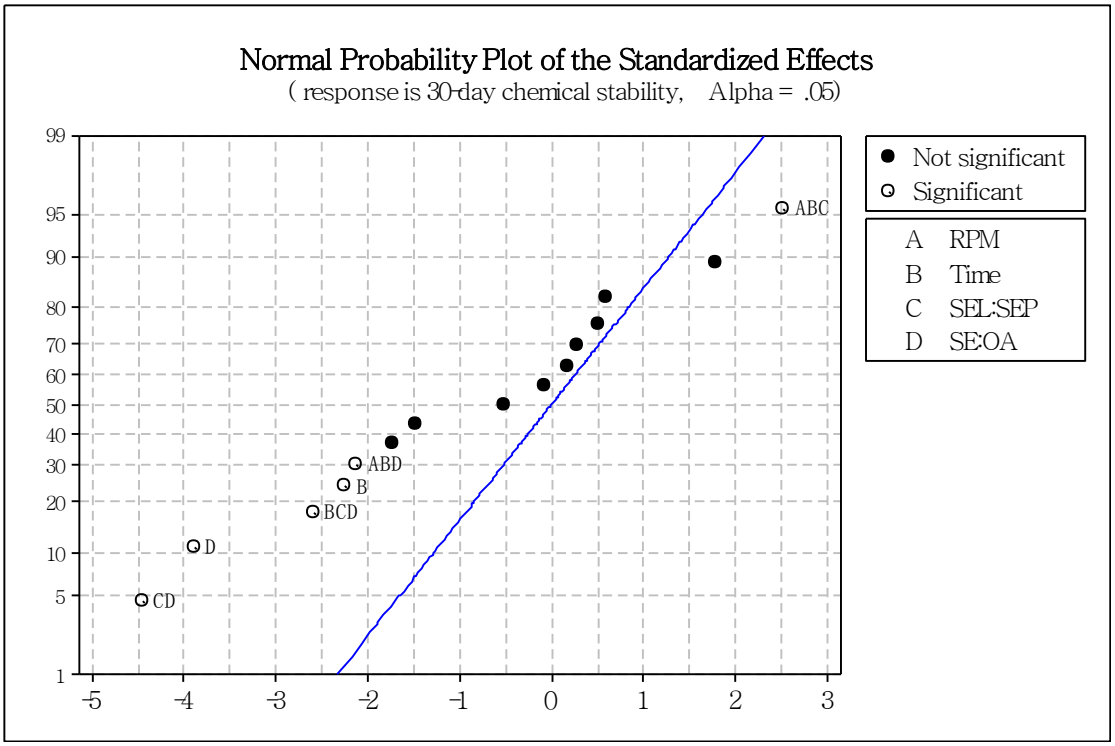
Normal Probability Plot of the Standardized Effects
(response is 30-day chemical stability, Alpha = .05)
Not significant
Significant
A RPM
B Time
C SEL:SEP
D SE:OA
ABC
ABD
B
BCD
D
CD

b

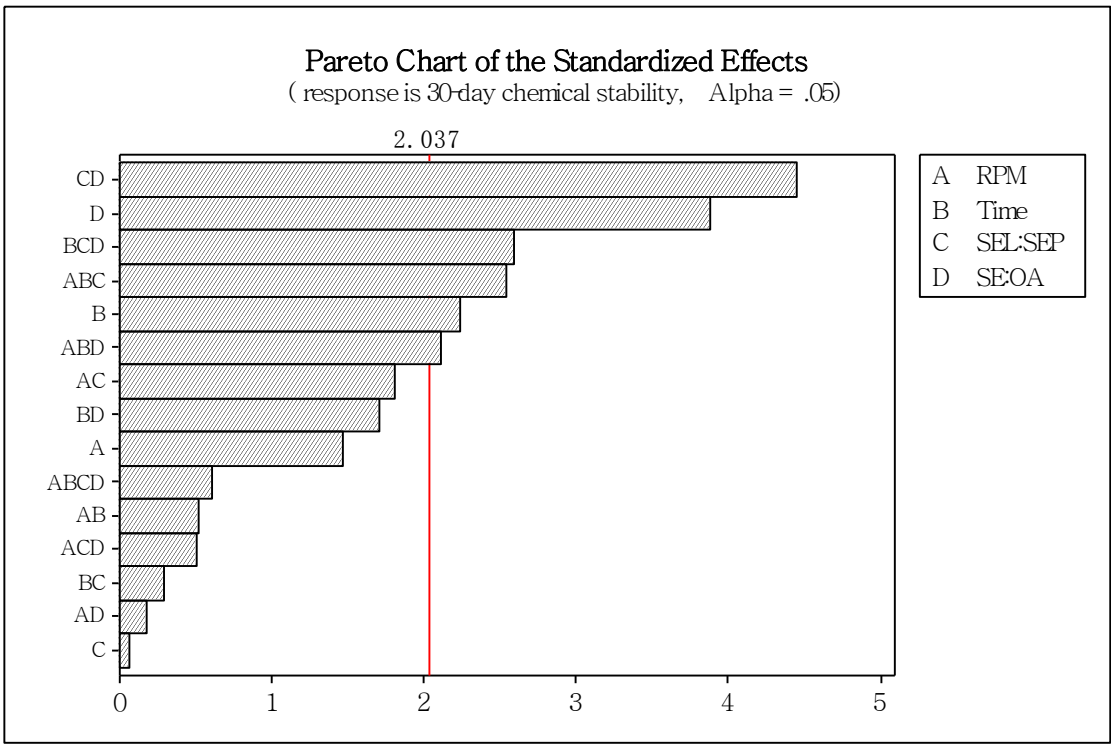
Pareto Chart of the Standardized Effects
(response is 30-day chemical stability, Alpha = .05)
2.037
A RPM
B Time
C SEL:SEP
D SE:OA
CD
D
BCD
ABC
B
ABD
AC
BD
A
ABCD
AB
ACD
BC
AD
C

c

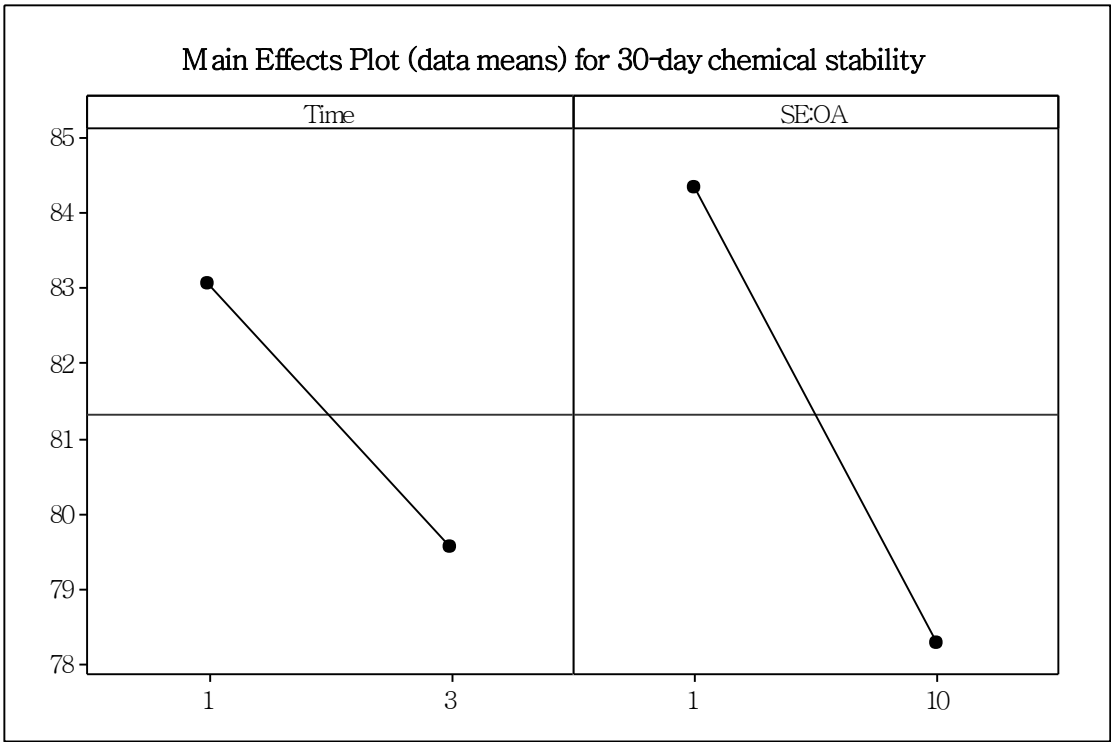
Main Effects Plot (data means) for 30-day chemical stability
Time
SE:OA
85
84
83
82
81
80
79
78
1
3
1
10

d1

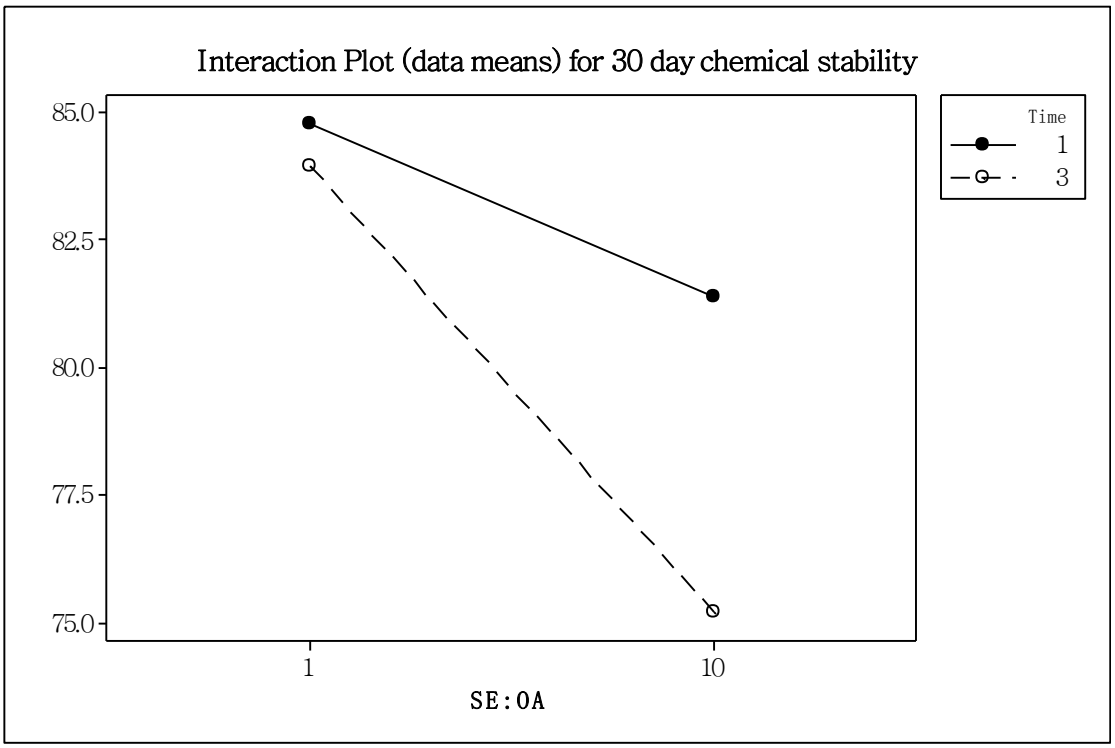
Interaction Plot (data means) for 30 day chemical stability
85.0
82.5
80.0
77.5
75.0
1
10
SE:OA
Time
1
3

d2

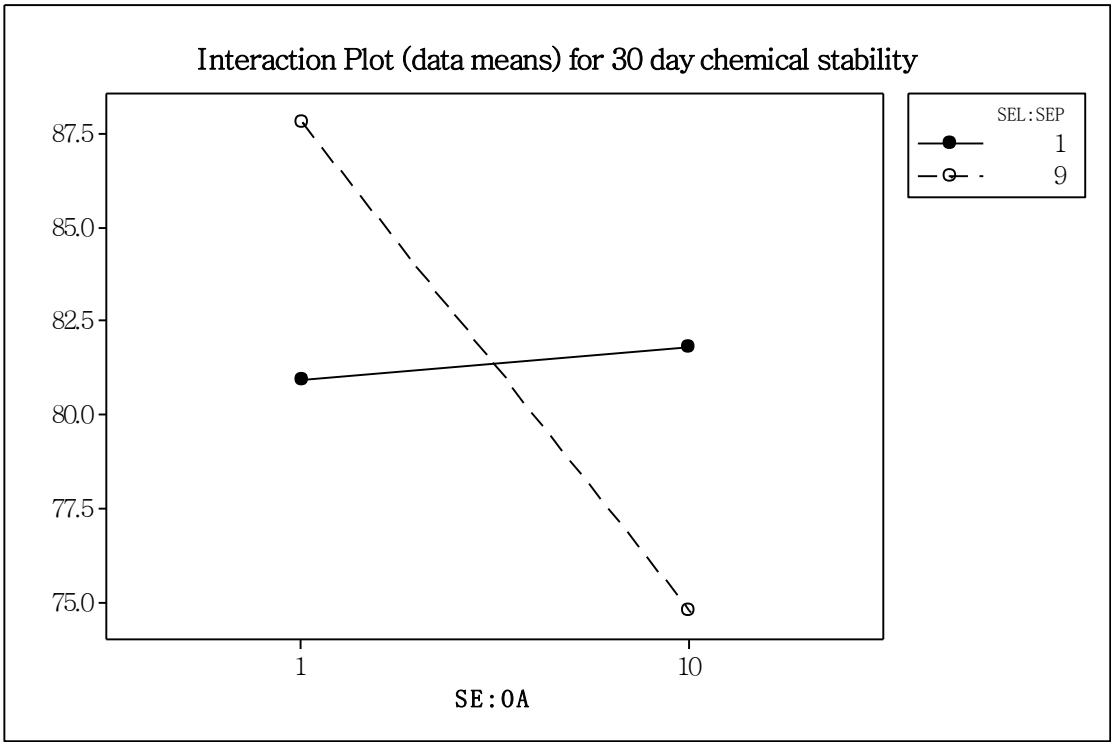

Figure 3.10 Minitab analysis of 30-day chemical stability influence factors. Normal Probability Plot of the Standardized Effects (3.10a), Pareto Chart of the Standardized Effects (3.10b), Main Effects Plot (data means) for 30-day relative concentration (3.10c), Interaction Plot (data means) for 30-day relative concentration between milling time and SE : OA (3.10d1), and Interaction Plot (data means) between SE : OA and SEL : SEP ratio (3.10d2).

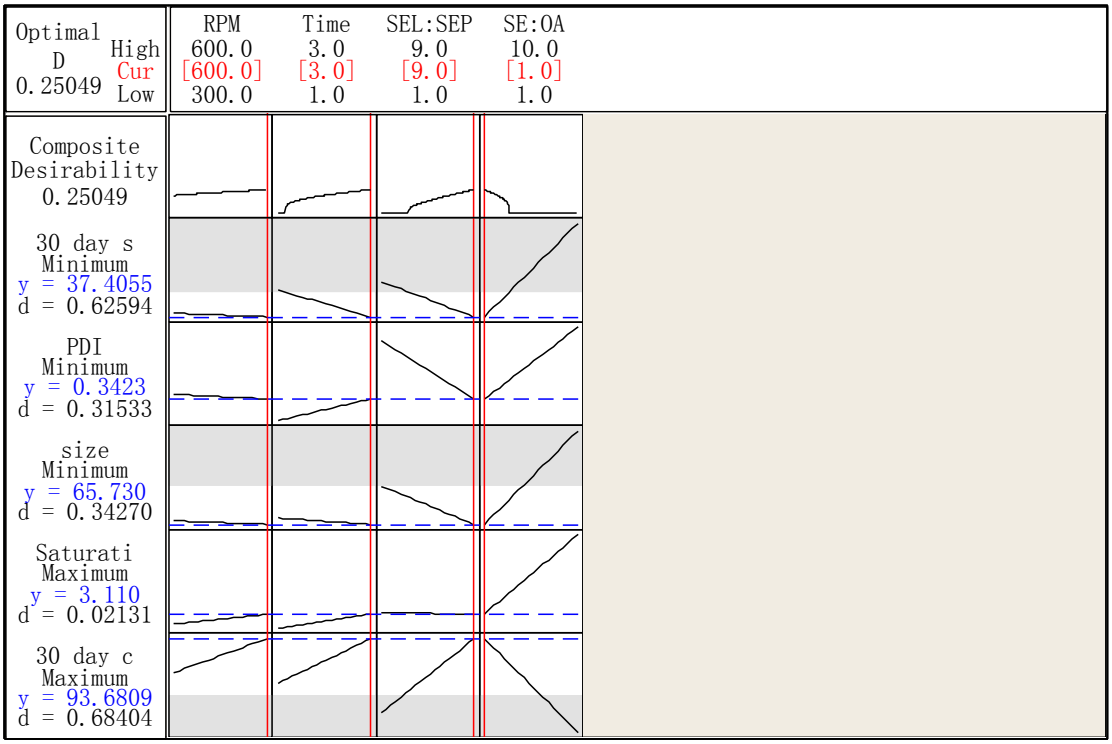

Figure 3.11 Response optimization of 30-day physical stability, PDI, particle size, saturation solubility and 30-day chemical stability with optimized conditions in brackets.

3.4.2 *IN VITRO* DISSOLUTION

The influence of SEOA NS on the dissolution rate of OA was investigated by the *in vitro* dissolution profiles of OA NS with coarse OA suspension as control (Figure 3.12). The dissolution rate of OA coarse suspension (suspended in N, N-DMAC : PEG400: water at 2 : 4 :1, v/v/v) was very low, only about 15 % of the drug dissolved after 120 min. On the contrary, the SEOA-GBD NS either in suspension form or as a lyophilized powder both showed a marked increase in the dissolution rate for OA as compared with the coarse OA suspension and 100 % of OA dissolution was achieved within 20 min.

The dissolution rate determined by dialysis bag method was also carried out to confirm the fast dissolution of OA from SEOA-GBD NS as free molecular form (can pass through dialysis bag) or in NS form (cannot pass dialysis bag). From Figure 3.12b, by dialysis bag method, no OA was detected even after 60 min in the dissolution medium and the dissolution rate increased very slowly thereafter with the percent of dissolved OA after 120 min not even reaching 5 % and was less than 10 % until after 1200 min dissolution time. The findings collectively had suggested that most of the fast dissolving OA measured during *in vitro* dissolution testing was not in the dissolved OA drug but nanoparticulates released by the NS product.

a.

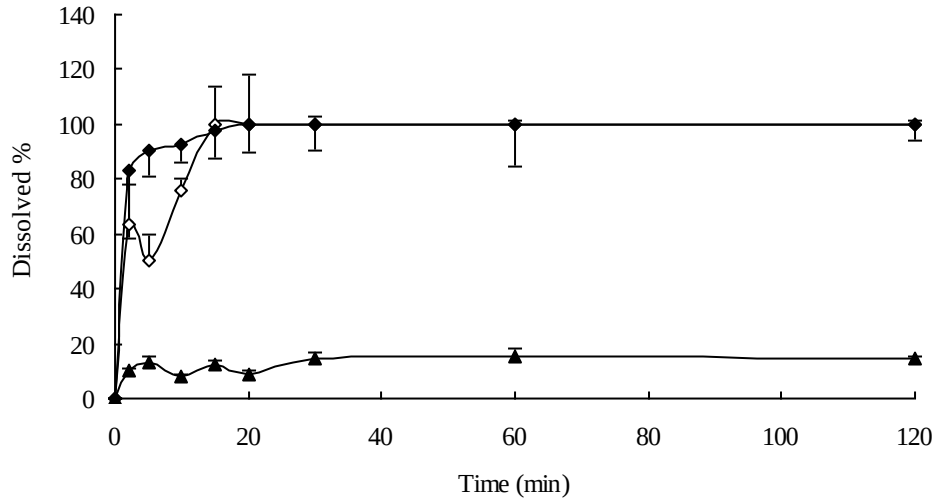

b.

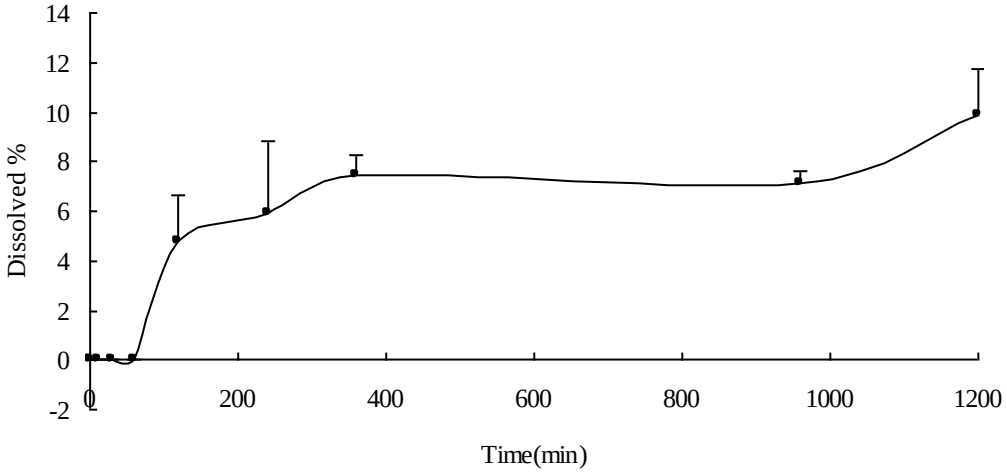

Figure 3.12 Dissolution profiles of OA coarse suspension (▲) (suspended in N,N-DMAC : PEG400 : Water at 2 : 4 : 1, v/v/v), SEOA-GBD NS (◇) and SEOA-GBD NS lyophilized powder(◆) (3.12a) and SEOA GBD NS in dialysis bag (▲) (3.12b) in pH 7.4 phosphate buffer solution containing 1 % sodium dodecyl sulfate (SDS) (n = 3).

3.4.3 CYTOTOXICITY OF SEOA NS

In NS form, the saturation solubility of OA was increased from 3.43 μg/mL (free OA) to 3110 μg/mL (SEOA-GBD NS). Owing to the increase in OA saturation solubility, the *in vitro* cytotoxicity to A549 cell lines measured by MTT assay was also observed to have increased. As shown in Figure 3.13, formulation of SE OA NS significantly increased the cytotoxicity of OA in both time- and dose-dependent manner (also see data in Table 3.6). The 72 h IC_{50} dropped from 120 μM of free OA to 45 μM and 24 h IC_{50} dropped from 130 μM of free OA to 78 μM. Although free OA is not considered potent in anti-lung cancer cells, formulated OA as NS form showed enhanced bioefficacy without any chemical modification. Thus, the usefulness of the natural derived hydrophobic compound can be changed by its physical transformation, to a NS form.

The enhanced anti-cancer effect is most likely due to the increased saturation solubility of OA rather than the surface-active effect of the sucrose-ester molecules. From the results discussed in Chapter 2 (Table 2.4), the control SE NS with SEL : SEP ratio of 9 : 1 (similar constituents as SEOA-GBD NS) had the 24 h IC_{50} of 249.10 μg/mL and 72 h IC_{50} of 212.60 μg/mL, which were much larger than SEOA-GBD NS IC_{50} values (6.82 times and 10.01 times).

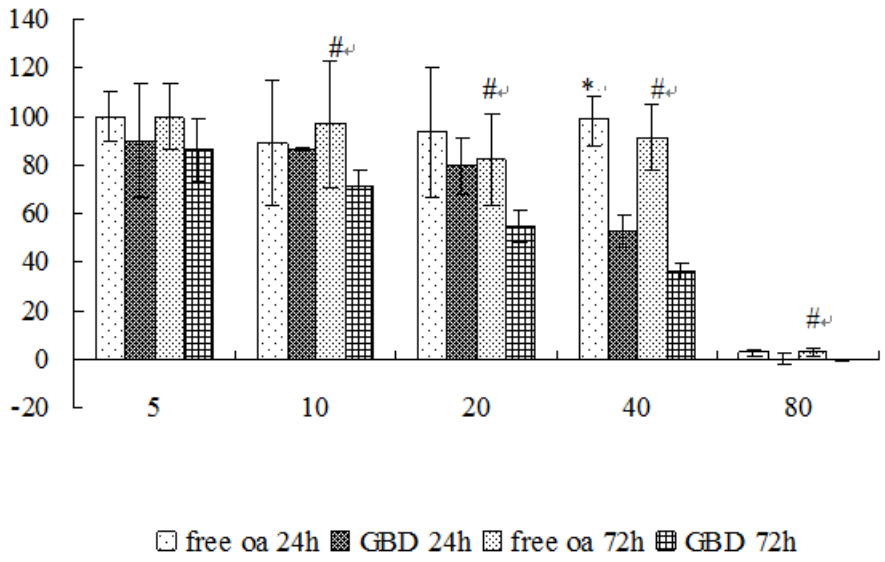

Figure 3.13 Dose- and time-dependent growth inhibition of A549 cells by Free OA dissolved in media containing 0.05 %DMSO, and SEOA-GBD NS.X axis shows OA concentration (μg/mL) and Y shows the percentages of viable A549 cells normalized to that of control (%).

*, $p<0.05$ between SEOA-GBD 24 h and free OA 24 h; #, $p<0.05$ between SEOA-GBD 72h and free OA 72 h. Data is presented as mean (μg/mL) ± std from three independent experiments repeated in quadruplicate.

Table 3.6 IC_{50} comparison of SEOA-GBD NS and free OA

Group	24 h (μg/mL)	72 h (μg/mL)
Free OA	59.70 ± 1.01 (130.00 μM)	56.80 ± 1.02 (120.00 μM)
SEOA-GBD NS	36.53 ± 1.06 (78.00 μM)	21.14 ± 1.06 (45.00 μM)

IC_{50} values were calculated by nonlinear regression (curve fit) of cytotoxicity data in graphs 6a-d using sigmoidal dose response (variable slope) equation, Graphpad Prism software (Graphpad 4.0, Graphpad software, Inc., La Jolla, CA USA).

3.4.4 SEOA NS PHARMACOKINETICS PROFILE

3.4.4.1 PHARMACOKINETICS RESULTS AFTER INTRAVENOUS ADMINISTRATION

Figure 3.14a shows the pharmacokinetics results of OA following a single iv bolus dose (2 mg/kg) of NS (Group I). It demonstrated that the plasma concentration of OA declined rapidly over the first hour of tissue distribution and was followed by a slower drop from the second hour onwards in the elimination profile. The maximum plasma concentration (C_{max}) was high (21.98 ± 5.79 μg /mL) and plasma elimination half-life ($T_{1/2}$) was found to be 88.41 ± 16.15 min. AUC and Cl values were calculated as 121.49 ± 27.37 μg.min/mL and 17.11 ± 3.67 mL/min/kg, respectively.

3.4.4.2 PHARMACOKINETICS RESULTS AFTER ORAL ADMINISTRATION

The plasma pharmacokinetic profiles and the pharmacokinetic parameters following single oral doses of SEOA NS (10 and 20 mg/kg) and dose of coarse OA (20 mg/kg) suspensions are shown in Figure 3.14b and Table 3.7. In all cases, OA in NS groups resulted in a significantly ($p<0.05$) higher C_{max} than the suspension formulations. However, there were no significant differences ($p>0.05$) in T_{max} and $T_{1/2.}$ The NS group (Groups IIb and IIIb) had a significantly higher bioavailability (F %) values (7.71 and 7.63 over 0.56) than the coarse OA suspension group (Group IV) ($p<0.05$), while between 10 mg/kg and 20 mg/kg NS groups, there was no statistically significant differences ($p>0.05$). The rF % values of

Group IIb to Group IV and Group IIIb to Group IV are 13.77 and 13.63 respectively. These findings indicated that the SEOA-GBD NS had enhanced the oral bioavailability when compared with coarse OA suspension.

The longer $T_{1/2,}$ although without statistical significance, exhibited by the coarse suspension formulation probably had indicated the sustained absorption of OA through the GI tract. This was possibly due to the slower dissolution of OA in the GI fluids from the coare suspension formulation and hence, the corresponding delayed absorption.

a

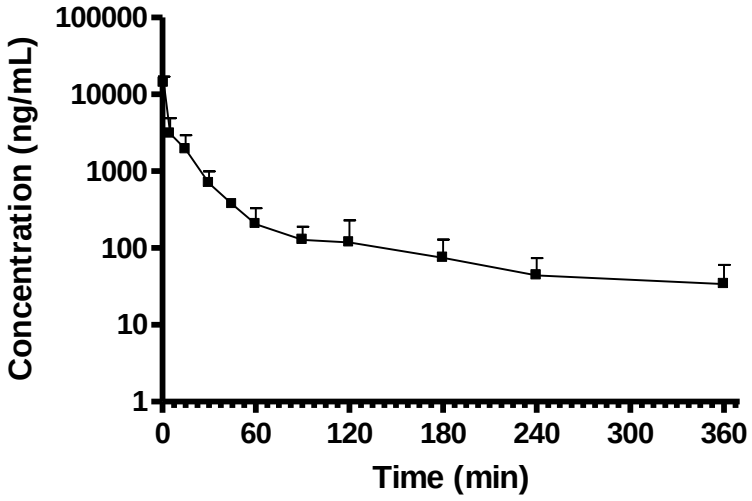

b

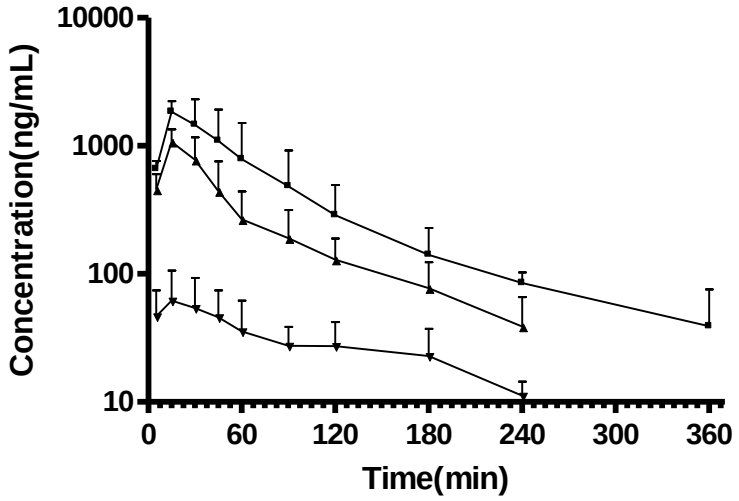

Figure 3.14 Mean plasma concentration-time profiles comparison of OA in rats after (a) IV injection at 2 mg/kg (■,n=5), (b) oral administration of OA NS at 10(▲, n=5),20 (■, n=5) mg/kg doses and oral administration of OA coarse suspension (▼, n=5, control) at 20 mg/kg dose. Vertical bars represent standard deviation.

Table 3.7 Oral pharmacokinetics profiles of SEOA NS and coarse suspension

Parameter	Group IIb	Group IIIb	Group IV
Formulation	NS	NS	Suspension
Dose (mg/kg)	10.00	20.00	20.00
AUC (μg.min/mL)	65.57 ± 18.62 [a, c]	129.86 ± 65.98 [a, b]	6.70 ±3.40 [b, c]
T_{max} (min)	18.00 ± 6.71	21.00 ± 8.22	13.00 ± 4.50
C_{max} (ng/mL)	1101.60 ± 250.84 [a, c]	1896.00 ± 436.38 [a, b]	70.00 ± 42.70 [b,c]
$T_{1/2}$ (min)	68.00 ± 53.96	65.42 ± 15.25	102.10 ± 16.56
F %	7.71 ± 2.19	7.63 ± 3.88	0.56 ± 0.28 [b, c]

Data is presented as Mean ± Std, N=5.
[a], *p<0.05* between Groups IIb and IIIb; [b], *p<0.05* between IIIb and IV; [c], *p<0.05* between 2 and 4

3.5. CONCLUSION

SEOA NS was prepared by the wet ball milling, a top-down method and critically evaluated. The SE : OA ratio, SEL : SEP ratio, milling time and milling speed had their influences on the characteristics of SEOA NS produced. The preparation of the SEAOA SE by a DOE method and analysed by the statistical software enabled the critical evaluation of the formulation parameters and the optimized product could be identified together with the ideal parameters for preparation. The mean particle sizes of most SEOA NS prepared were less than 100 nm. Except for some variations, the PDI of most formulations were found to be relatively low. The NS particles were generally spherical in shape and observed to be covered by distinct diffuse coating, possibly of the surfactant, SE, on the periphery of particles or their aggregates. Preparation of OA as NS by wet ball milling increased its saturation solubility considerably, ranging from 2.08 to 5.49 mg/mL. SEOA-GBD NS was the optimized formulation. SEOA-GBD NS increased the OA dissolution rate markedly. Most of the dissolved OA existed in the NS in solution and not dissolved as the free molecular form. Formulation of OA as NS significantly and substantially increased the cytotoxicity of OA. It reduced the proliferation rate of A549 cell lines to a much greater extent than control OA at a time- and dose-dependent manner. This increased activity was attributed to the nanonized drug and not the SE. NS of OA not only increased its saturation solubility and dissolution rate to a great extent but also change the pharmacokinetic profile of OA after oral administration. Oral bioavailability of OA was enhanced by the NS formulation, which showed much higher C_{max} and rF % than the coarse suspension group. Dose-independent pharmacokinetics of OA

was observed after oral administration at the range of 10 to 20 mg/kg.

CHAPTER 4.

GENERAL CONCLUSIONS

CHAPTER 4. GENERAL CONCLUSIONS

NS provides the opportunity of improving saturation solubility, dissolution rate, bioefficacy and pharmacokinetic attribute for low aqueous solubility compounds with therapeutic efficacy, especially many potential compounds from natural sources. Although there are compounds with many promising properties such as low toxic and ready biodegradability (104-106), the bioavailability of the compounds would eventually determine their usefulness as a therapeutic agent. Thus, for a poorly water soluble drug, the ability of the drug to dissolve upon ingestion and present a reasonable bioavailability so as to give the required therapeutic blood level is of paramount importance. Amongst the methods of enhancing drug solubility, the method of producing nanosized and physiologically acceptable dispersions by only the application of gentle heat and moderate shear stress (109) is highly desirable. Thus, this study was directed at the search of desirable methods to produce nanoparticles. As nanoparticles required a stabilizing agent, a popular class of surfactant used in the preparation of beverages was explored. Highly purified SE was selected as it is generally regarded as non-toxic and posses a good taste. SEs were not well studied as stabilizers in preparing nanoscaled products. This present study was the first to employ SEs as main stabilizer for the preparation of NS.

Two approaches for the preparation of nanoparticles were evaluated, namely the emulsion-solvent evaporation method (ESE) and wet ball milling (WBM) method. Both of the methods applied to prepare SEOA NS yielded nanosized –range of particles (below 100 nm). NS produced were found to be spherical in shape and covered by distinct SE coating on

the periphery, as examined by the TEM. Saturation solubility of NS prepared via bottom-up and top-down methods were both much higher than the free drug. The saturation solubility of manufactured NS ranged from 0.66 mg/mL (SEOA91101 NS) to 1.89 mg/mL (SEOA4121 NS), and 2.08 mg/mL (SEOA-EAC NS) to 5.49 mg/mL (SEOA-HBD NS) respectively. As a consequence, the *in vitro* dissolution rate and cytotoxicity of SEOA NS prepared via the two methods were also much higher than free drug. The oral bioavailability produced a big increase, a 6-7 folds increase (SEOA4121 NS) to 12 folds increase (SEOA-GBD NS).

However, as there were differences in the preparation routes, the two methods also produced NS particles with some contrasts in their characteristics (Table 4.1).

Firstly, the average particle size and PDI of the two production methods' products were similar and statistically insignificant ($p>0.05$). However, the average particle size for WBM's products ranged much wider (with bigger variation) than ESE's products. The median size of WBM (77.09 nm and 0.35 PDI) NS was much smaller than ESE's group (101.6 nm and 0.57 PDI). This had implied that the WBM method produced much widely distributed NS since the production parameters for WBM method also ranged much wider than the ESE method.

Secondly, WBM produced NS had much higher saturation solubility (3.79 mg/mL to 0.88 mg/mL) and less EE % (37.87 % to 55.77 %) than ESE. Top-down method utilized more energy resulting in more heat generated. Therefore, the higher energy method enabled much more hydrophobic OA to be entrapped, coated and presented as NS. However, the lower EE % indicated that the increase of solubility had its maximum limit. In addition, with the restriction of SE stabilization ability and Ostwald ripening effect, too high a saturation solubility led to instability and product failure.

Thirdly, when comparing the stability index, ESE method was superior in both chemical and physical stability (*p<0.05*). The higher input of energy and heat generation caused some level of instability.

However, it was well accepted that Ostwald ripening had some major impact on physical stability of NS (80, 142, 143). According to Lifshitz–Slesov–Wagner (LSW) theory (77, 78), $\omega = \frac{dr_N^3}{dt} = \frac{8}{9}[C(\infty)\gamma V_m D/\rho RT]$, Ostwald ripening rate ω (indicating as change rate of particle size) correlated with the saturation solubility C(∞) and interfacial tension γ.

Table 4.1 character comparison between bottom-up and top-down methods

	emulsion-solvent-evaporation	wet ball milling
Particle size (nm)	112.85 ± 27.15	93.67 ± 52.31
PDI	0.54 ± 0.09	0.53 ± 0.29
Saturation solubility (mg/mL)	0.88 ± 0.42 **	3.79 ± 1.24
EE %	55.77 ± 22.33 *	37.87 ± 12.36
15-day size change (%)	37.68 ± 22.62 *	765.15 ± 1033.94
30-day size change (%)	185.57 ± 132.60 *	1173.22 ± 1525.96
30-day relative con. (%)	87.06 ± 5.43 *	81.32 ± 6.59

Data represent 3 independent experiments repeated in triplicate. Values are presented as means ± std. *, *p<0.05*, **, *P<0.01*. Statistics were carried out by independent- samples T test.

Since the saturation solubility of WBM increased much higher than ESE, as according to LSW theory, the Ostwald ripening rates were much faster in the WBM than the ESE method. Although more surfactant reduced the interfacial tension and slowed down the rate of change, the increase in saturation solubility appeared to override the slowing down effect.

Last but not least, to add further discussion to the stability issue, it was valuable to compare the most stable NS prepared by the two methods. As discussed earlier, the SEL : SEP ratio and SE : OA ratio played important roles in determining the NS characteristics prepared by both of the two methods. The most stable formulation in ESE method was SEOA 91101 NS (SEL : SEP at 9 : 1, w/w; SE : OA at 10 : 1, w/w) and in WBM method was SEOA-GBD NS (600 rpm, 3 h, SEL : SEP at 9 : 1, w/w; SE : OA at 1 : 1, w/w). Although both the NS products were similar in SEL : SEP ratio, they were rather different in their SE : OA ratio.

When using ESE, the amount of SE needed was constant and that of OA varied. SE : OA at 10 : 1 (w/w) had the least amount of OA and the saturation solubility of produced NS was the smallest. With similar lowing of the interfacial tension effect (same amount of SE) and lowest saturation solubility, SEOA 91101 NS received the lowest Ostwald ripening rate and hence most stable. Although SELOA and SEPOA also had the 10 : 1 ratio of SE : OA, the SEL : SEP at 9 : 1 (w/w) also aided in maintaining stable NS structure, they were not as stable as SEOA 91101 NS.

On the contrary, WBM varied in the amount of SE and OA was kept constant. Although the increase in SE could contributed to a reduction in the interfacial tension and slow down the Ostwald ripening process, the effects of increased saturation solubility which also arose from larger SE : OA ratio (10 : 1) could override the slowing down effect resulted in worsening the physical stability. This deduction may explain the anomaly why in WBM method, the SE : OA at 1 : 1 was more stable than 10 : 1. Similarly, SEL : SEP at 9 : 1 (w/w) was shown to be the better stabilizing factor.

As a suspension form, SEOA NS was only stable for a limited time span. The future work should focus on formulating more stable products that could be optimized as SEOA NS suitable to be incorporated into tablets and posses the required shelf-life as required for general marketed product. DOE will be applied in optimizing the production settings with multiple responses and variables. Pharmacokinetics study (bioavailability and distribution among others), pharmacokinetic-pharmacodynamic interaction and toxicology studies will be carried out to compare SEOA NS in tablets with the marketed drug products by using both normal animals and disease model animals. In our study, although the solubility and bioefficacy of SEOA NS has been enhanced greatly comparing to free drug, the cytotoxicity to A549 cell line is still weak. We will try to evaluate the liverprotection effect by *in vitro* and *in vivo*. Further directions may also include the clinical trials to ascertain the findings in this study.

REFERENCE

1. J.A. Dimasi. New drug development in the United States from 1963 to 1999. Clin Pharmacol Ther. 69:286-296 (2001).
2. C.P. Adamsand V.V. Brantner. Spending on new drug development1. Health Economics. 19:130-141 (2010).
3. A.L. Harvey. Natural products in drug discovery. Drug Discov Today. 13:894-901 (2008).
4. M.S. Butler. Natural products to drugs: natural product-derived compounds in clinical trials. Nat Prod Rep. 25:475-516 (2008).
5. N. Rasenack, H. Hartenhauer, and B.W. Muller. Microcrystals for dissolution rate enhancement of poorly water-soluble drugs. Int J Pharm. 254:137-145 (2003).
6. L. Liang, H.A. Tajmir-Riahi, and M. Subirade. Interaction of beta-lactoglobulin with resveratrol and its biological implications. Biomacromolecules. 9:50-56 (2008).
7. A. Betancor-Fernandez, A. Perez-Galvez, H. Sies, and W. Stahl. Screening pharmaceutical preparations containing extracts of turmeric rhizome, artichoke leaf, devil's claw root and garlic or salmon oil for antioxidant capacity. J Pharm Pharmacol. 55:981-986 (2003).
8. G. Eibes, M.T. Moreira, G. Feijoo, and J.M. Lema. Enzymatic degradation of low soluble compounds in monophasic water: solvent reactors. Kinetics and modeling of anthracene degradation by MnP. Biotechnol Bioeng. 100:619-626 (2008).
9. F.R. Kinder, Jr., R.W. Versace, K.W. Bair, J.M. Bontempo, D. Cesarz, S. Chen, P. Crews, A.M. Czuchta, C.T. Jagoe, Y. Mou, R. Nemzek, P.E. Phillips, L.D. Tran, R.M. Wang, S. Weltchek, and S. Zabludoff. Synthesis and antitumor activity of ester-modified analogues of bengamide B. J Med Chem. 44:3692-3699 (2001).
10. R. Thiericke. Drug discovery from Nature: automated high-quality sample preparation. J Autom Methods Manag Chem. 22:149-157 (2000).
11. J. Liu. Pharmacology of oleanolic acid and ursolic acid. J Ethnopharmacol. 49:57-68 (1995).
12. N.Y. Kim, M.K. Lee, M.J. Park, S.J. Kim, H.J. Park, J.W. Choi, S.H. Kim, S.Y. Cho, and J.S. Lee. Momordin Ic and oleanolic acid from Kochiae Fructus reduce carbon tetrachloride-induced hepatotoxicity in rats. J Med Food. 8:177-183 (2005).
13. J. Liu, Q. Wu, Y.F. Lu, and J. Pi. New insights into generalized hepatoprotective effects of oleanolic acid: key roles of metallothionein and Nrf2 induction. Biochem Pharmacol. 76:922-928 (2008).
14. Z. Ovesna, A. Vachalkova, K. Horvathova, and D. Tothova. Pentacyclic triterpenoic acids: new chemoprotective compounds. Minireview. Neoplasma. 51:327-333 (2004).
15. H.Y. Hsu, J.J. Yang, and C.C. Lin. Effects of oleanolic acid and ursolic acid on inhibiting tumor growth and enhancing the recovery of hematopoietic system postirradiation in mice. Cancer Lett. 111:7-13 (1997).
16. T. Oguro, J. Liu, C.D. Klaassen, and T. Yoshida. Inhibitory effect of oleanolic acid on 12-O-tetradecanoylphorbol-13-acetate-induced gene expression in mouse skin. Toxicol Sci. 45:88-93 (1998).
17. Y. Kashiwada, H.K. Wang, T. Nagao, S. Kitanaka, I. Yasuda, T. Fujioka, T. Yamagishi, L.M. Cosentino, M. Kozuka, H. Okabe, Y. Ikeshiro, C.Q. Hu, E. Yeh, and K.H. Lee. Anti-AIDS agents. 30. Anti-HIV activity of oleanolic acid, pomolic acid, and structurally related

triterpenoids. J Nat Prod. 61:1090-1095 (1998).

18. F. Mengoni, M. Lichtner, L. Battinelli, M. Marzi, C.M. Mastroianni, V. Vullo, and G. Mazzanti. In vitro anti-HIV activity of oleanolic acid on infected human mononuclear cells. Planta Med. 68:111-114 (2002).
19. G.B. Singh, S. Singh, S. Bani, B.D. Gupta, and S.K. Banerjee. Anti-inflammatory activity of oleanolic acid in rats and mice. J Pharm Pharmacol. 44:456-458 (1992).
20. S.J. Tsaiand M.C. Yin. Antioxidative and anti-inflammatory protection of oleanolic acid and ursolic acid in PC12 cells. J Food Sci. 73:H174-178 (2008).
21. K.K. Dharmappa, R.V. Kumar, A. Nataraju, R. Mohamed, H.V. Shivaprasad, and B.S. Vishwanath. Anti-inflammatory activity of oleanolic acid by inhibition of secretory phospholipase A2. Planta Med. 75:211-215 (2009).
22. H. Matsuda, Y. Dai, Y. Ido, T. Murakami, M. Yoshikawa, and M. Kubo. Studies on Kochiae Fructus. V. Antipruritic effects of oleanolic acid glycosides and the structure-requirement. Biol Pharm Bull. 21:1231-1233 (1998).
23. S. Begum, I. Sultana, B.S. Siddiqui, F. Shaheen, and A.H. Gilani. Structure and spasmolytic activity of eucalyptanoic acid from Eucalyptus camaldulensis var. obtusa and synthesis of its active derivative from oleanolic acid. J Nat Prod. 65:1939-1941 (2002).
24. D. Gao, Q. Li, Y. Li, Z. Liu, Z. Liu, Y. Fan, Z. Han, J. Li, and K. Li. Antidiabetic potential of oleanolic acid from Ligustrum lucidum Ait. Can J Physiol Pharmacol. 85:1076-1083 (2007).
25. A. Petronelli, G. Pannitteri, and U. Testa. Triterpenoids as new promising anticancer drugs. Anticancer Drugs. 20:880-892 (2009).
26. I. Sogno, N. Vannini, G. Lorusso, R. Cammarota, D.M. Noonan, L. Generoso, M.B. Sporn, and A. Albini. Anti-angiogenic activity of a novel class of chemopreventive compounds: oleanic acid terpenoids. Recent Results Cancer Res. 181:209-212 (2009).
27. Y. Chen, J. Liu, X. Yang, X. Zhao, and H. Xu. Oleanolic acid nanosuspensions: preparation, in-vitro characterization and enhanced hepatoprotective effect. J Pharm Pharmacol. 57:259-264 (2005).
28. D.W. Jeong, Y.H. Kim, H.H. Kim, H.Y. Ji, S.D. Yoo, W.R. Choi, S.M. Lee, C.K. Han, and H.S. Lee. Dose-linear pharmacokinetics of oleanolic acid after intravenous and oral administration in rats. Biopharm Drug Dispos. 28:51-57 (2007).
29. P.J. Sinkoand A.N. Martin. Martin's physical pharmacy and pharmaceutical sciences : physical chemical and biopharmaceutical principles in the pharmaceutical sciences, Lippincott Williams & Wilkins, Philadelphia, 2006.
30. A. Dokoumetzidisand P. Macheras. A century of dissolution research: From Noyes and Whitney to the biopharmaceutics classification system. International journal of pharmaceutics. 321:1-11 (2006).
31. D.E. Wursterand P.W. Taylor. Dissolution Rates. J Pharm Sci. 54:169-175 (1965).
32. M.R. Caira, K.A. Alkhamis, and R.M. Obaidat. Preparation and crystal characterization of a polymorph, a monohydrate, and an ethyl acetate solvate of the antifungal fluconazole. J Pharm Sci. 93:601-611 (2004).
33. S. Li, S. Wong, S. Sethia, H. Almoazen, Y.M. Joshi, and A.T. Serajuddin. Investigation of solubility and dissolution of a free base and two different salt forms as a function of pH. Pharm Res. 22:628-635 (2005).
34. M. Rahamathulla, G. Hv, and N. Rathod. Solubility and dissolution improvement of

Rofecoxib using solid dispersion technique. Pak J Pharm Sci. 21:350-355 (2008).

35. R.A. Schwendenerand H. Schott. Lipophilic 1-beta-D-arabinofuranosyl cytosine derivatives in liposomal formulations for oral and parenteral antileukemic therapy in the murine L1210 leukemia model. J Cancer Res Clin Oncol. 122:723-726 (1996).
36. A.G. Floyd. Top ten considerations in the development of parenteral emulsions. Pharm Sci Technolo Today. 4:134-143 (1999).
37. M.J. Lawrenceand G.D. Rees. Microemulsion-based media as novel drug delivery systems. Adv Drug Deliv Rev. 45:89-121 (2000).
38. M.A. Hammadand B.W. Muller. Solubility and stability of lorazepam in bile salt/soya phosphatidylcholine-mixed micelles. Drug Dev Ind Pharm. 25:409-417 (1999).
39. T. Loftssonand M.E. Brewster. Pharmaceutical applications of cyclodextrins. 1. Drug solubilization and stabilization. J Pharm Sci. 85:1017-1025 (1996).
40. V.J. Stellaand R.A. Rajewski. Cyclodextrins: their future in drug formulation and delivery. Pharm Res. 14:556-567 (1997).
41. M.J. Akers. Excipient-drug interactions in parenteral formulations. J Pharm Sci. 91:2283-2300 (2002).
42. A.B. Stefaniak, S.J. Chipera, G.A. Day, P. Sabey, R.M. Dickerson, D.C. Sbarra, M.G. Duling, R.B. Lawrence, M.L. Stanton, and R.C. Scripsick. Physicochemical characteristics of aerosol particles generated during the milling of beryllium silicate ores: implications for risk assessment. J Toxicol Environ Health A. 71:1468-1481 (2008).
43. S.S. Lanke, S.G. Gayakwad, J.G. Strom, and J. D'Souza M. Oral delivery of low molecular weight heparin microspheres prepared using biodegradable polymer matrix system. J Microencapsul:1-8 (2008).
44. V.B. Patravale, A.A. Date, and R.M. Kulkarni. Nanosuspensions: a promising drug delivery strategy. J Pharm Pharmacol. 56:827-840 (2004).
45. J. Chingunpitak, S. Puttipipatkhachorn, P. Chavalitshewinkoon-Petmitr, Y. Tozuka, K. Moribe, and K. Yamamoto. Formation, Physical Stability and In Vitro Antimalarial Activity of Dihydroartemisinin Nanosuspensions Obtained by Co-grinding Method. Drug Dev Ind Pharm. 34:314-322 (2008).
46. D. Zhang, T. Tan, L. Gao, W. Zhao, and P. Wang. Preparation of azithromycin nanosuspensions by high pressure homogenization and its physicochemical characteristics studies. Drug Dev Ind Pharm. 33:569-575 (2007).
47. B.E. Rabinow. Nanosuspensions in drug delivery. Nat Rev Drug Discov. 3:785-796 (2004).
48. F. Gonzáles-Caballero, de Dios Garcia López-Durán, J. Suspension formulation. In F. Nielloudand G. Marti-Mestres (eds.), Pharmaceutical Emulsions and Suspensions, Drugs and the Pharmaceutical Sciences, Vol. 105, Marcel Dekker,Inc, New York, 2000, pp. 127-190.
49. B. Van Eerdenbrugh, G. Van den Mooter, and P. Augustijns. Top-down production of drug nanocrystals: nanosuspension stabilization, miniaturization and transformation into solid products. Int J Pharm. 364:64-75 (2008).
50. X.S. Li, J.X. Wang, Z.G. Shen, P.Y. Zhang, J.F. Chen, and J. Yun. Preparation of uniform prednisolone microcrystals by a controlled microprecipitation method. Int J Pharm. 342:26-32 (2007).
51. G. Liversidge, K. Cundy, J. Bishop, and D. Czekai. Surface modified drug nanoparticles, Google Patents, 1992.

52. E.L. Parrot. Comminution, *Encyclopedia of Pharmaceutical Technology*, Marcel Decker Inc., New York, 1990, pp. 101–121.
53. R. Hütterauch, Fricke, S., Zielke, P. Mechanical activation of pharmaceutical systems. Pharm Res:302-306 (1985).
54. S. Buchmann, W. Fischli, F. Thiel, and R. Alex. Aqueous suspension, an alternative intravenous formulation for animal studies. European Journal of Pharmaceutics and Biopharmaceutics. 42:S10 (1996).
55. R. BRUNOand R. MCILWRICK. Microfluidizer(R) processor technology for high performance particle size reduction, mixing and dispersion. Paperback APV. 42:77-89 (2001).
56. M. Tunick, D. Van Hekken, P. Cooke, and E. Malin. Transmission electron microscopy of mozzarella cheeses made from microfluidized milk. J Agric Food Chem. 50:99-103 (2002).
57. J.U. Junghannsand R.H. Muller. Nanocrystal technology, drug delivery and clinical applications. Int J Nanomedicine. 3:295-309 (2008).
58. R. Muller, R. Becker, B. Kruss, and K. Peters. Pharmaceutical nanosuspensions for medicament administration as systems with increased saturation solubility and rate of solution, Google Patents, 1999.
59. K. Krauseand R. Müller. Production and characterisation of highly concentrated nanosuspensions by high pressure homogenisation* 1. International journal of pharmaceutics. 214:21-24 (2001).
60. M. Grau, O. Kayser, and R. Müller. Nanosuspensions of poorly soluble drugs--reproducibility of small scale production. International journal of pharmaceutics. 196:155-159 (2000).
61. F. Kesisoglou, S. Panmai, and Y. Wu. Nanosizing--oral formulation development and biopharmaceutical evaluation. Adv Drug Deliv Rev. 59:631-644 (2007).
62. R.O. Williams, 3rd, J. Brown, and J. Liu. Influence of micronization method on the performance of a suspension triamcinolone acetonide pressurized metered-dose inhaler formulation. Pharm Dev Technol. 4:167-179 (1999).
63. R. Müllerand K. Peters. Nanosuspensions for the formulation of poorly soluble drugs:: I. Preparation by a size-reduction technique. International journal of pharmaceutics. 160:229-237 (1998).
64. T. Barberand B. Healthcare. Pharmaceutical particulate matter: analysis and control, Interpharm Press Buffalo Grove, 1993.
65. J. Knapp, T. Barber, and A. Lieberman. Liquid-and surface-borne particle measurement handbook, Marcel Dekker, 1996.
66. B. Du, X.T. Li, Y. Zhao, Y.M. A, and Z.Z. Zhang. Preparation and characterization of freeze-dried 2-methoxyestradiol nanoparticle powders. Pharmazie. 65:471-476 (2010).
67. D. Xia, P. Quan, H. Piao, S. Sun, Y. Yin, and F. Cui. Preparation of stable nitrendipine nanosuspensions using the precipitation-ultrasonication method for enhancement of dissolution and oral bioavailability. European Journal of Pharmaceutical Sciences (2010).
68. Z. Zhu, K. Margulis-Goshen, S. Magdassi, Y. Talmon, and C.W. Macosko. Polyelectrolyte stabilized drug nanoparticles via flash nanoprecipitation: a model study with beta-carotene. J Pharm Sci. 99:4295-4306 (2010).
69. I. Friedrichand C.C. Muller-Goymann. Characterization of solidified reverse micellar solutions (SRMS) and production development of SRMS-based nanosuspensions. Eur J

Pharm Biopharm. 56:111-119 (2003).

70. R. Erni, M. Rossell, C. Kisielowski, and U. Dahmen. Atomic-resolution imaging with a sub-50-pm electron probe. Physical review letters. 102:96101 (2009).
71. X. Pu, J. Sun, Y. Wang, X. Liu, P. Zhang, X. Tang, W. Pan, J. Han, and Z. He. Development of a chemically stable 10-hydroxycamptothecin nanosuspensions. Int J Pharm. 379:167-173 (2009).
72. Y. Wang, Z. Liu, D. Zhang, X. Gao, X. Zhang, C. Duan, L. Jia, F. Feng, Y. Huang, Y. Shen, and Q. Zhang. Development and in vitro evaluation of deacety mycoepoxydiene nanosuspension. Colloids Surf B Biointerfaces (2010).
73. A. Dolenc, J. Kristl, S. Baumgartner, and O. Planinsek. Advantages of celecoxib nanosuspension formulation and transformation into tablets. International journal of pharmaceutics. 376:204-212 (2009).
74. E. Nicolaides, M. Symillides, J. Dressman, and C. Reppas. Biorelevant dissolution testing to predict the plasma profile of lipophilic drugs after oral administration. Pharmaceutical research. 18:380-388 (2001).
75. J.B. Dressmanand C. Reppas. In vitro-in vivo correlations for lipophilic, poorly water-soluble drugs. Eur J Pharm Sci. 11 Suppl 2:S73-80 (2000).
76. X. Li, L. Gu, Y. Xu, and Y. Wang. Preparation of fenofibrate nanosuspension and study of its pharmacokinetic behavior in rats. Drug Dev Ind Pharm. 35:827-833 (2009).
77. I. Lifshitzand V. Slyozov. The kinetics of precipitation from supersaturated solid solutions. Journal of Physics and Chemistry of Solids. 19:35-50 (1961).
78. C. Wagner. Theorie der Alterung von Niederschl gen durch Uml sen (Ostwald©\Reifung). Zeitschrift f¨r Elektrochemie, Berichte der Bunsengesellschaft f¨r physikalische Chemie. 65:581-591 (1961).
79. P. Gassmann, M. List, A. Schweitzer, and H. Sucker. Hydrosols: alternatives for the parenteral application of poorly water soluble drugs. European Journal of Pharmaceutics and Biopharmaceutics. 40:64-72 (1994).
80. S. Verma, R. Gokhale, and D.J. Burgess. A comparative study of top-down and bottom-up approaches for the preparation of micro/nanosuspensions. Int J Pharm. 380:216-222 (2009).
81. A. Ain-Aiand P. Gupta. Effect of arginine hydrochloride and hydroxypropyl cellulose as stabilizers on the physical stability of high drug loading nanosuspensions of a poorly soluble compound. International journal of pharmaceutics. 351:282-288 (2008).
82. P. Mishra, L. Shaal, R. M¨ller, and C. Keck. Production and characterization of Hesperetin nanosuspensions for dermal delivery. International journal of pharmaceutics. 371:182-189 (2009).
83. S. Kobierski, K. Ofori-Kwakye, R. M¨ller, and C. Keck. Resveratrol nanosuspensions for dermal application-production, characterization, and physical stability. Pharmazie. 64:741-747 (2009).
84. K. Lee, S. Givens, D. Chase, and J. Rabolt. Electrostatic polymer processing of isotactic poly (4-methyl-1-pentene) fibrous membrane. Polymer. 47:8013-8018 (2006).
85. R. Lopez, J. Seto, D. Blankschtein, and R. Langer. Enhancing the transdermal delivery of rigid nanoparticles using the simultaneous application of ultrasound and sodium lauryl sulfate. Biomaterials (2010).
86. H. Shubar, S. Lachenmaier, M. Heimesaat, U. Lohman, R. Mauludin, R. Mueller, R. Fitzner,

K. Borner, and O. Liesenfeld. SDS-coated atovaquone nanosuspensions show improved therapeutic efficacy against experimental acquired and reactivated toxoplasmosis by improving passage of gastrointestinal and blood-brain barriers. Journal of Drug Targeting:1-11 (2010).

87. H. Shubar, I. Dunay, S. Lachenmaier, M. Dathe, F. Bushrab, R. Mauludin, R. M¨ller, R. Fitzner, K. Borner, and O. Liesenfeld. The role of apolipoprotein E in uptake of atovaquone into the brain in murine acute and reactivated toxoplasmosis. Journal of Drug Targeting. 17:257-267 (2009).
88. J. Pardeikeand R.H. Muller. Nanosuspensions: a promising formulation for the new phospholipase A2 inhibitor PX-18. Int J Pharm. 391:322-329 (2010).
89. V. Teeranachaideekul, V. Junyaprasert, E. Souto, and R. M¨ller. Development of ascorbyl palmitate nanocrystals applying the nanosuspension technology. International journal of pharmaceutics. 354:227-234 (2008).
90. S. Verma, B.D. Huey, and D.J. Burgess. Scanning probe microscopy method for nanosuspension stabilizer selection. Langmuir. 25:12481-12487 (2009).
91. R.H. Mullerand C.M. Keck. Challenges and solutions for the delivery of biotech drugs--a review of drug nanocrystal technology and lipid nanoparticles. J Biotechnol. 113:151-170 (2004).
92. L. Peltonenand J. Hirvonen. Pharmaceutical nanocrystals by nanomilling: critical process parameters, particle fracturing and stabilization methods. J Pharm Pharmacol. 62:1569-1579 (2010).
93. S. Farrokhpay. A review of polymeric dispersant stabilisation of titania pigment. Adv Colloid Interface Sci. 151:24-32 (2009).
94. A. Tual, E. Bourles, P. Barey, A. Houdoux, M. Desprairies, and J. Courthaudon. Effect of surfactant sucrose ester on physical properties of dairy whipped emulsions in relation to those of O/W interfacial layers. Journal of colloid and interface science. 295:495-503 (2006).
95. T. Hira, K. Takahashi, and H. Hara. Sucrose fatty acid esters suppress pancreatic secretion accompanied by peptide YY release in pancreatico-biliary diverted rats. Experimental Physiology. 92:687 (2007).
96. S.B. Calderilla-Fajardo, J. Cazares-Delgadillo, R. Villalobos-Garcia, D. Quintanar-Guerrero, A. Ganem-Quintanar, and R. Robles. Influence of sucrose esters on the in vivo percutaneous penetration of octyl methoxycinnamate formulated in nanocapsules, nanoemulsion, and emulsion. Drug Dev Ind Pharm. 32:107-113 (2006).
97. J.T. Ongand E. Manoukian. Micellar solubilization of timobesone acetate in aqueous and aqueous propylene glycol solutions of nonionic surfactants. Pharm Res. 5:704-708 (1988).
98. B. Youan. Microencapsulation of superoxide dismutase into poly (Å-caprolactone) microparticles by reverse micelle solvent evaporation. Drug Delivery. 10:283-288 (2003).
99. C. Rodriguez, D.P. Acharya, S. Hinata, M. Ishitobi, and H. Kunieda. Effect of ionic surfactants on the phase behavior and structure of sucrose ester/water/oil systems. J Colloid Interface Sci. 262:500-505 (2003).
100. O. Glatter, D. Orthaber, A. Stradner, G. Scherf, M. Fanun, N. Garti, V. Clement, and M.E. Leser. Sugar-Ester Nonionic Microemulsion: Structural Characterization. J Colloid Interface Sci. 241:215-225 (2001).
101. H.A. Ayala-Bravo, D. Quintanar-Guerrero, A. Naik, Y.N. Kalia, J.M. Cornejo-Bravo, and A.

Ganem-Quintanar. Effects of sucrose oleate and sucrose laureate on in vivo human stratum corneum permeability. Pharm Res. 20:1267-1273 (2003).

102. J. Cazares-Delgadillo, A. Naik, Y.N. Kalia, D. Quintanar-Guerrero, and A. Ganem-Quintanar. Skin permeation enhancement by sucrose esters: a pH-dependent phenomenon. Int J Pharm. 297:204-212 (2005).
103. A. Muller, J. Gagnaire, Y. Queneau, M. Karaoglanian, J. Maitre, and A. Bouchu. Winsor behaviour of sucrose fatty acid esters: choice of the cosurfactant and effect of the surfactant composition. Colloids and Surfaces A: Physicochemical and Engineering Aspects. 203:55-66 (2002).
104. I. Baker, B. Matthews, H. Suares, I. Krodkiewska, D. Furlong, F. Grieser, and C. Drummond. Sugar fatty acid ester surfactants: structure and ultimate aerobic biodegradability. Journal of Surfactants and Detergents. 3:1-11 (2000).
105. M. Ferrer, F. Comelles, F. Plou, M. Cruces, G. Fuentes, J. Parra, and A. Ballesteros. Comparative surface activities of di-and trisaccharide fatty acid esters. Langmuir. 18:667-673 (2002).
106. K. Parker, K. James, and J. Hurford. Sucrose Ester Surfactants ¡ªA Solventless Process and the Products Thereof, Vol. 41, ACS Publications, p. 97¨C114.
107. B. Arica Yegin, J.P. Benoit, and A. Lamprecht. Paclitaxel-loaded lipid nanoparticles prepared by solvent injection or ultrasound emulsification. Drug Dev Ind Pharm. 32:1089-1094 (2006).
108. H. Bunjes, M.H. Koch, and K. Westesen. Influence of emulsifiers on the crystallization of solid lipid nanoparticles. J Pharm Sci. 92:1509-1520 (2003).
109. S. Ullrich, H. Metz, and K. Mader. Sucrose ester nanodispersions: microviscosity and viscoelastic properties. Eur J Pharm Biopharm. 70:550-555 (2008).
110. J. Kuntsche, M.H. Koch, F. Steiniger, and H. Bunjes. Influence of stabilizer systems on the properties and phase behavior of supercooled smectic nanoparticles. J Colloid Interface Sci. 350:229-239 (2010).
111. V. Klang, N. Matsko, A.M. Zimmermann, E. Vojnikovic, and C. Valenta. Enhancement of stability and skin permeation by sucrose stearate and cyclodextrins in progesterone nanoemulsions. Int J Pharm. 393:152-160 (2010).
112. S. Takegami, K. Kitamura, H. Kawada, Y. Matsumoto, T. Kitade, H. Ishida, and C. Nagata. Preparation and characterization of a new lipid nano-emulsion containing two cosurfactants, sodium palmitate for droplet size reduction and sucrose palmitate for stability enhancement. Chem Pharm Bull (Tokyo). 56:1097-1102 (2008).
113. A. Lippacher, R.H. Muller, and K. Mader. Semisolid SLN dispersions for topical application: influence of formulation and production parameters on viscoelastic properties. Eur J Pharm Biopharm. 53:155-160 (2002).
114. H.Y. Ji, B.S. Shin, D.W. Jeong, E.J. Park, E.S. Park, S.D. Yoo, and H.S. Lee. Interspecies scaling of oleanolic acid in mice, rats, rabbits and dogs and prediction of human pharmacokinetics. Arch Pharm Res. 32:251-257 (2009).
115. M. Song, T.J. Hang, Y. Wang, L. Jiang, X.L. Wu, Z. Zhang, J. Shen, and Y. Zhang. Determination of oleanolic acid in human plasma and study of its pharmacokinetics in Chinese healthy male volunteers by HPLC tandem mass spectrometry. J Pharm Biomed Anal. 40:190-196 (2006).
116. M. Konopleva, T. Tsao, Z. Estrov, R.M. Lee, R.Y. Wang, C.E. Jackson, T. McQueen, G.

Monaco, M. Munsell, J. Belmont, H. Kantarjian, M.B. Sporn, and M. Andreeff. The synthetic triterpenoid 2-cyano-3,12-dioxooleana-1,9-dien-28-oic acid induces caspase-dependent and -independent apoptosis in acute myelogenous leukemia. Cancer Res. 64:7927-7935 (2004).

117. Z. Gao, D.J. Maloney, L.M. Dedkova, and S.M. Hecht. Inhibitors of DNA polymerase beta: activity and mechanism. Bioorg Med Chem. 16:4331-4340 (2008).

118. SUCROSE MONOLAURATE - Compound Summary (CID 4182596) http://pubchem.ncbi.nlm.nih.gov/summary/summary.cgi?cid=4182596&loc=ec_rcs.

119. Sucrodet - Compound Summary (CID 5360814) http://pubchem.ncbi.nlm.nih.gov/summary/summary.cgi?cid=5360814&loc=ec_rcs.

120. T. Cheng, Y. Zhao, X. Li, F. Lin, Y. Xu, X. Zhang, Y. Li, R. Wang, and L. Lai. Computation of octanol- water partition coefficients by guiding an additive model with knowledge. J Chem Inf Model. 47:2140-2148 (2007).

121. P.C. Lerk, H.H. Sucker, and H.F. Eicke. Micellization and solubilization behavior of sucrose laurate, a new pharmaceutical excipient. Pharm Dev Technol. 1:27-36 (1996).

122. G. Cornaire, J. Woodley, P. Hermann, A. Cloarec, C. Arellano, and G. Houin. Impact of excipients on the absorption of P-glycoprotein substrates in vitro and in vivo. Int J Pharm. 278:119-131 (2004).

123. J.V. Henry, P.J. Fryer, W.J. Frith, and I.T. Norton. Emulsification mechanism and storage instabilities of hydrocarbon-in-water sub-micron emulsions stabilised with Tweens (20 and 80), Brij 96v and sucrose monoesters. J Colloid Interface Sci. 338:201-206 (2009).

124. O. Amsalem, A. Aserin, and N. Garti. Phospholipids-embedded fully dilutable liquid nanostructures. Part 2: The role of sodium diclofenac. Colloids Surf B Biointerfaces. 81:422-429 (2010).

125. R. Bodmeier, H. Chen, P. Tyle, and P. Jarosz. Spontaneous formation of drug-containing acrylic nanoparticles. Journal of microencapsulation. 8:161-170 (1991).

126. A. Romero-P ¨ţez, E. Garc ¨a-Garc ¨a, A. Zavaleta-Mancera, J. Ram ¨ţez-Bribiesca, A. Revilla-V ¨¢zquez, L. Hern ¨¢ndez-Calva, R. L ¨®pez-Arellano, and R. Cruz-Monterrosa. Designing and evaluation of sodium selenite nanoparticles in vitro to improve selenium absorption in ruminants. Veterinary research communications. 34:71-79 (2010).

127. Z. Rahman, A. Zidan, M. Habib, and M. Khan. Understanding the quality of protein loaded PLGA nanoparticles variability by Plackett-Burman design. International journal of pharmaceutics. 389:186-194 (2010).

128. J. Zhuand R. Hayward. Spontaneous generation of amphiphilic block copolymer micelles with multiple morphologies through interfacial instabilities. Journal of the American Chemical Society. 130:7496-7502 (2008).

129. S. Khoeeand M. Yaghoobian. An investigation into the role of surfactants in controlling particle size of polymeric nanocapsules containing penicillin-G in double emulsion. European journal of medicinal chemistry. 44:2392-2399 (2009).

130. E. Pisani, E. Fattal, J. Paris, C. Ringard, V. Rosilio, and N. Tsapis. Surfactant dependent morphology of polymeric capsules of perfluorooctyl bromide: Influence of polymer adsorption at the dichloromethane-water interface. Journal of colloid and interface science. 326:66-71 (2008).

131. S. Das, H.S. Lin, P.C. Ho, and K.Y. Ng. The impact of aqueous solubility and dose on the pharmacokinetic profiles of resveratrol. Pharm Res. 25:2593-2600 (2008).

132. A. Noyesand W. Whitney. The rate of solution of solid substances in their own solutions. Journal of the American Chemical Society. 19:930-934 (1897).
133. H.V. Carey, M.T. Andrews, and S.L. Martin. Mammalian hibernation: cellular and molecular responses to depressed metabolism and low temperature. Physiol Rev. 83:1153-1181 (2003).
134. O.H.C.a.B.H. Stewart. Physicochemical and drug-delivery considerations for oral drug bioavailability Drug Discovery Today. 1:12 (1996).
135. D. Montgomery. Design and Analysis of Experiments, 5th edn, 2001, John Wiley & Sons, Inc.: New York.
136. P. Haaland. Experimental design in biotechnology, CRC, 1989.
137. B. Singh, R. Kumar, and N. ABUJA. Optimizing drug delivery systems using systematic design of experiments. Part I: Fundamental aspects. Critical reviews in therapeutic drug carrier systems. 22:27-105 (2005).
138. P. Mathews. Design of Experiments with MINITAB, Asq Pr, 2005.
139. H. Tye. Application of statistical 'design of experiments' methods in drug discovery. Drug Discov Today. 9:485-491 (2004).
140. A.M. Cerdeira, M. Mazzotti, and B. Gander. Miconazole nanosuspensions: Influence of formulation variables on particle size reduction and physical stability. Int J Pharm. 396:210-218 (2010).
141. X. He, M.R. Barone, P.J. Marsac, and D.C. Sperry. Development of a rapidly dispersing tablet of a poorly wettable compound: formulation DOE and mechanistic study of effect of formulation excipients on wetting of celecoxib. Int J Pharm. 353:176-186 (2008).
142. S. Verma, S. Kumar, R. Gokhale, and D.J. Burgess. Physical stability of nanosuspensions: Investigation of the role of stabilizers on Ostwald ripening. Int J Pharm (2010).
143. B. Van Eerdenbrugh, L. Froyen, J. Van Humbeeck, J.A. Martens, P. Augustijns, and G. Van den Mooter. Drying of crystalline drug nanosuspensions-the importance of surface hydrophobicity on dissolution behavior upon redispersion. Eur J Pharm Sci. 35:127-135 (2008).